# *Colloquium*: Spin-orbit effects in superconducting hybrid structures

Morten Amundsen[*]

*Nordita, KTH Royal Institute of Technology and Stockholm University, Hannes Alfvéns väg 12, SE-106 91 Stockholm, Sweden and Center for Quantum Spintronics, Department of Physics, Norwegian University of Science and Technology, NO-7491 Trondheim, Norway*

Jacob Linder[†]

*Center for Quantum Spintronics, Department of Physics, Norwegian University of Science and Technology, NO-7491 Trondheim, Norway*

Jason W. A. Robinson[‡]

*Department of Materials Science and Metallurgy, University of Cambridge, 27 Charles Babbage Road, Cambridge CB3 0FS, United Kingdom*

Igor Žutić[§]

*Department of Physics, University at Buffalo, State University of New York, Buffalo, New York 14260, USA*

Niladri Banerjee[‖]

*Department of Physics, Blackett Laboratory, Imperial College London, London SW7 2AZ, United Kingdom*

(published 28 May 2024)

Spin-orbit coupling (SOC) relates to the interaction between an electron's motion and its spin and is ubiquitous in solid-state systems. Although the effect of SOC in normal-state phenomena has been extensively studied, its role in superconducting hybrid structures and devices elicits many unexplored questions. In conjunction with broken symmetries and material inhomogeneities within superconducting hybrid structures, SOC may have contributions beyond its effects in homogeneous materials. Notably, even with well-established magnetic or nonmagnetic materials and conventional *s*-wave spin-singlet superconductors, SOC leads to emergent phenomena including equal-spin-triplet pairing and topological superconductivity (hosting Majorana states), a modified current-phase relationship in Josephson junctions, and nonreciprocal transport, including superconducting diode effects. SOC is also responsible for transforming quasiparticles in superconducting structures, which enhances the spin Hall effect and changes the spin dynamics. Taken together, SOC in superconducting hybrid structures and the potential for electric tuning of the SOC strength create interesting possibilities to advance superconducting spintronic devices for energy-efficient computing and enable topological fault-tolerant quantum computing. By providing a description of experimental techniques and theoretical methods to study SOC, this Colloquium describes the current understanding of resulting phenomena in superconducting structures and offers a framework to select and design a growing class of materials systems where SOC plays an important role.

DOI: 10.1103/RevModPhys.96.021003

**CONTENTS**



[*]morten.amundsen@ntnu.no
[†]jacob.linder@ntnu.no
[‡]jjr33@cam.ac.uk
[§]zigor@buffalo.edu
[‖]n.banerjee@imperial.ac.uk

 

## I. INTRODUCTION

As a relativistic effect, the motion of an electron in an electric field creates a magnetic field in its rest frame (Jackson, 1998). The resulting spin-orbit coupling (SOC) in solid-state systems can have different contributions. In addition to the coupling of the electron spin with the average electric field from the periodic crystal potential, other SOC terms arise due to an applied or built-in electric field, for example, due to broken inversion symmetry. One can also distinguish among intrinsic, extrinsic, and synthetic SOC, which are due to electronic structure, impurities, and magnetic textures, respectively. With SOC, at a given wave vector $\mathbf{k}$ the twofold spin degeneracy is removed, resulting in a $k$-dependent Zeeman energy and an effective magnetic field (Winkler, 2003; Žutić, Fabian, and Das Sarma, 2004). In superconducting heterostructures, the role of SOC can be even more striking by transforming the orbital and spin symmetry of the Cooper pairs, through which exotic states may emerge, even from simple $s$-wave spin-singlet superconductors.

For decades, SOC effects have been identified as crucial for many normal-state phenomena, such as spin-photon and spin-charge conversion (Meier and Zakharchenya, 1984), various topological states (Shen, 2012; Armitage, Mele, and Vishwanath, 2018), the family of spin Hall effects (D'yakonov and Perel', 1971a; Maekawa *et al.*, 2012), magnetocrystalline anisotropy, and noncollinear spin textures (including skyrmions and chiral domain walls) (Tsymbal and Žutić, 2019). They also formed the basis for early spintronic applications, which can be traced back to the discovery of anisotropic magnetoresistance in 1857 (Thomson, 1857; Žutić, Fabian, and Das Sarma, 2004). In contrast, the relevance of SOC in superconducting structures was largely absent or limited to specific aspects without fully recognizing many connections (Tedrow and Meservey, 1971; Meservey and Tedrow, 1994; Golubov, Kupriyanov, and Il'ichev, 2004; Bergeret, Volkov, and Efetov, 2005; Buzdin, 2005). Motivated by recent advances in studies of hybrid superconducting structures where SOC plays a prominent role, this Colloquium provides an experimental and theoretical framework to highlight many such connections between different phenomena and emerging applications in these structures.

The quest to realize topological superconductivity and elusive Majorana states for fault-tolerant topological quantum computing in structures with strong SOC relies on equal-spin-triplet superconductivity (Nayak *et al.*, 2008; Elliot and Franz, 2015). This triplet superconductivity is also sought in superconducting spintronics (Eschrig, 2015; Linder and Robinson, 2015; Ohnishi *et al.*, 2020; Yang, Ciccarelli, and Robinson, 2021), as it supports dissipationless spin currents and allows for the coexistence of superconductivity and ferromagnetism. Josephson junctions (JJs) with tunable SOC, which enable spin-triplet superconductivity, are important building blocks for topological superconductivity and superconducting spintronics (Mayer *et al.*, 2020; Dartiailh *et al.*, 2021). These JJs also reveal the superconducting diode effect (Dartiailh *et al.*, 2021; Baumgartner *et al.*, 2022), an example of a nonreciprocal phenomenon (Nadeem, Fuhrer, and Wang, 2023). While nonreciprocal effects are technologically important (Shockley, 1952; Marder, 2010) and have been known since the 19th century in the normal state (Faraday, 1846; Kerr, 1877), experimental demonstrations of superconducting counterparts were largely absent until recently (Nadeem, Fuhrer, and Wang, 2023). Analogous to multiferroic materials that allow electrical control of magnetic properties and, conversely, magnetic control of electrical properties, we can view SOC in the superconducting state as enabling various magnetoelectric effects (Tkachov, 2017) and facilitating the coupling between different order parameters. Since SOC changes the properties of quasiparticles in superconductors, it has also been shown to produce strongly enhanced spin Hall phenomena in superconducting structures.

With controllable SOC, the previous efforts to integrate superconductors and ferromagnets can be radically simplified. Instead of engineering complex noncollinear magnetic structures at the superconductor/ferromagnet ($S/F$) interface (Keizer *et al.*, 2006; Khaire *et al.*, 2010; Robinson, Witt, and Blamire, 2010; Usman *et al.*, 2011; Robinson *et al.*, 2012; Banerjee, Robinson, and Blamire, 2014), a single common $F$ with SOC in a superconducting heterostructure with broken inversion symmetry is sufficient to support spin-triplet superconductivity and large magnetoresistive effects (Banerjee *et al.*, 2018; Jeon *et al.*, 2018, 2020; Jeon, Ciccarelli *et al.*, 2019; González-Ruano *et al.*, 2020, 2021; Martínez *et al.*, 2020; Cai *et al.*, 2021). Theoretically the observed role of SOC in singlet-to-triplet pair conversion has been studied for both ballistic and diffusive transport (Yokoyama, Tanaka, and Inoue, 2006; Feng *et al.*, 2008; Bergeret and Tokatly, 2013, 2014; Högl *et al.*, 2015; Jacobsen, Ouassou, and Linder, 2015) and preceded by the related effect of spin-active interfaces (Žutić and Das Sarma, 1999; Eschrig *et al.*, 2003; Halterman and Valls, 2009; Linder, Yokoyama, and Sudbø, 2009) and SOC generated $k$-anisotropic triplet condensates (Gor'kov and Rashba, 2001; Edelstein, 2003).

Another example where SOC fundamentally modifies the underlying physics is within superconducting random-access memories using ferromagnetic JJs. Here nonvolatile control of the zero and $\pi$ ground-state phase encoding binary information (Dayton *et al.*, 2018; Birge and Houzet, 2019) needs to be revisited in the presence of SOC where, in addition to the spin-singlet and spin-triplet states, their admixture is also possible.

The resulting anomalous Josephson effect (Buzdin, 2008; Reynoso *et al.*, 2008) supports an arbitrary phase shift other than just zero and $\pi$, leading to novel challenges and opportunities for nonbinary information processing and storage. Just as magnetic JJs are the building blocks for superconducting memories, their nonmagnetic counterparts are the key elements for low-power and high-speed superconducting logic (Holmes, Ripple, and Manheimer, 2013; Tafuri, 2019) and superconducting quantum computing (Wendin, 2017; Krantz *et al.*, 2019). This means that SOC may not only modify such devices but also provide entirely new functionalities in their operation, as the current-phase relation, Josephson energy, critical temperature, and critical current can all strongly change with SOC. As in the normal state, SOC is the major source of spin relaxation and decoherence, as well as the underlying mechanism for spin dynamics, in the superconducting state (Žutić, Fabian, and Das Sarma, 2004). Since both long and short spin-relaxation times (Nishikawa *et al.*, 1995; Lindemann *et al.*, 2019) can be desirable in the normal state, their SOC-controlled tunability in the superconducting state would be similarly advantageous. Taken together, the presence of SOC and its tunability in hybrid superconducting structures offers an intriguing prospect to both identify novel phenomena and advance various quantum technologies ranging from storing, transferring, and processing information to improving quantum sensing. While some of the resulting efforts simply extend the current concepts and applications of superconductivity, others, like topological quantum computing, would radically change the paths toward realizing computational architectures (Cai, Žutić, and Han, 2023). Even if the most ambitious proposals remain aspirational, the advances in our understanding of SOC have already transformed the way that we view various superconducting phenomena.

Focusing on more common materials, where their superconductivity is well established, simplifies the understanding of the role of SOC. For example, a large part of this Colloquium focuses on hybrids with conventional elemental or nitride *s*-wave superconductors, including Nb, Al, V, and NbN. However, we note that other superconducting systems to investigate SOC effects are possible; for over two decades superconducting spintronics has been studied with high-temperature *d*-wave superconductors (Vas'ko *et al.*, 1997; Wei *et al.*, 1999; Chen *et al.*, 2001), where even their normal-state properties remain under debate. In mentioning other oxide superconductors, two-dimensional superconductors, such as $NbSe_2$, and proximity-induced superconductivity in group III-V and group IV semiconductor nanostructures, we complement our Colloquium by providing relevant reviews on these topics.

While we recognize that significant development is required before SOC-driven superconducting phenomena can be applied in the field of spintronics or quantum technologies, sufficient progress has already been made both theoretically and experimentally where one can start to think about potential areas of application. Using dissipationless supercurrents offers alternatives for energy-efficient information-communication and quantum technologies. Data centers alone are predicted to require 8% of globally generated electrical power by 2030 (Jones, 2018). A potential solution may combine superconducting electronics with recent advances in spintronics (Tsymbal and Žutić, 2019; Hirohata *et al.*, 2020) to seamlessly integrate logic and memory (Birge and Houzet, 2019) and thereby overcome the von Neumann bottleneck (Dery *et al.*, 2012). Through this Colloquium we hope to drive future innovations benefiting fields like superconducting spintronics and Majorana physics, which will help solve material challenges that are key to progress in these areas. We start with an introduction to relevant theoretical and experimental background of superconductivity in the presence of SOC in hybrid structures, continue by discussing recent developments, and conclude with open questions while highlighting promising research directions.

## II. BACKGROUND

This section reviews basic concepts that build a basis for the results outlined in the following sections. We start by describing SOC, specifically, the Rashba and Dresselhaus models, in bulk materials and structures with inversion asymmetry. We then introduce the physics emerging from SOC superconductivity in proximity structures and include a discussion on theoretical methods that can be used to study such systems. The purpose of this section is thus to provide a set of theoretical concepts necessary when discussing the interesting spintronics phenomena that arise due to the combination of superconductivity and SOC in heterostructures.

### A. Spin-orbit coupling

Coupling between the motion of an electron and its spin stems from the fact that, in the reference frame of the electron, it is the positively charged lattice that moves. Moving charges create a magnetic field that may couple to the electron spin. In a Lorentz-invariant formulation, a SOC term emerges, as shown in the Dirac equation (Dirac, 1928)

$$\begin{pmatrix} mc^2+V(\boldsymbol{r}) & -i\hbar c\boldsymbol{\sigma}\cdot\boldsymbol{\nabla} \\ -i\hbar c\boldsymbol{\sigma}\cdot\boldsymbol{\nabla} & -mc^2+V(\boldsymbol{r}) \end{pmatrix}\begin{pmatrix}\psi_e\\ \psi_h\end{pmatrix}=(\varepsilon+mc^2)\begin{pmatrix}\psi_e\\ \psi_h\end{pmatrix}, \quad (1)$$

and, taking the nonrelativistic limit, $\varepsilon, V \ll mc^2$, where $\varepsilon$ is the particle energy without its rest mass. In Eq. (1) $V(\boldsymbol{r})$ is the lattice potential, $m$ is the free electron mass, and $\boldsymbol{\sigma}$ is a vector of Pauli matrices. The resulting Hamiltonian is $H = p^2/2m + V(\boldsymbol{r}) + (\hbar/4m^2c^2)\boldsymbol{\sigma}\cdot(\boldsymbol{\nabla}V\times\boldsymbol{p})$ for the electron wave function $\psi_e$, where irrelevant terms are discarded. The last term represents SOC, which is large near a lattice site (Fabian *et al.*, 2007). Within the second quantization formalism, in the basis of the Bloch functions it takes the form (Samokhin, 2009)

$$H_{\mathrm{SO}} = \sum_{k}\sum_{nn'}\sum_{ss'}\boldsymbol{Q}_{nn'}(\boldsymbol{k})\cdot\boldsymbol{\sigma}_{ss'}c^{\dagger}_{kns}c_{kn's'}, \quad (2)$$

where $\boldsymbol{Q}_{nn'}$ is a phenomenological model function that expresses the coupling between momentum and spin, with $n$ and $n'$ band indices and $\boldsymbol{k}$ the crystal momentum. For a centrosymmetric material, the terms $\boldsymbol{Q}_{nn}$ vanish and SOC can be described only by models containing at least two bands. However, in a noncentrosymmetric material the one-band model $\sum_{nn'}\boldsymbol{Q}_{nn'}\to\boldsymbol{Q}$ in Eq. (2) is possible, while

$\boldsymbol{Q}(\boldsymbol{k}) = -\boldsymbol{Q}(-\boldsymbol{k})$. One can distinguish bulk inversion asymmetry (BIA) from structure inversion asymmetry (SIA), which leads to a spin splitting and SOC,

$$H_{\mathrm{SO}}(\boldsymbol{k}) = \hbar\boldsymbol{\sigma}\cdot\boldsymbol{\Omega}(\boldsymbol{k})/2, \tag{3}$$

where $\boldsymbol{\Omega}(\boldsymbol{k})$ is the Larmor frequency for the electron spin precession in the conduction band (Žutić, Fabian, and Das Sarma, 2004) or, equivalently, the SOC field. In Eq. (3) the momentum scattering $\boldsymbol{\Omega}(\boldsymbol{k})$ is responsible for spin dephasing. Related SOC manifestations in semiconductors usually focus on effective models that capture the low-energy properties of the conduction and valence bands. An example of BIA is the Dresselhaus SOC (Dresselhaus, 1955) given by $\boldsymbol{\Omega}_D = (2\gamma/\hbar)[k_x(k_y^2 - k_z^2), k_y(k_z^2 - k_x^2), k_z(k_x^2 - k_y^2)]$, where $\gamma$ is the SOC strength. In two-dimensional (2D) systems with quantum confinement along the unit vector $\hat{n}$, $\boldsymbol{\Omega}_D$ can be linearized in $\boldsymbol{k}$ as

$$\boldsymbol{\Omega}_D^{\mathrm{2D}} \sim k_n^2[2n_x(n_y k_y - n_z k_z) + k_x(n_y^2 - n_z^2)]\hat{\mathbf{x}} + \mathrm{c.p.}, \tag{4}$$

where $k_n^2$ is the expectation value of the square of the wave number operator normal to the plane in the lowest subband state, while $\hat{\boldsymbol{n}} = (n_x, n_y, n_z)$ is the confinement unit vector of the quantum well and c.p. denotes the cyclic index permutation. For a rectangular well of width $a$, $k_n^2 = (\pi/a)^2$, while for a triangular well $k_n^2$ is as given by de Sousa and Das Sarma (2003). With a strong confinement, $k_\parallel^2 \ll k_n^2$, where $\boldsymbol{k}_\parallel$ is the in-plane (IP) wave vector ($\perp\hat{n}$); cubic terms in $\boldsymbol{k}$ in $\boldsymbol{\Omega}_D$ from Eq. (4) can be neglected.

For commonly considered quantum well confinements, one obtains for [001] $\boldsymbol{\Omega}_D^{\mathrm{2D}} \sim k_n^2(-k_x, k_y, 0)$, for [111] $\boldsymbol{\Omega}_D^{\mathrm{2D}} \sim k_n^2(\boldsymbol{k}\times\boldsymbol{n})$, and for [110] $\boldsymbol{\Omega}_D^{\mathrm{2D}} \sim k_n^2 k_x(-1, 1, 0)$, as shown in Fig. 1. Several features can be readily seen: BIA [100] displays a "breathing" pattern, while BIA [110] $\boldsymbol{\Omega}(\boldsymbol{k})$ is perpendicular to the plane such that, within the linear in $\boldsymbol{k}$ approximation, the perpendicular spins do not dephase.

An extensively studied SIA example is given by Bychkov-Rashba (or simply Rashba) SOC (Bychkov and Rashba, 1984), which arises in asymmetric quantum wells or in deformed bulk systems and is expressed by

$$\boldsymbol{\Omega}_R = 2\alpha(\boldsymbol{k}\times\boldsymbol{n}), \tag{5}$$

where $\alpha$ parametrizes its strength and the inversion symmetry is broken along the $\boldsymbol{n}$ direction. We see in Fig. 1 that its functional form $\boldsymbol{\Omega}_R$ coincides with BIA $\boldsymbol{\Omega}_D^{\mathrm{2D}}$ in [111] quantum wells. A desirable property of Rashba SOC is that $\alpha$ is tunable with an applied electric field. While these linearized forms of the Rashba and Dresselhaus SOC are the most common models, there is increasing interest in the study of phenomena that go beyond their range of validity.

For example, in Rashba SOC there is a growing class of materials where cubic terms in $k$ can play an important role or can even be dominant (Alidoust, Shen, and Žutić, 2021). Finally, while we have focused here on intrinsic SOC, we note that extrinsic SOC caused by impurities plays a key role in spintronics both with and without superconductors, thus giving rise to important contributions to spin Hall effects and spin relaxation (Žutić, Fabian, and Das Sarma, 2004).

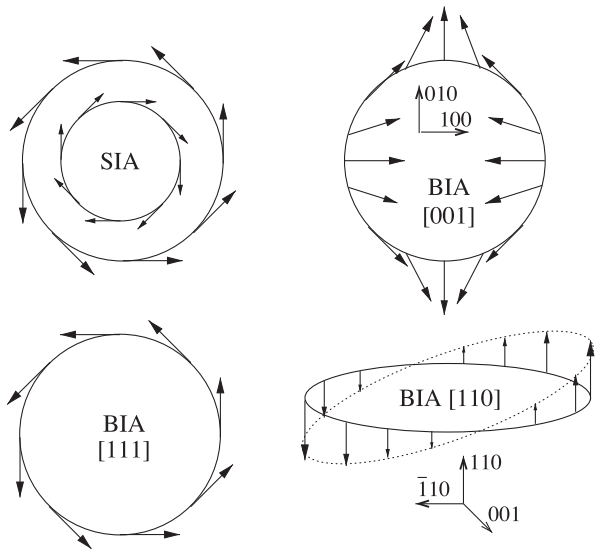


FIG. 1. Vector fields $\boldsymbol{\Omega}(\boldsymbol{k})$ on a circular Fermi surface for structure inversion asymmetry (SIA) and bulk inversion asymmetry (BIA). Since $\boldsymbol{\Omega}(\boldsymbol{k})$ is the spin-quantization axis, the vector pattern is also the pattern of the spin on the Fermi surface. As opposite spins have different energies, the Fermi circle splits into two concentric circles with opposite signs of spin. Only the SIA case is shown, but the analogy extends to all examples. The field for BIA [110] is perpendicular to the plane, with the magnitude varying along the Fermi surface. All other cases have constant fields lying in the plane. From Žutić, Fabian, and Das Sarma, 2004.

### B. Validity of Rashba and Dresselhaus models

The validity of effective low-energy SIA and BIA SOC models can be examined from electronic structure calculations using a first-principles, $\boldsymbol{k}\cdot\boldsymbol{p}$ method, or a tight-binding model. Another contribution to Rashba-like spin splitting $H_L = -\mathbf{p}\cdot\mathbf{E}$ arises in systems with localized orbital momentum $\mathbf{L}$ (Park *et al.*, 2011, 2012), where $\mathbf{E}$ is the electric field and where the electric dipole moment $\mathbf{p} \propto \mathbf{L}\times\mathbf{k}$ is produced by the asymmetric charge distribution. Rashba SOC strength is renormalized by the orbital contribution, while local symmetry breaking can induce local orbital Rashba spin splitting even in centrosymmetric systems (Lee and Kwon, 2020).

Going beyond the Rashba and Dresselhaus models might be necessary for interfacial SOC in junctions with interface-induced symmetry reduction in the individual bulk constituents and for multiorbital configurations (Mercaldo *et al.*, 2020). This is exemplified in an Fe/GaAs junction, where the cubic and $T_d$ symmetries of bulk Fe and GaAs, respectively, are reduced to $C_{2v}$ (Fabian *et al.*, 2007; Žutić *et al.*, 2019).

Since the interfacial SOC is present only near the interface, its effects can be controlled electrically via a gate voltage or an applied external bias capable of pushing the carrier wave function into or away from the interface. Interfacial SOC can also be controlled magnetically, as it strongly depends on the orientation of $\mathbf{M}$ in the Fe layer, as illustrated from the first-principles calculation in Figs. 2(b) and 2(c) (Gmitra *et al.*, 2013). The bias dependence of the SOC can be inferred from the transport anisotropy in Figs. 2(d) and 2(e).

While the resulting interfacial SOC for the Fe/GaAs junction corresponds to neither the Rashba nor the

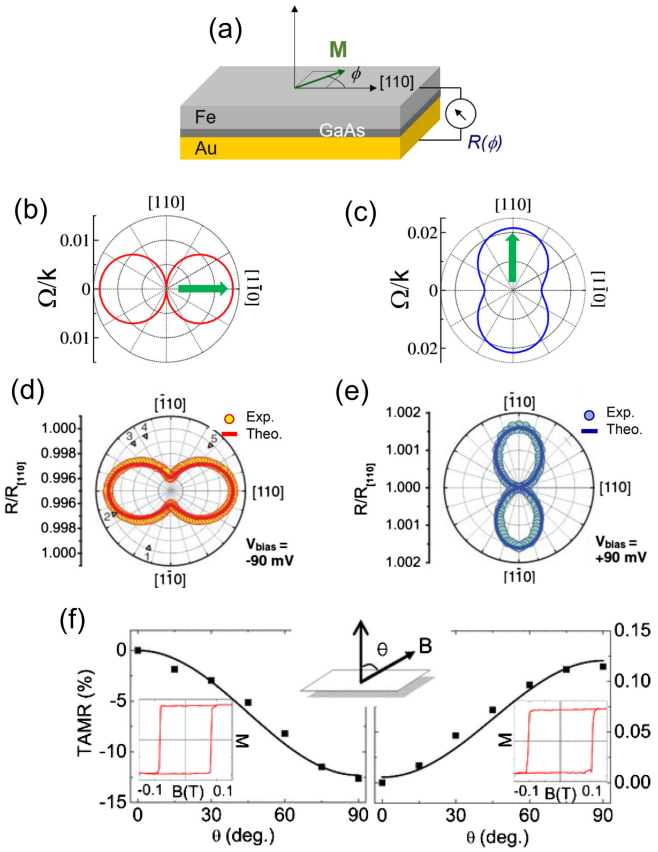


FIG. 2. (a) Schematic of a Fe/GaAs slab. For in-plane TAMR, **M** is rotated in the plane of Fe. (b) Angular **k**-space dependence of the amplitude of the interfacial SOC field for **M** along the GaAs $[1\bar{1}0]$ direction (green arrow). (c) Same as in (b) but for **M** along the $[110]$ direction (Gmitra *et al.*, 2013). The tunneling resistance $R(\phi)$ is normalized to its $\phi = 0$ value $R_{[110]}$. (d), (e) Measurements for bias $\pm 90$ meV (Moser *et al.*, 2007). (f) Angular dependence of the TAMR in the out-of-plane (OOP) configuration. Left panel: $CoPt/AlO_x/Pt$ tunnel junctions. Right panel: $Co/AlO_x/Pt$ tunnel junctions. An extra Pt layer with strong SOC yields in $CoPt/AlO_x/Pt$ TAMR that is 2 orders of magnitude larger than that in $Co/AlO_x/Pt$. Insets: **M** measurements in OOP magnetic fields (Park *et al.*, 2008). Adapted from Žutić *et al.*, 2019.

Dresselhaus model, its existence can be probed through tunneling anisotropic magnetoresistance (TAMR), which gives the dependence of the tunneling current in a junction with only one magnetic electrode on the orientation of **M** (Gould *et al.*, 2004). For an IP rotation of **M** in Fig. 2(a), we can define TAMR as the normalized resistance difference,

$$\mathrm{TAMR} = [R(\phi) - R_{[110]}]/R_{[110]}, \tag{6}$$

where $R(\phi = 0) \equiv R_{[110]}$ is the resistance along the $[110]$ crystallographic axis. The out-of-plane (OOP) TAMR is defined analogously. TAMR appears because the electronic structure depends on the **M** orientation due to SOC. The surface or an interface electronic structure can strongly deviate from its bulk counterparts and host pure or resonant bands. With SOC, the dispersion of these states depends on the **M** orientation (Chantis *et al.*, 2007). As a result, the tunneling conductance, which in a crystalline junction is sensitive to the transverse wave vector, develops both OOP and IP MR [shown in Figs. 2(d)–2(f)] whose angular dependence reflects the crystallographic symmetry of the interface. For example, the TAMR inherits the $C_{4v}$ symmetry for the Fe(001) surface (Chantis *et al.*, 2007) and the reduced $C_{2v}$ symmetry for the Fe(001)/GaAs interface (Moser *et al.*, 2007).

Our prior discussion of SOC and its manifestations in the normal-state properties have important superconducting counterparts and enable entirely new phenomena that are absent in the normal state. Even when the SOC results in only a small normal-state transport anisotropy, as shown in Figs. 2(d) and 2(e), the superconducting analogs of such phenomena can lead to much greater effects (Martínez *et al.*, 2020; Cai *et al.*, 2021).

### C. Triplet superconductivity

Conventional $s$-wave superconductors are well described by Bardeen-Cooper-Schrieffer (BCS) microscopic theory. The superconducting correlations consist of Cooper pairs in a spin-singlet state and carry no net spin, unlike the proximity-induced spin-triplet superconducting correlations. There are materials believed to exhibit intrinsic triplet superconductivity such as Bechgaard salts (Sengupta *et al.*, 2001), $UPt_3$ (Joynt and Taillefer, 2002), and ferromagnetic superconductors (Aoki *et al.*, 2011). A direct interaction between superconductivity and SOC was also found in noncentrosymmetric superconductors, where electron pairing is a mixture of spin-singlet and spin-triplet configurations (Smidman *et al.*, 2017).

Through proximity effects, triplet superconducting correlations can be generated using only conventional materials. In $S/F$ bilayers, the spin splitting in the latter leads to oscillations in the pair correlation between the singlet and triplet spin configurations due to a process akin to Fulde-Ferrell-Larkin-Ovchinnikov (FFLO) oscillations (Fulde and Ferrell, 1964; Larkin and Ovchinnikov, 1964; Buzdin, 2005). Nevertheless, such a coupling between $S$ and homogeneous $F$ is rapidly suppressed as one moves away from the interface region, leading to a short-range proximity effect. The situation is different in $F$ with an inhomogeneous **M** direction, where the spin of the short-range triplet correlations is orthogonal to **M**. Here the short-range triplets decay over the coherence length of the Cooper pairs in the $F$ layer. If the orientation of **M** changes, the triplet spin will obtain a component parallel to **M**. This component, referred to as a long-range triplet component, is not influenced by the spin splitting to the same degree as their short-range counterparts. Notably it may persist for long distances, as in nonmagnetic metals (Petrashov *et al.*, 1994; Giroud *et al.*, 1998; Lawrence and Giordano, 1999; Petrashov *et al.*, 1999) of the order of $\sqrt{D/2\pi T}$ in the diffusive limit, where $D$ is the diffusion coefficient of the $F$ region and $T$ is the temperature (Bergeret, Volkov, and Efetov, 2001, 2005; Kadigrobov, Shekhter, and Jonson, 2001).

Engineered superconducting hybrid structures used to generate spin-polarized triplets have been extensively studied. The use of magnets with rare earth materials (holmium) with intrinsically inhomogeneous **M** in JJs has provided evidence of triplet pair creation (Sosnin *et al.*, 2006; Robinson, Witt, and Blamire, 2010). Alternatively, noncollinear magnetism

can be engineered in magnetic multilayers (Khaire *et al.*, 2010; Banerjee, Robinson, and Blamire, 2014). However, intrinsically inhomogeneous magnets are rare, and controlling **M** misalignment in ferromagnetic multilayers is difficult. Magnetic vortices are emerging as a viable candidate for tunable sources of noncollinear magnetism and corresponding triplet generation (Fermin, van Dinter *et al.*, 2022; Fermin, Scheinowitz *et al.*, 2022).

An effective inhomogeneous **M** is generated in a homogeneous $F$ in the presence of SOC. This takes the form of a Dzyaloshinskii-Moriya exchange interaction (Dzyaloshinsky, 1958; Moriya, 1960) that cants **M**, thereby creating helical spin textures (Ferriani *et al.*, 2008) and skyrmions (Rößler, Bogdanov, and Pfleiderer, 2006; Heinze *et al.*, 2011). Such magnetic structures at the $S/F$ interface can generate spin-polarized triplets. Furthermore, the formation of triplets in $S/F$ structures with an interfacial SOC generated due to broken inversion symmetry has been an area of intense study (Mel'Nikov *et al.*, 2012; Bergeret and Tokatly, 2013, 2014; Högl *et al.*, 2015; Jacobsen, Kulagina, and Linder, 2016; Banerjee *et al.*, 2018; Jeon *et al.*, 2018, 2020; Satchell and Birge, 2018; Simensen and Linder, 2018; Jeon, Ciccarelli *et al.*, 2019; Satchell, Loloee, and Birge, 2019; Vezin *et al.*, 2020; Cai *et al.*, 2021).

### D. Theoretical frameworks

In the following we describe common theoretical models that describe SOC in superconducting hybrid structures with increasing realism. We start by highlighting basic features of the proximity effect in such systems.

#### 1. General considerations of spin-dependent fields

To understand the response of a superconductor to magnetic interactions, we consider the BCS model in an infinite domain, with spin splitting of the type

$$H = \sum_{ks} \xi_k c_{ks}^\dagger c_{ks} - \sum_{ks} [s\Delta c_{ks}^\dagger c_{-k,-s}^\dagger + s\Delta^* c_{-k,-s} c_{ks}] - \sum_{kss'} \boldsymbol{h}(\boldsymbol{k}) \cdot \boldsymbol{\sigma}_{ss'} c_{ks}^\dagger c_{ks'}, \tag{7}$$

where $\xi_k = \hbar^2 \boldsymbol{k}^2/2m - \mu$, $\mu$ is the chemical potential, $m$ is the electron rest mass, $\Delta$ is the superconducting order parameter, and $\boldsymbol{h}$ relates to the spin splitting. The operator $c_{ks}^\dagger$ ($c_{ks}$) creates (annihilates) an electron with momentum $k$ and spin $s$. Consider the case where $\boldsymbol{h} = h_0\hat{\boldsymbol{z}}$ is independent of momentum and therefore reduces to a Zeeman field. Insight into the superconducting behavior can be gained by inspecting the normal-state dispersions ($\Delta = 0$), as shown in Fig. 3(a). The Zeeman field splits the energy bands of the two spin species: the spin-up band is lowered in energy and the spin-down band is raised. The corresponding gap induced in the band structure of the two spin species when superconductivity is introduced, $E_g^\uparrow$ and $E_g^\downarrow$, respectively, is $E_g^s = \Delta - sh$ and indicates a difference in the strength of the hybridization between electrons and holes for the two opposite spins. We can study the effect of superconductivity via the opposite-spin electron pair correlations, which are given as $F_{\uparrow\downarrow}(\boldsymbol{k}, t) = \langle c_{k\uparrow}^\dagger(t) c_{-k\downarrow}^\dagger(0)\rangle$. We note that this quantity can

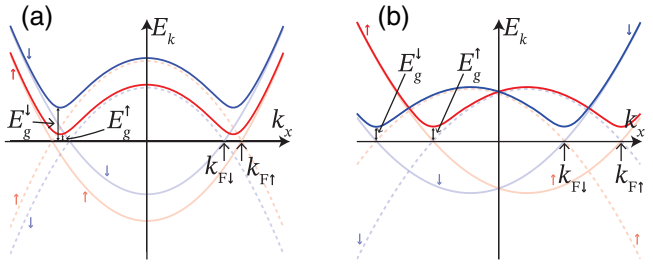


FIG. 3. The band structure of a superconductor with (a) a Zeeman field and (b) SOC of the form $H_{SO} = \alpha k_x \sigma_z$. $E_g^s$ indicates the superconducting gap of the two branches. The faint, solid (dashed) lines represent the normal-state electron (hole) band structures of the two spins. The arrow accompanying each band indicates its spin index.

represent a scattering process between a spin-down hole and a spin-up electron and therefore involves no exchange of spin. This is because $c_{-k\downarrow}^\dagger$ creates a spin-down electron, which is equivalent to the removal of a spin-up hole.

A similar analysis applies to $F_{\downarrow\uparrow}(\boldsymbol{k}, t) = \langle c_{k\downarrow}^\dagger(t) c_{-k\uparrow}^\dagger(0)\rangle$, which now involves spin-down particles. The Zeeman field changes the relative size of the pair correlations. The superconducting correlations have to be antisymmetric under the combined interchange of spin, momentum, band, and time indices, a relationship known as the SPOT rule (Berezinskii, 1974; Linder and Balatsky, 2019). The singlet pairing (odd in spin index) $F_s \propto F_{\uparrow\downarrow} - F_{\downarrow\uparrow}$ is the most conventional form of superconductivity and is typically $s$ wave (even parity), single band (even in band index), and even frequency (even in time index). However, since $F_{\uparrow\downarrow}$ and $F_{\downarrow\uparrow}$ now are different, one obtains a triplet component $F_t \propto F_{\uparrow\downarrow} + F_{\downarrow\uparrow}$. Since we have no $k$ dependence in either the order parameter or the Zeeman field, we typically get $s$-wave correlations, meaning that the triplets must be odd frequency. Hence, we derive $F_{s\bar{s}} = -s\Delta/[(i\omega + sh)^2 - \xi_k^2 - |\Delta|^2]$, with $\bar{s} = -s$, from which we see that $F_t \propto ih\omega$, which is odd when $\omega \to -\omega$.

In the model considered here, even-frequency triplets require oppositely aligned spins with mismatched momenta so that an odd-parity component appears. This is possible in the presence of a Zeeman field and a spatially modulated superconducting order parameter. This is the FFLO phase (Fulde and Ferrell, 1964; Larkin and Ovchinnikov, 1964), which has not been observed experimentally in the bulk. Such triplets are more readily obtained by considering a spin splitting of the form $\boldsymbol{h} = h_0 k_x \hat{\boldsymbol{z}}$, i.e., a form of SOC. The normal-state dispersions are shown in Fig. 3(b), plotted along $k_x$. There is a relative horizontal shift of the energy bands of the two spins, meaning that spin-up particles on average have a positive momentum along $k_x$, while spin-down particles have a negative momentum. Hence, even in the absence of **M** there is an equilibrium spin current [including in the normal state (Rashba, 2003; Sonin, 2007, 2010; Tokatly, 2008; Droghetti *et al.*, 2022)]. The momentum shift of the normal-state dispersions leads to a similar relative momentum shift in the pair correlations $F_{s\bar{s}} = -s\Delta/[(i\omega)^2 - (\xi_k - sh_0 k_x)^2 - |\Delta|^2]$ that gives rise to $p_x$-wave triplets $F_t \propto h_0 k_x$.

When $F_{\uparrow\downarrow} \neq F_{\downarrow\uparrow}$, it means that one spin species has a greater hybridization with their corresponding hole branch

than the other. In other words, we have spin-dependent scattering processes in the electron-hole sector and hence might expect an observable **M** to appear. However, to obtain **M** it is a requirement that the relative phase difference between the singlet and the triplet differs from $\pi/2$; otherwise, $F_{\uparrow\downarrow} \propto |F_s| + i|F_t|$ and $F_{\downarrow\uparrow} \propto |F_s| - i|F_t|$ remain equal in magnitude (Linder, Amundsen, and Risinggård, 2017). For the Zeeman field, the odd-frequency triplets indeed incur such a phase shift of $\pi/2$, and therefore do not directly contribute to **M**. However, the even-frequency triplets are not phase shifted relative to the singlet correlations. This produces a superconducting contribution to the spin currents since $F_{\uparrow\downarrow} \propto |F_s| + |F_t|$ for $k_x > 0$, $F_{\uparrow\downarrow} \propto |F_s| - |F_t|$ for $k_x < 0$, and the converse for $F_{\downarrow\uparrow}$. In other words, there is preferential particle-hole scattering of one spin species for $k_x > 0$, and for the other spin species for $k_x < 0$.

### 2. Superconducting proximity effect

The superconducting proximity effect in a metallic material is enabled by the process of Andreev reflection (Žutić, Fabian, and Das Sarma, 2004; Buzdin, 2005; Deutscher, 2005; Eschrig, 2018). In this process, an incoming electron from the metallic side enters the superconducting material, crosses the quasiparticle branch when it has penetrated far enough that its energy equals the local value of the superconducting gap, and then travels back as a holelike excitation that enters the normal metal. In the process of the incident electron crossing branch, a total charge of $-2e$ is transferred to the superconducting condensate, thereby resulting in the creation of a Cooper pair. On the normal-metal side, the incoming electron becomes correlated to the hole that tunnels back into the normal metal, thus creating a superconducting phase coherence that extends a long distance.

Before we discuss how SOC modifies the proximity effect, consider $F$ with the two bands split by an exchange field modeled by $H = \boldsymbol{h} \cdot \boldsymbol{\sigma}$, where $\boldsymbol{h}$ is the exchange field. This causes the superconducting proximity effect to behave qualitatively differently than with a normal metal (Bergeret, Volkov, and Efetov, 2001, 2005; Kadigrobov, Shekhter, and Jonson, 2001; Buzdin, 2005). To begin, there will appear odd-frequency triplets due to the presence of superconducting correlations in a spin-split material. In addition, since the $S/F$ interface breaks translation invariance, momentum in the direction normal to the interface is not a good quantum number. This leads to mixing between odd- and even-parity pair correlations, and thus odd-parity, even-frequency triplets. Consider the wave vectors of an electron excitation with a given spin, such as spin up, and a hole excitation with the opposite spin at a given energy $\varepsilon$. The electron (hole) will have wave vectors $\pm k_\uparrow$ ($\mp k_\downarrow$). The mismatch $\Delta k = k_\uparrow - k_\downarrow$ between the electron and hole gives the Cooper pair wave function induced in $F$ a finite center-of-mass momentum even in the absence of any net current through the system. For this reason, the superconducting correlations will not only decay as one moves deeper into the $F$ region but also oscillate (Bergeret, Volkov, and Efetov, 2005; Buzdin, 2005). This is shown in Fig. 4. The decay is caused by the mismatch in wave vectors for the electrons and holes, causing a decoherence

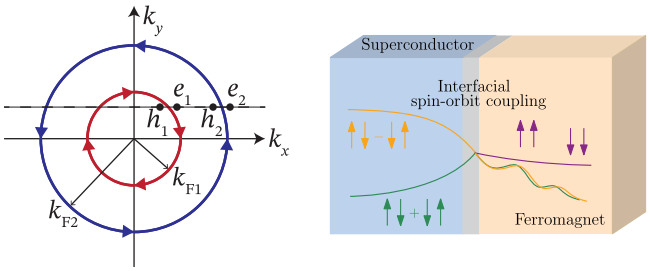


FIG. 4. Left panel: Rashba SOC in two dimensions. The outer blue and inner red bands have the opposite spins for a given angle in the $(k_x, k_y)$ plane. For an electron incident toward the interface with a direction away from the interface normal $(k_y \neq 0)$, Andreev reflection is possible via both interband and intraband scattering. Thus, the superconducting proximity becomes a mix of oscillatory and nonoscillatory terms inside the material with SOC. Right panel: by adding a heavy-metal (HM) layer with interfacial Rashba at the $S/F$ interface, the proximity effect for spins parallel to $M$ can be extended through the generation of $\uparrow\uparrow$ and $\downarrow\downarrow$ triplet pairs. Conversely, for spins perpendicular to **M** in $F$ the spin-zero singlet and spin-zero triplet pairs remain short range and oscillatory in $F$. The HM layer provides strong atomic SOC and SIA, which produces an effective Rashba SOC localized at the interface.

during propagation that reduces their correlation away from the interface.

We now discuss the superconductor proximity effect in hybrid structures with SOC (Reeg and Maslov, 2015). An important point that distinguishes the magnetic and SOC cases is that the dimensionality is important for the qualitative behavior of the proximity effect. Consider first the one-dimensional (1D) case, for example, $S$/nanowire with SOC. We can model an antisymmetric Rashba-like SOC via $H_{\mathrm{SO}} = \alpha \boldsymbol{g}_{\boldsymbol{k}} \cdot \boldsymbol{\sigma}$, where $\alpha$ is the magnitude of the SOC and $\boldsymbol{g}_{\boldsymbol{k}} = (0, 0, k_x)$ for a nanowire extending along the $x$ axis (Cayao and Black-Schaffer, 2018). We again consider an electron and a hole with opposite spins at an energy $\varepsilon$ in Fig. 3(b), as these are the excitations involved in the Andreev-reflection process inducing superconductivity in the SOC metal. The band structure in the SOC metal is now unlike that in the ferromagnetic case. By considering electrons and holes with opposite-spin labels, we see that such pairs have momenta $\pm k_{F\uparrow}$ or $\pm k_{F\downarrow}$, respectively. Therefore, there is no mismatch[1] in the momentum magnitude between the electrons and the Cooper pair wave function does not acquire any center-of-mass momentum. Thus, Andreev reflection involves only intraband (same band) excitations in the 1D case, and there is no oscillatory behavior of the superconducting correlations inside the SOC metal. In the diffusive limit, a decay length $\hbar/m\alpha$ of the triplet correlations in a SOC metal

[1]When the Andreev-reflection process involves quasiparticles with excitation energy $\varepsilon$, there is a small mismatch between the wave vectors due to different signs for $\varepsilon$ in the wave vector expression for electrons and holes. This mismatch also occurs in the normal-metal case and does not cause oscillations of the energy-integrated superconducting correlation function in the normal metal.

(Reeg and Maslov, 2015) can be compared to the decay length $\sqrt{D/h}$ of triplets in $F$.

The situation changes qualitatively when it goes into two dimensions. We can model a 2D system with Rashba SOC via the same $H_{\mathrm{SO}}$, but this time with a $\boldsymbol{g_k}$ vector that depends on both $k_x$ and $k_y$ for a system that lies in the $x$-$y$ plane such as a two-dimensional electron gas (2DEG). A Rashba-like SOC is described by $\boldsymbol{g_k} = (-k_y, k_x, 0)$ and gives rise to the band structure shown in Fig. 4.

As shown in Fig. 4, the Fermi surface consists of two circles where the spin expectation value of an excitation on one of the circles varies as the electron moves around the circle. Assume for simplicity that we are dealing with a ballistic SOC/$S$ structure such that translational invariance is maintained in the direction parallel to the interface. Momentum in this direction is conserved during the Andreev-reflection process (say, $k_y$ for a structure extending along the $x$ axis). Considering the case $k_y = 0$ first, we recover the 1D situation shown in Fig. 3(b). But for $k_y \neq 0$ (the dashed black line in the left panel of Fig. 4), the proximity effect changes its nature. Since the Fermi surfaces do not have a definite spin, an electron on the outer blue circle ($e_2$) can be Andreev reflected as a hole on both the outer blue ($h_2$) and inner red ($h_1$) Fermi surfaces. Both of these holes carry some weight of the opposite spin to the $e_2$ electron when $k_y \neq 0$, whereas only a hole on the same Fermi surface has the opposite spin when $k_y = 0$. As a result, both intraband and interband Andreev scattering are possible. The intraband scattering gives rise to a nonoscillatory superconducting correlation decaying inside the SOC metal, like in the 1D case. But the interband Andreev scattering is seen to feature a momentum magnitude mismatch between the electron and holes involved: $k_{F1} - k_{F2}$. Thus, for interband Andreev scattering we return to a similar situation as in the ferromagnetic case, where the induced superconducting correlations oscillate. The superconducting proximity effect in a SOC metal consists of both oscillatory and nonoscillatory terms, in contrast to both the ferromagnetic and 1D SOC metal cases. Odd-frequency triplet superconductivity due to SOC has also been studied in topological insulators (Cayao and Black-Schaffer, 2017; Cayao *et al.*, 2022).

Cooper pairs consisting of electrons with spins that are collinear with $\mathbf{M}$ in $F$ penetrate a long distance. This is because there is no longer any momentum mismatch between such electrons, as both belong to the same spin-polarized Fermi surface. This long-range superconducting proximity effect in $F$ can be achieved by incorporating SOC, for example, by adding (1) an interfacial heavy-metal (HM) layer, thereby causing SOC scattering, or (2) $F$ with intrinsic SOC. Case (1) is illustrated in Fig. 4, where spin-dependent scattering at the interface due to the HM layer creates long-range triplet pairs in $F$. Such pairs can survive $\sim$1 μm, even in strongly polarized $F$ (Keizer *et al.*, 2006). The number density of triplet pairs created in this way depends on the direction of $\mathbf{M}$ in the $F$ layer (Jacobsen, Ouassou, and Linder, 2015). In case (2), long-range triplet pairs are also created via the following two physical mechanisms (Bergeret and Tokatly, 2013): spin precession induced by the SOC and anisotropic spin relaxation. One can map the diffusive-limit equation of motion for the anomalous Green's functions (describing the Cooper pairs), known as the Usadel equation, to the spin-diffusion equation of Bergeret and Tokatly (2014). This analogy is useful since it shows that the different triplet Cooper pair components behave similarly to the spin components of an electron in a diffusive metal with SOC. Finally, there is an interplay between the spin and orbital degrees of freedom even in the absence of SOC when a $F$ couples to an intrinsic triplet $S$ (Gentile *et al.*, 2013).

### 3. Ginzburg-Landau formalism

The Ginzburg-Landau formalism is a symmetry-based method to explore the behavior of superconducting systems (Ginzburg and Landau, 1950). It involves expanding the free energy in the complex superconducting order parameter $\psi$, thereby indicating the strength of the superconductivity, and is valid close to the superconducting transition temperature ($T_c$). The method is highly successful and consistent with BCS theory (Gor'kov, 1959). Since $\psi$ describes singlet superconductivity, this approach cannot be used to obtain information about the triplet correlations and thus is of limited use in making predictions relevant for superconducting spintronics, such as the generation of long-range triplets. Nevertheless, it is still possible to indirectly extract some information about spin-dependent phenomena (through their influence on $\psi$). A prominent example of this is the inclusion of a Rashba-type SOC and an exchange field $\boldsymbol{h}$, in which case the free energy density is given as (Edelstein, 1996; Samokhin, 2004; Kaur, Agterberg, and Sigrist, 2005)

$$f(\boldsymbol{r}) = a|\psi(\boldsymbol{r})|^2 + \gamma|\tilde{\boldsymbol{\nabla}}\psi(\boldsymbol{r})|^2 + \frac{b}{2}|\psi(\boldsymbol{r})|^4 + \frac{\boldsymbol{B}^2}{2\mu_0} - i\alpha(\boldsymbol{r})(\boldsymbol{n}\times\boldsymbol{h})\{\psi^*(\boldsymbol{r})\tilde{\boldsymbol{\nabla}}\psi(\boldsymbol{r}) - \psi(\boldsymbol{r})[\tilde{\boldsymbol{\nabla}}\psi(\boldsymbol{r})]^*\}, \quad (8)$$

where $\tilde{\boldsymbol{\nabla}} = \boldsymbol{\nabla} - (2ie/\hbar)\boldsymbol{A}$ and $\boldsymbol{B} = \boldsymbol{\nabla}\times\boldsymbol{A}$. Furthermore, $a$, $b$, and $\gamma$ are phenomenological parameters, $\boldsymbol{n}$ is the unit vector along the direction of broken inversion symmetry, and $\alpha$ characterizes the SOC magnitude (in general, it can have a nonlinear dependence on the atomic SOC strength). Applying Eq. (8) to a Josephson weak link, a nonzero phase difference appears between the superconducting banks (Buzdin, 2008). This is seen when one minimizes Eq. (8) with respect to $\psi$ and $\boldsymbol{A}$, giving the Euler-Lagrange equation

$$a\psi - \gamma\tilde{\boldsymbol{\nabla}}^2\psi + b\psi|\psi|^2 - 2i\alpha(\boldsymbol{n}\times\boldsymbol{h})\cdot\tilde{\boldsymbol{\nabla}}\psi = 0, \quad (9)$$

$$\boldsymbol{j} = \frac{4e\gamma}{\hbar}\Im(\psi^*\boldsymbol{\nabla}\psi) - \left(\frac{8e^2\gamma}{\hbar^2}\boldsymbol{A} + \frac{4e\alpha}{\hbar}(\boldsymbol{n}\times\boldsymbol{h})\right)|\psi|^2. \quad (10)$$

To derive Eqs. (9) and (10) for $\psi$ microscopically, one can derive the quasiclassical Eilenberger equation (discussed later), find the solution for the anomalous Green's function perturbatively in orders of $\Delta$, and then insert this solution into the self-consistent gap equation. Equation (9) can be solved in the normal metal, where $\psi$ is a small pair correlation due to its proximity to the superconductors. When the higher-order nonlinear term is neglected at $\boldsymbol{B} = \boldsymbol{0}$ in one dimension with the exchange field in the $z$ direction, $\psi(x) = |\Delta|e^{i\alpha h x/\gamma}[e^{i\phi_R}\sinh\kappa(x+L/2) - e^{i\phi_L}\sinh\kappa(x-L/2)]/\sinh\kappa L$,

with $\kappa^2 = a/\gamma - \alpha^2 h^2/\gamma^2$ and $\phi_{R/L} = \mp(\phi - \alpha h L/\gamma)/2$. Transparent boundary conditions have been assumed, i.e., $\psi(\pm L/2) = |\Delta| e^{i\phi_{R/L}}$, where $|\Delta|$ and $\phi$ are the absolute value of the superconducting gap, assumed to be equal in the two superconductors, and its phase, respectively. Inserting $\psi(x)$ into Eq. (10), one finds the current-phase relation

$$j = j_c \sin(\phi - \phi_0), \tag{11}$$

where $j_c = \kappa|\Delta|^2/\sinh \kappa L$ and $\phi_0 = \alpha h L/\gamma$. The SOC has introduced a phase shift into the conventional Josephson current. This is further discussed later in this Colloquium.

Equation (10) also reveals spontaneous edge currents in $S/F$ structures, as noted by Mironov and Buzdin (2017). If the interfacial SOC is substantial, $\boldsymbol{j}$ may be nonzero even if the orbital effect is negligible ($\boldsymbol{A} = \boldsymbol{0}$) and $\psi$ is uniform. In this case, $\boldsymbol{j}$ is directed along $\boldsymbol{n} \times \boldsymbol{h}$ parallel to the interface. This has interesting applications, such as in a superconducting loop near a ferromagnetic insulator. Circulating spontaneous supercurrents have been predicted (Robinson, Samokhvalov, and Buzdin, 2019) that may find use in single flux quantum logic, similar to proposals involving $\pi$ junctions (Feofanov *et al.*, 2010). Superconducting vortices generated by these spontaneous currents without an applied external magnetic field have also been predicted at $S/F$ interfaces (Olthof *et al.*, 2019).

#### 4. Bogoliubov–de Gennes method

In the following, we consider a superconducting system within the mean-field approximation. This can be described by a Hamiltonian of the form

$$H = \sum_{ss'} \int d\boldsymbol{r}\, \psi_s^\dagger(\boldsymbol{r}) h_{ss'}(\boldsymbol{r}) \psi_{s'}(\boldsymbol{r}) + \tfrac{1}{2} \int d\boldsymbol{r} [\Delta(\boldsymbol{r}) \psi_\uparrow^\dagger(\boldsymbol{r}) \psi_\downarrow^\dagger(\boldsymbol{r}) + \Delta^*(\boldsymbol{r}) \psi_\downarrow(\boldsymbol{r}) \psi_\uparrow(\boldsymbol{r})], \tag{12}$$

where $\psi_s(\boldsymbol{r})$ is the field operator for an electron with spin $s$, $h$ is the single particle Hamiltonian containing SOC (Simensen and Linder, 2018), and in a homogeneous system $\Delta$ is the $s$-wave superconducting gap. The presence of $\Delta$ introduces the added complication that the electron and hole bands hybridize, described by the Nambu basis $\Psi(\boldsymbol{r}) = (\psi_\uparrow(\boldsymbol{r})\, \psi_\downarrow(\boldsymbol{r})\, \psi_\uparrow^\dagger(\boldsymbol{r})\, \psi_\downarrow^\dagger(\boldsymbol{r}))^T$, in which case Eq. (12) can be written as

$$H = H_0 + \tfrac{1}{2} \int d\boldsymbol{r}\, \Psi^\dagger(\boldsymbol{r}) \hat{H} \Psi(\boldsymbol{r}), \tag{13}$$

where $H_0$ describes a trivial energy shift and

$$\hat{H} = \begin{pmatrix} h & \Delta i\sigma_y \\ -\Delta^* i\sigma_y & -h^* \end{pmatrix}. \tag{14}$$

The diagonalization of Eq. (14) is referred to as the Bogoliubov–de Gennes method (de Gennes, 1999), in which the quasiparticles (the eigenvalues) become a mixture of particles and holes.

Generally two approaches are used when studying superconducting hybrid structures using the Bogoliubov–de Gennes method. A continuum formulation may be used, in which case the scattering at interfaces between materials is taken into account via generalizing the Griffin-Demers or Blonder-Tinkham-Klapwijk (BTK) formalism (Griffin and Demers, 1971; Blonder, Tinkham, and Klapwijk, 1982). This entails matching the wave functions obtained from Eq. (13) in adjacent materials at every interface and includes both normal reflection and tunneling processes, as well as Andreev reflection of opposite or equal spins (Žutić and Das Sarma, 1999). While the BTK formalism assumes a step-function profile for the pair potential, the continuum formulation can also be solved self-consistently (Halterman, Valls, and Wu, 2015; Wu *et al.*, 2018; Setiawan, Wu, and Levin, 2019; Valls, 2022).

The other way of applying the Bogoliubov–de Gennes method is in a tight-binding approach on a lattice (Zhu, 2016). It is appropriate when one wants to study the equilibrium properties of superconducting systems, for instance, the superconducting pair correlation in hybrid structures due to the proximity effect. The Hamiltonian then becomes a discrete $4N \times 4N$ matrix, where $N$ is the number of lattice sites. An advantage of the Bogoliubov–de Gennes method is its conceptual simplicity, the drawback being the limitation in system size that is manageable computationally. It is a microscopic theory valid at arbitrary temperature.

#### 5. Quasiclassical theory

The Green's function method is a powerful tool to describe condensed matter systems. Here we review the Keldysh technique, which is applicable to equilibrium and nonequilibrium systems. For an in-depth discussion, see Rammer and Smith (1986). In many systems there is a dominating energy scale, such as the Fermi energy $E_F$ in metals, such that all other contributions to the Hamiltonian may be considered small in comparison. In that case, and for metals, in particular, the relevant contribution to several physical quantities of interest comes from near the Fermi level (referred to as the low-energy region). The Gor'kov equations, however, contain information about the entire spectrum. The quasiclassical approximation simplifies these equations by retaining only their low-energy component, i.e., terms that are at most linear in $\Xi/E_F$, where $\Xi$ is any of the energy or self-energy scales involved: $\Xi \in \{|\Delta|, |\boldsymbol{h}|, \alpha, \ldots\}$ (Serene and Rainer, 1983; Rammer and Smith, 1986; Millis, Rainer, and Sauls, 1988; Belzig *et al.*, 1999; Chandrasekhar, 2004).

The quasiclassical theory for SOC was established by Vorontsov, Vekhter, and Eschrig (2008), Gorini *et al.* (2010), Eschrig, Iniotakis, and Tanaka (2012), and Raimondi *et al.* (2012). Linear-in-momentum models of SOC such as the Rashba and Dresselhaus models may be introduced by an effective SU(2) gauge field, for which the derivative operator may be replaced by its gauge covariant equivalent. Within the quasiclassical approximation, it is given as $\tilde{\nabla} \bullet = \nabla \bullet - (ie/\hbar)[\boldsymbol{A}, \bullet]$, when acting on a $2 \times 2$ Green's function matrix $\bullet$ in spin space, where $A_k = A_{0,k}\sigma_0 + \alpha_{klm}\sigma_l k_m$, with $A_{0,k}$ a scalar gauge field stemming from a potential external magnetic field, and $\alpha_{klm}$ is a generic tensor describing

the SOC. For ballistic systems, the SOC has the form of a momentum-dependent exchange field, which is intuitively reasonable, and has interesting consequences in ballistic Josephson weak links (Konschelle, Tokatly, and Bergeret, 2016).

The quasiclassical approximation of the Gor'kov equation of motion for the Green's function of a ballistic system is the Eilenberger equation (Eilenberger, 1968), which takes the form

$$\hbar \boldsymbol{v}_{\mathrm{F}} \cdot \tilde{\boldsymbol{\nabla}} \check{g} + i[\varepsilon \check{\tau}_z + \check{\Sigma}, \check{g}] = 0 \tag{15}$$

to lowest order, where the quasiparticle energy $\varepsilon$ is the Fourier conjugate to $t - t'$ assuming a stationary system, $\boldsymbol{v}_{\mathrm{F}}$ is the Fermi velocity, and $\check{\Sigma}$ contains the self-energies and molecular fields acting on the itinerant electrons (such as a Zeeman field) under study. Furthermore, a caron denotes an $8 \times 8$ matrix in Nambu-Keldysh space and $\check{g} = (i/\pi) \int d\xi \check{G}$ is the quasiclassical Green's function, with $\xi = \hbar^2 \boldsymbol{k}^2/2m - \mu$. The uniqueness of Eq. (15) is assured by the accompanying constraint $(\check{g})^2 = \hat{I}$, with $\hat{I}$ the $4 \times 4$ identity matrix (Shelankov, 1985).

A high concentration of impurities may also be treated within the quasiclassical approximation, using conventional impurity averaging techniques (Abrikosov, Gor'kov, and Dzyaloshinski, 1975). This has the effect that quasiparticle motion takes the form of a random walk due to frequent impurity scatterings, so that momentum-dependent effects are strongly suppressed. The equation of motion then becomes

$$D \tilde{\boldsymbol{\nabla}} \cdot \check{g} \tilde{\boldsymbol{\nabla}} \check{g} + i[\varepsilon \check{\tau}_z + \check{\Sigma}_{\mathrm{diff}} + \boldsymbol{h} \cdot \check{\boldsymbol{\sigma}}, \check{g}] = 0, \tag{16}$$

where $D$ is the diffusion constant. The self-energy term $\check{\Sigma}_{\mathrm{diff}}$ differs from $\check{\Sigma}$ in Eq. (15) in that the nonmagnetic impurity potential that appears in the latter in a diffusive system has been averaged out. We have also separated a potential exchange (or Zeeman) field $\boldsymbol{h}$ from $\check{\Sigma}_{\mathrm{diff}}$, as such a field is typically necessary to obtain spin-dependent effects due to the lowest-order contribution from SOC in the diffusive limit. Equation (16) takes the form of a diffusion equation, and a net particle current, representing a drift in the random walk, may be identified by Fick's first law: $\check{\boldsymbol{j}} = -D\check{g}\tilde{\boldsymbol{\nabla}}\check{g}$. This drift has a profound effect on diffusive systems: impurity scattering becomes anisotropic and gives rise to momentum-dependent effects that cancel out in an isotropic system.

Information about the superconducting correlations is found in the anomalous Green's function $f$. They are off-diagonal $2 \times 2$ blocks extracted from $\check{g}$; see Belzig *et al.* (1999) for a more detailed discussion. The effect of SOC on diffusive superconducting hybrid structures (Bergeret and Tokatly, 2013; Bergeret and Tokatly, 2014) is most evident in the limit where the proximity effect is weak, so $f$ is small. By parametrizing into singlet $f_s$ and triplet $\boldsymbol{f}$ components using the $d$ vector notation (Leggett, 1975) $f = (f_s + \boldsymbol{f} \cdot \boldsymbol{\sigma}) i\sigma_y$, one finds that for Rashba SOC $\boldsymbol{A} = \alpha \boldsymbol{n} \cdot (\boldsymbol{\nabla} \times \boldsymbol{\sigma})$, where $\boldsymbol{n}$ is a unit vector pointing in the direction of symmetry breaking, the Usadel equation becomes $D\boldsymbol{\nabla}^2 f_s + 2i\varepsilon f_s + 2i\boldsymbol{h} \cdot \boldsymbol{f} = 0$ and $D\nabla^2 \boldsymbol{f} + 4iD\alpha[\boldsymbol{n} \times (\nabla \times \boldsymbol{f}) - \nabla \times (\boldsymbol{n} \times \boldsymbol{f})] + (2i\varepsilon - 4D\alpha^2)\boldsymbol{f} + 2i\boldsymbol{h} f_s = 0$. A similar set of equations may be derived for the linear Dresselhaus model. Inspection of these equations reveals that the singlet superconducting correlation is independent of the SOC to this level of accuracy, which is reasonable, as it is independent of spin. The triplets, however, are influenced. The term proportional to $\alpha^2$ in the previous equation is also present in homogeneous systems and is a consequence of the frequent impurity scatterings in the diffusive limit. As momentum direction is averaged out by these scattering processes, so too is the spin direction (because of the SOC). This is an effect akin to the D'yakonov-Perel' spin relaxation (D'yakonov and Perel', 1971a) and leads to an increased decay of the triplet superconducting correlations. The terms proportional to $\alpha$ represent a precession of the pair correlation spins, resulting in a mixture of the triplet components. This observation, along with the experimental accessibility of the diffusive limit, has led to these systems receiving significant attention (Alidoust and Halterman, 2015a, 2015b; Jacobsen, Ouassou, and Linder, 2015; Jacobsen, Kulagina, and Linder, 2016; Amundsen and Linder, 2017). The formalism has also been extended to incorporate magnetoelectric effects and particle-hole asymmetry (Konschelle, Tokatly, and Bergeret, 2015; Bobkova and Bobkov, 2017; Silaev, Tokatly, and Bergeret, 2017; Tokatly, 2017; Virtanen, Bergeret, and Tokatly, 2022), as well as extrinsic SOC, i.e., as induced by impurities (Bergeret and Tokatly, 2016; Huang, Tokatly, and Bergeret, 2018; Virtanen, Bergeret, and Tokatly, 2021). This extension allows for the description of additional physical effects such as anomalous Josephson currents and spin Hall effects in the superconducting state. Recent works reconciled the nonlinear quasiclassical equations including SOC with a normalized Green's function (Virtanen, Bergeret, and Tokatly, 2021, 2022) and also expanded the theory to include boundary conditions describing interfacial SOC (Amundsen and Linder, 2019), thereby giving rise to a supercurrent spin Hall effect (Linder and Amundsen, 2022).

## III. EXPERIMENTAL TECHNIQUES

Here we provide some intuitive guidelines on designing experiments to investigate $S/F$ proximity effects in the context of SOC-driven triplet pair formation. Although the techniques are similar to standard $S/F$ proximity effects, we highlight, where appropriate, the expected differences in the outcomes when one considers the triplet pair formation due to SOC.

### A. Transition temperature measurements

Measuring $T_c$ of a thin film $S$ proximity coupled to $F$ layers is a common method of exploring $S/F$ structures. The $S/F$ proximity depends on the depairing effect of the magnetic exchange field on the Cooper pairs and/or the generation of triplet pairs affecting the singlet pairing amplitude in $S$.

The majority of $T_c$ measurements are carried out on unpatterned thin films using a four-point current-bias technique. A low bias current is used to avoid current-induced nonequilibrium shifts in $T_c$. To control the magnetic state of the $F$ layer(s), magnetic fields are applied that are negligible relative to the upper critical field of the $S$ layer. There is an orbital depairing effect from the applied magnetic field that can suppress $T_c$ and must be accounted for during the analyses

of the proximity effect. This is usually not a problem for IP magnetic fields as the coercive fields of transition metal $F$'s are small relative to the IP upper critical field of the $S$ layer. However, the situation is more complex for OOP magnetic fields, where the coercive fields of $F$ layers tend to be large and are often comparable to or greater than the magnetic field required to nucleate superconducting vortices. Further complication arises from the dipolar fields injected into $S$ from magnetic domain walls. These factors should be considered during the analyses of the results and often requires control samples including isolated $S$ films and $S/F$ structures with insulating barriers to break the proximity effect between the $S$ and $F$ layers (Singh *et al.*, 2015; Banerjee *et al.*, 2018).

Careful consideration is required when selecting the $F$ material. For $S/F/F'$ or $F/S/F'$ spin valves, the key challenge is to obtain stable parallel, antiparallel, or noncollinear magnetic states over a range of reasonable magnetic fields. Here $F$ and $F'$ refer to two distinct $F$ layers with sufficiently different coercive fields. This requires specific anisotropies, e.g., Co/Ni multilayers (Satchell, Loloee, and Birge, 2019), or a large OOP field to be applied to reorient one $F$ layer (e.g., Ni) (Singh *et al.*, 2015).

### B. Josephson junctions

JJs with $F$ barriers have been key to demonstrating triplet creation, with one of the first experiments detecting supercurrents through the highly spin-polarized half-metallic $CrO_2$ (Keizer *et al.*, 2006). The absence of minority spin states in $CrO_2$ means that any supercurrent flowing through it must be mediated by the spin-charge triplet current; however, magnetic control of singlets to triplet pair formation was found to be challenging and highly irreproducible. Since then, advances in triplet supercurrent transport in JJs have been made, as discussed in Sec. IV.E.

Owing to the small electrical resistance of metallic $S/F$ heterostructures, nanopatterning is required for straightforward measurements of device voltage, such as in JJs. For JJs with magnetic barriers, a further advantage of nanopatterning is that the $F$ layers can be magnetically single domain, meaning that even at high applied magnetic fields, the barrier flux can be small relative to a flux quanta. This allows the magnetic state of the barrier to be manipulated without a significant lowering of the JJ critical current. The presence of a barrier magnetic moment adds to the magnetic flux from the external magnetic field and can distort the magnetic field dependence of the Josephson critical current. A further complication in nanopatterned JJs is that dipolar fields from the $F$ layers can distort the single domain state, introducing additional complex nanomagnetic states. These issues need careful consideration when one designs JJs with magnetic barriers (Blamire *et al.*, 2013).

Optical or electron beam lithography techniques are routinely used for fabricating $S/F$ devices, including JJs. These techniques were described by Blamire, Aziz, and Robinson (2011).

### C. Magnetization dynamics

An injected normal-state current from a thin film $F$ into a $S$ in $S/F$ structures can introduce a nonequilibrium quasiparticle spin accumulation with relaxation lengths much larger than in normal metals (Yang *et al.*, 2010), differing also from the charge relaxation length (Hübler *et al.*, 2012; Quay *et al.*, 2013). This has been explained by the Zeeman splitting of the quasiparticle bands, combined with an energy imbalance (Bobkova and Bobkov, 2015; Silaev *et al.*, 2015; Bergeret *et al.*, 2018). Alternatively, when one follows the original experiment on spin dynamics of ferromagnets in proximity to superconductors (Bell *et al.*, 2008), it may be possible to create a superconducting spin current in the $S$ layer mediated via triplet pairs (Jeon, Ciccarelli *et al.*, 2019). This experiment involved spin pumping from a layer of NiFe [permalloy (Py)] in a Pt/Nb/Py/Nb/Pt structure. Here the effective Gilbert damping $\alpha$, which is proportional to the spin-current density, of the precessing $\mathbf{M}$ of Py increased below $T_c$, indicating an enhancement of the spin current above the normal state that differs from the spin pumping via the Andreev bound states (Yao *et al.*, 2021).

Spin pumping in $S/F$ structures can be performed using broadband ferromagnetic resonance (FMR). For FMR experiments on $S/F/S$ structures, the $S$ layer thickness should be below the magnetic penetration depth (∼100 nm for Nb); otherwise, the dc-resonance field shifts to lower values (Li *et al.*, 2018; Jeon *et al.*, 2019; Golovchanskiy *et al.*, 2020). Jeon *et al.* (2019) attributed this to Meissner screening fields generated in the $S$ layer. An alternative explanation by Silaev (2022) suggested that a gap is spontaneously induced in the magnon spectrum through the Anderson-Higgs mechanism, causing a shift in the dc-resonance field of a $S/F/S$ structure.

### D. Spectroscopic techniques

The nature of a triplet induced in a $F$, $S$, or normal-metal ($N$) layer is theoretically different from the usually dominant singlet state. Although odd-frequency triplet and singlet states share the common feature of an $s$-wave order parameter, unlike the singlet state the orbital and spin components of the triplet state are even with respect to the electron exchange, and this implies that their correlation function must be odd in frequency or, equivalently, odd under exchange of the time coordinates (Bergeret, Volkov, and Efetov, 2001; Linder and Balatsky, 2019). Consequently, an odd-frequency triplet state can enhance the quasiparticle density of states (DOS) and conductance of a $S/F$ bilayer (Petrashov *et al.*, 1999; Kontos *et al.*, 2002). This can be shown by considering the Green's function for an odd-frequency superconductor at small energies, where it looks like a normal metal with an effective mass renormalization (increase), thereby enhancing the DOS (Linder and Balatsky, 2019). For a singlet state, there is no enhancement in the DOS, so the observation of a conductance peak around zero voltage is an indication of odd-frequency superconductivity. This quantized peak was predicted as a signature of Majorana zero modes (see Sec. IV.A) (Sengupta *et al.*, 2001), but alternative explanations are possible (Das Sarma and Pan, 2021; Yu *et al.*, 2021).

The standard technique to probe the induced superconducting DOS involves tunnel junctions or scanning tunneling microscopy measurements of the current-voltage ($I$-$V$) characteristics. Below $T_c$, the $I$-$V$ characteristics are nonlinear at voltages near the gap edge. For $S$/insulator/$N$ junctions, that

is around $V = \pm\Delta/e$, where $e$ is the electron charge and $\Delta$ is the energy gap. Such measurements can provide high-resolution spectroscopic information because $dI/dV$ is proportional to the quasiparticle excitations, i.e., to the superconducting DOS. Tunneling studies have been extensively used to probe the singlet state (SanGiorgio *et al.*, 2008; Boden, Pratt, and Birge, 2011) and the triplet state (Kalcheim *et al.*, 2012, 2014, 2015) in different $S/F$ structures.

### E. Low-energy muon spin rotation technique

Low-energy muon spin rotation (LE-$\mu$SR) has been used to probe the depth dependence of superconductivity and magnetism in $S/F$ structures. LE-$\mu$SR offers a high sensitivity to magnetic fluctuations and spontaneous fields $< 0.1$ G with a depth-resolved sensitivity of a few nanometers (Flokstra *et al.*, 2014; Di Bernardo *et al.*, 2015; Fittipaldi *et al.*, 2021).

Muons are spin-half elementary particles with a charge matching an electron but over 200 times heavier. Implanted muons can provide detailed information about their local magnetic environment within a material (Hillier *et al.*, 2022), so the muon spin rotation technique is a sensitive tool for probing subsurface superconductivity in the Meissner state. Spin-polarized positive muons $\mu^+$ are generated from $\pi^+$ decay and are moderated by passing them through a cryosolid, typically Ar, to obtain $\mu^+$ in the low-energy range ($\sim$15 eV). These $\mu^+$ are accelerated by an adjustable sample bias that tunes their energies from 0.5 to 30 keV for their precise implantation depth within a material. The spins of the implanted $\mu^+$ precess about a local magnetic field and a decaying $\mu^+$ emits a positron in the direction of the $\mu^+$ spin. This decay of the positron intensity is measured as a difference in the number of counts by two detectors placed near the sample.

To study the Meissner state of the $S$ or $S/F$ structure, a magnetic field $B_{\mathrm{ext}}$ is applied parallel to the sample plane and perpendicular to the initial spin polarization of the $\mu^+$ beam. This induces a precession of the $\mu^+$ spins at an average frequency of $\bar{\omega}_s = \gamma_\mu \bar{B}_{\mathrm{loc}}$, where $\bar{B}_{\mathrm{loc}}$ is the average local field experienced by the implanted muons and $\gamma_\mu = 2\pi \times 135.5\ \mathrm{MHz\,T^{-1}}$ is the gyromagnetic ratio of $\mu^+$. If the stopping distribution is $p(z, E)$ at a depth $z$ and energy $E$ of the implanted muons, then the precession frequency is $\bar{\omega}_s = \gamma_\mu \int B_{\mathrm{loc}}(z) p(z, E) dz$. The asymmetry spectrum $A_s(t, E)$, which measures the normalized difference in the counts of the left and right detectors, is proportional to $e^{-\bar{\lambda}t}[\cos \gamma_\mu \bar{B}_{\mathrm{loc}} t + \phi_0 t]$ for a given implantation energy $E$. Here $\bar{\lambda}$ is the mean muon depolarization rate and $\phi_0 E$ is the starting phase of the muon precession. A series of mean-field values $\bar{B}_{\mathrm{loc}}$ is determined from the asymmetry fits as a function of the muon implantation energy $E$, which provides the final $B_{\mathrm{loc}}(z)$ profile inside the sample.

In the context of $S/F$ proximity effects and triplet pairs, this technique was used to detect a paramagnetic Meissner effect in Au/Ho/Nb (Di Bernardo *et al.*, 2015), enhanced flux expulsion in Cu/Nb/Co (Flokstra *et al.*, 2018), remotely induced magnetism in a normal metal in a superconducting spin valve structure (Flokstra *et al.*, 2016) and Au/$C_{60}$/Cu/$C_{60}$/Nb (Rogers *et al.*, 2021) structures, observed as a local enhancement of the magnetic field in Au above the externally applied field, in contrast to the well-known Meissner effect in the superconducting state. In the presence of SOC, the Meissner response has been predicted to be tunable from paramagnetic to diamagnetic (Espedal, Yokoyama, and Linder, 2016).

## IV. RECENT DEVELOPMENTS

In this section we sumarize the recent theoretical and experimental developments with a specific motivation to show how triplet pairing induced by SOC provides a common link to a wide range of phenomena: from Majorana zero modes to superconducting spintronics.

### A. Majorana zero modes

Majorana fermions are particles that have the peculiar property of being their own antiparticles. They are real solutions of the Dirac equation and represent a potential new, as of yet, undetected fundamental particle (Elliot and Franz, 2015). In condensed matter systems, predicted Majorana fermions are chargeless quasiparticle excitations (Aguado, 2017). This property makes superconductors ideal candidates to host such states, as the quasiparticles of superconducting systems (the bogoliubons) can consist of an equal mixture of electronlike and holelike excitations of the normal-state system, as discussed in Sec. II.D.4. However, these superconductors cannot be conventional with a spin-singlet configuration. Instead, topological superconductors are sought with equal-spin (also referred to as spinless) pairings that, as topological insulators, feature a band inversion and a nontrivial topology (Shen, 2012; Culcer *et al.*, 2020). Defects (such as vortices) and quasiparticles in topological superconductors or boundaries between topological and trivial regions can bind localized Majorana zero modes (MZMs) (Aasen *et al.*, 2016). These zero-energy (pinned at the Fermi level) topologically protected degenerate states, in which quantum information can be nonlocally stored, are separated by the topological gap from the excited states.

Much interest in MZMs comes from their exotic non-Abelian statistics (unlike the Majorana fermions in particle physics), which both is fundamentally interesting and offers a prospect for fault-tolerant topological quantum computing (Ivanov, 2001; Kitaev, 2003; Nayak *et al.*, 2008; Alicea *et al.*, 2011; Das Sarma, Freedman, and Nayak, 2015). An interchange of the position of two MZMs known as braiding yields a non-Abelian phase and transforms quantum states within a degenerate ground-state manifold. The result is a quantum gate that is topologically protected from local perturbations that limit conventional quantum computers (Lahtinen and Pachos, 2017). A complementary signature of the non-Abelian statistics comes from bringing together, or fusing, two MZMs that removes their degeneracy and yields either an ordinary fermion or a vacuum state (Cooper pair condensate) (Beenakker, 2020). Experimental reports of MZM detection remain under debate and do not include their non-Abelian statistics.

In one dimension, MZMs are found at the ends of the Kitaev chain with triplet $p$-wave superconductivity (Kitaev, 2001). In two dimensions, MZMs appear in $p_x \pm ip_y$

superconductors, as localized states bound to vortices, as well as distributed chiral edge states at interfaces (Read and Green, 2000). Higher-order topological superconductors analogous to their insulating counterparts (Benalcazar, Bernevig, and Hughes, 2017; Schindler, Cook *et al.*, 2018; Schindler *et al.*, 2018) can host MZMs on surfaces with a codimension larger than 1, for example, in the 0D corners of 2D systems, or 1D hinges of 3D systems.

There are materials believed to exhibit intrinsic topological superconductivity, such as $Sr_2RuO_4$ (Mackenzie and Maeno, 2003; Kallin, 2012), $UTe_2$ (Shishidou *et al.*, 2021), and $Cu_xBi_2Se_3$ (Kriener *et al.*, 2011; Sasaki *et al.*, 2011). However, challenges in relying on them are seen in the extensively studied $Sr_2RuO_4$. While doubts about the claimed $p_x \pm ip_y$ (Mackenzie and Maeno, 2003; Nelson *et al.*, 2004; Kallin, 2012) have been raised (Žutić and Mazin, 2005), experimental evidence against the $p$ wave (Petsch *et al.*, 2020) now involves even the discoverer of $Sr_2RuO_4$ (Maeno *et al.*, 1994).

An alternative to the elusive intrinsic $p$-wave superconductors is using the proximity-induced topological superconductivity. Chiral triplet superconducting correlations can be induced on the semimetallic surface states of a topological insulator near a conventional $s$-wave superconductor (Fu and Kane, 2008; Rosenbach *et al.*, 2021). The proximity-induced topological superconductivity is also predicted when the topological insulator is replaced by a semiconductor nanowire with strong Rashba SOC and a Zeeman field (Alicea, 2010; Lutchyn, Sau, and Das Sarma, 2010; Oreg, Refael, and von Oppen, 2010; Sau *et al.*, 2010; Brouwer *et al.*, 2011; Das *et al.*, 2012; Deng *et al.*, 2012; Mourik *et al.*, 2012; Rokhinson, Liu, and Furdyna, 2012). For orthogonal Rashba SOC and Zeeman fields (Figs. 3 and 4), the spin degeneracy at $k = 0$ is removed. The resulting spin canting and depletion of one spin support $p$-wave triplet topological superconductivity with the effective gap $\Delta_p(k) \propto \alpha k\Delta/2\sqrt{h^2 + \alpha^2 k^2}$ when $\mu$ is within the Zeeman gap $h$ (Lutchyn, Sau, and Das Sarma, 2010; Oreg, Refael, and von Oppen, 2010; Aguado, 2017).

With strong SOC, noncentrosymmetric superconductors (Tanaka *et al.*, 2010; Yada *et al.*, 2011) lead to both $p$-wave and $s$-wave superconducting correlations. These materials support topologically nontrivial states with edge modes (Tanaka *et al.*, 2009; Smidman *et al.*, 2017) and generate tunable higher-order topological states by rotating an IP magnetic field $B_{||}$ to switch between the corner and edge modes (Zhu, 2018; Pahomi, Sigrist, and Soluyanov, 2020; Ikegaya *et al.*, 2021). MZMs are reported using a large Rashba SOC ($\sim$110 meV) in Au(111) surface states (Wei *et al.*, 2019; Manna *et al.*, 2020).

Instead of native SOC, MZMs can be hosted in systems with synthetic SOC realized through magnetic textures and the resulting fringing fields (Kjaergaard, Wölms, and Flensberg, 2012; Klinovaja, Stano, and Loss, 2012; Nadj-Perge *et al.*, 2014; Kim, Tewari, and Tserkovnyak, 2015; Fatin *et al.*, 2016; Marra and Cuoco, 2017; Wu *et al.*, 2017; Kim *et al.*, 2018; Desjardins *et al.*, 2019; Güngördü and Kovalev, 2022; Steffensen *et al.*, 2022; Huang and Kotetes, 2023). Magnetic textures $\mathbf{B}(\mathbf{r})$ remove the need for an applied magnetic field, and their tunability reconfigures regions that support topological superconductivity to create, control, and braid MZMs (Fatin *et al.*, 2016; Yang *et al.*, 2016; Matos-Abiague *et al.*, 2017; Boutin, Lemyre, and Garate, 2018; Güngördü, Sandhoefner, and Kovalev, 2018; Mohanta *et al.*, 2019; Zhou *et al.*, 2019). The emergent SOC is understood by noting that the Zeeman interaction $g_{\text{eff}}\mu_B\mathbf{B}(\mathbf{r})/2 \cdot \boldsymbol{\sigma}$, where $g_{\text{eff}}$ is the effective $g$ factor, is diagonalized by performing local spin rotations aligning the spin-quantization axis to the local $\mathbf{B}(\mathbf{r})$, which has been known for more than 45 years (Matos-Abiague *et al.*, 2017). In a rotated frame, the Zeeman energy $|g_{\text{eff}}\mu_B\mathbf{B}(\mathbf{r})/2|\sigma_z$ is simplified, while the kinetic energy acquires an extra term due to the non-Abelian field that yields the synthetic SOC.

Since the role of magnetic textures would be more pronounced in proximitized materials with large $|g_{\text{eff}}|$, such as narrowband semiconductors or magnetically doped semiconductors (Fatin *et al.*, 2016; Mohanta *et al.*, 2019; Zhou *et al.*, 2019), it was surprising that MZMs were reported in a carbon nanotube (Desjardins *et al.*, 2019; Yazdani, 2019), where the weak inherent SOC renders $|g_{\text{eff}}|$ small. Experimentally a multilayer Co/Pt magnetic texture generated a strong fringing field $\approx$0.4 T in the nearby carbon nanotube, which resulted in both the Zeeman interaction and the characteristic SOC energy $\approx$1.1 meV (Desjardins *et al.*, 2019), exceeding the SOC values for InAs or InSb, which are common MZM candidates. Tuning the magnetic textures, which needs to be accurately studied through micromagnetic simulations (Desjardins *et al.*, 2019; Mohanta *et al.*, 2019; Zhou *et al.*, 2019), revealed through the oscillations of the superconductivity-induced subgap states in carbon-nanotube-based JJs with $s$-wave Pd/Nb electrodes.

Experiments with 2DEGs have revealed a strong proximity effect when they are coupled to a superconductor, even in the presence of strong SOC (Wan *et al.*, 2015; Kjaergaard *et al.*, 2016; Shabani *et al.*, 2016). Planar JJs with $B_{||}$, where the superconducting correlations in the 2DEG can be tuned into a topologically nontrivial phase via a phase difference between the superconducting banks, are predicted to produce MZMs (Hell, Flensberg, and Leijnse, 2017; Hell, Leijnse, and Flensberg, 2017; Pientka *et al.*, 2017; Stern and Berg, 2019; Zhou *et al.*, 2020) and are accompanied by related experiments reporting topological superconducitivity (Fornieri *et al.*, 2019; Ren *et al.*, 2019; Dartiailh *et al.*, 2021). When a superconducting quantum interference device (SQUID) geometry is used as shown in Figs. 5(a) and 5(b), gate voltage can change both the carrier density and the strength of the Rashba SOC, which can determine the presence or absence of topological superconductivity. Two individually gated JJs in the SQUID thus control the current to flow through both or just one of them (Dartiailh *et al.*, 2021). Figures 5(c) and 5(d) show that with gate control the JJ current can become nonmonotonic with $B_{||}$, as expected with the closing of the $s$-wave and the reopening of the $p$-wave superconducting gap predicted for proximitized nanowires (Alicea, 2010; Lutchyn, Sau, and Das Sarma, 2010; Oreg, Refael, and von Oppen, 2010; Sau *et al.*, 2010). The observed JJ current anisotropy, where its nonmonotonic character is lost for $B_{||}$, which is sufficiently misaligned with the $N/S$ interface

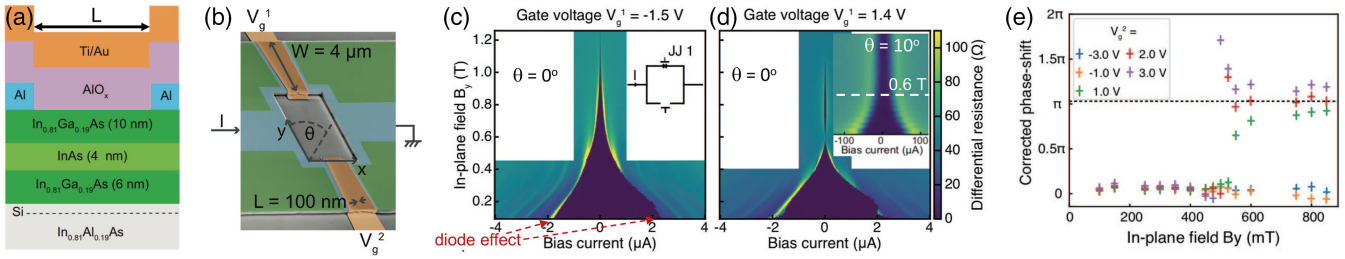


FIG. 5. Experimental evidence for topological superconductivity. (a) Schematic diagrams of a planar JJ. (b) SEM micrograph of a SQUID formed of two JJs with a width $W = 4$ μm and separation between the $S$ contacts (Al) $L = 100$ nm. Each JJ is independently gated with the voltage tuning both the carrier density and the SOC. The $x$ direction is collinear to the current flow in the JJs. Differential resistance of JJ1 as a function of an applied in-plane field at gate voltages: (c) $V_g^1 = -1.5$ V and (d) $V_g^1 = 1.4$ V. In both cases, JJ2 is depleted ($V_g^2 = -7$ V) and does not participate in the transport. Marked asymmetry signifies the superconducting diode effect. In (d), as expected for the transition to topological superconductivity, a minimum of the critical current is observed at around 0.6 T for JJ1 for the in-plane field $B_y$ at $\theta = 0°$; see (b). Inset: for $\theta = 10°$ such minimum is lost. (e) Phase signature of a topological transition from SQUID interferometry. Phase shift between the SQUID oscillation at $V_g^2 = -4$ V and the oscillation at a different value as a function of $B_y$. The linear $B_y$ contribution (due to the anomalous Josephson effect) has been subtracted to highlight the phase jump of $\sim\pi$ at three higher $V_g^2$ values. From Dartiailh *et al.*, 2021.

[Fig. 5(d), inset], further supports the expected proximity-induced $p$-wave superconductivity.

An independent signature of the topological superconductivity is obtained from the SQUID measurements, which in Fig. 5(e) reveal an approximate $\pi$ jump in the superconducting phase difference expected across the transition to topological superconductivity (Hell, Leijnse, and Flensberg, 2017; Pientka *et al.*, 2017). These various signatures of the topological superconductivity are obtained on the same sample and indicate a topological transition at ∼0.6 T. In contrast, $B_{||}$ required to reach the $0 - \pi$ transition expected from the FFLO-like mechanism (Yokoyama, Eto, and Nazarov, 2014) in the studied samples is $B_{0-\pi} = (\pi/2)\hbar v_F/g\mu_B L \approx 14.4$ T (Dartiailh *et al.*, 2021). In another Al/InAs planar JJ, topological superconductivity was reported at an even lower $B_{||} \sim 0.2$ T (Banerjee *et al.*, 2023). With phase bias $\pi$, idealized JJs could host MZMs even at $B_{||} = 0$, but determining the optimal topological gap is complicated by crystalline and magnetic anisotropy and a finite geometry (Paudel *et al.*, 2021; Pekerten *et al.*, 2022). With multiple gates, planar JJs can be used to fuse MZMs and probe the non-Abelian statistics (Zhou *et al.*, 2022).

Curved nanostructures for next-generation spintronic devices (Nagasawa *et al.*, 2013; Gentile, Cuoco, and Ortix, 2015; Ying *et al.*, 2016; Chang and Ortix, 2017; Das *et al.*, 2019; Francica, Gentile, and Cuoco, 2019; Salamone *et al.*, 2021, 2022) could host MZMs. SOC forcing motion along curved geometries can lead to nontrivial spin-dependent effects. Furthermore, bending a nanowire introduces a strain field that itself acts as a source of SOC. When superconducting order is introduced to such systems, curvature-dependent triplet superconducting correlations, a necessary ingredient for MZMs, may appear (Ying *et al.*, 2017). The manipulation of curvature can be used to exert control over, and even induce, nontrivial topology and MZMs (Francica, Cuoco, and Gentile, 2020; Chou *et al.*, 2021).

### B. Superconducting critical temperature

Some theory (Tagirov, 1999; Baladié *et al.*, 2001) and measurements of $F/S/F$ trilayers with both weak (CuNi) and strong (NiFe) $F$ layers showed that $T_c$ is higher for antiparallel $F$-layer moments versus parallel $F$-layer moments (Gu *et al.*, 2002; Moraru, Pratt, and Birge, 2006). This can be understood from the higher net pair-breaking exchange field for parallel $F$-layer moments, which strongly suppresses singlet superconductivity. However, other experiments (Rusanov, Habraken, and Aarts, 2006) observed a higher $T_c$ in the $P$ state that can be partially understood from a suppression of inverse crossed Andreev reflection in the $P$ state (Fominov *et al.*, 2010; Mironov and Buzdin, 2014). For noncollinear $F$-moment alignments in $F/S/F$ and $S/F/F$ systems (Leksin *et al.*, 2012; Wang *et al.*, 2014), the proximity effect between the $S$ and $F$ layers is enhanced due to the generation of triplet Cooper pairs. The increased proximity effect results in a reduction of $T_c$ by up to 120 mK for 3$d$ ferromagnets (Leksin *et al.*, 2012; Wang *et al.*, 2014) and 1 K for half-metallic ferromagnets such as $CrO_2$ (Singh *et al.*, 2015).

The principle of detecting triplets via a magnetic-state-dependent modulation of $T_c$ was experimentally used to detect control of short-range triplets (Banerjee *et al.*, 2018); see Sec. II.C for a definition of short-range triplets. Using a Pt/Co/Pt trilayer proximity coupled to an $s$-wave superconductor (Nb), a strong suppression of $T_c$ for magnetic fields applied IP and partial compensation of $T_c$ suppression for OOP fields were detected. This was in sharp contrast to a pure Nb or Nb/Co multilayers where relatively little $T_c$ suppression is seen for IP fields with negligible orbital depairing and a strong OOP $T_c$ suppression arising from orbital effects. The unconventional modulation is explained by the fact that, in $S/F$ structures without SOC, the short-range triplet energy does not depend on $\mathbf{M}$ orientation, thereby making the $T_c$ independent of the $\mathbf{M}$ angle $\theta$ with the film plane. However, in the presence of SOC arising from the interfacial symmetry breaking in Pt/Co/Pt trilayers, an increasing IP field increases the "leakage" of the Cooper pairs through the triplet channel. This leakage drains the superconductor of Cooper pairs, and the superconducting gap is reduced. An OOP has the opposite effect and closes this parallel triplet channel, thereby reducing the $T_c$ suppression. The dependence of the magnitude of $T_c$ modulation is expected to depend on the strength of both the

SOC and **M**, with the former most likely depending on the exact interface structure (Bregazzi *et al.*, 2024). Moreover, disorder will suppress odd-parity superconducting correlations due to the randomization of electron momentum generated by the lack of translational symmetry at the interface, which in turn modifies $T_c$.

### C. Modification of magnetic anisotropy

A consequence of a SOC-driven modulation of superconductivity is the potential for a reciprocal effect, i.e., a reorientation of **M** due to superconductivity (Johnsen, Banerjee, and Linder, 2019). A reduction in $T_c$ of the superconductor for an IP **M** translates to a reduction in the condensation energy due to a suppression of the superconducting gap. The free energy of the superconducting state will thus favor an OOP **M**. **M** angle dependence of free energy means that, for a sufficiently low-anisotropy barier in the $F$ layer $T_c$ can trigger an IP-to-OOP **M** reorientation. This is modeled as a $S/\mathrm{HM}/F$ structure. When one uses the tight-binding Bogoliubov–de Gennes method on a lattice (see Sec. III), the system is described by the following Hamiltonian:

$$\begin{aligned} H = & -t\sum_{\langle ij\rangle,\sigma} c^{\dagger}_{i,\sigma}c_{j,\sigma} - \sum_{i,\sigma}\mu_i c^{\dagger}_{i,\sigma}c_{i,\sigma} - \sum_i U_i n_{i,\uparrow}n_{i,\downarrow} \\ & - \frac{i}{2}\sum_{\langle ij\rangle,\alpha,\beta} \lambda_i c^{\dagger}_{i,\alpha}\hat{n}\cdot(\boldsymbol{\sigma}\times\boldsymbol{d}_{ij})_{\alpha,\beta}c_{j,\beta} \\ & + \sum_{i,\alpha,\beta} c^{\dagger}_{i,\alpha}(\boldsymbol{h}_i\cdot\boldsymbol{\sigma})_{\alpha,\beta}c_{i,\beta}. \end{aligned} \tag{17}$$

In Eq. (17) $t$ is the hopping integral, $\mu_i$ is the chemical potential at lattice site $\boldsymbol{i}$, $U<0$ is the attractive on-site interaction that gives rise to superconductivity, $\lambda_i$ is the Rashba SOC magnitude at site $\boldsymbol{i}$, $\hat{n}$ is a unit vector normal to the interface, $\boldsymbol{d}_{ij}$ is the vector from site $\boldsymbol{i}$ to site $\boldsymbol{j}$, $\boldsymbol{h}_i$ is the local magnetic exchange field, $c^{\dagger}_{i,\sigma}$ and $c_{i,\sigma}$ are the second quantization electron creation and annihilation operators at site $\boldsymbol{i}$ with spin $\sigma$, and $n_i \equiv c^{\dagger}_{i,\sigma}c_{i,\sigma}$. The superconducting term in the Hamiltonian is treated using a mean-field approach, where $c_{i,\uparrow}c_{i,\downarrow} = \langle c_{i,\uparrow}c_{i,\downarrow}\rangle + \delta$ and $c^{\dagger}_{i,\uparrow}c^{\dagger}_{i,\downarrow} = \langle c^{\dagger}_{i,\uparrow}c^{\dagger}_{i,\downarrow}\rangle + \delta^{\dagger}$ are inserted into Eq. (17) and neglect terms of second order in the fluctuations $\delta$ and $\delta^{\dagger}$. In addition, $\Delta_i \equiv U_i\langle c_{i,\uparrow}c_{i,\downarrow}\rangle$ is the superconducting order parameter, which is solved self-consistently. In the presence of a strong shape anisotropy favoring an IP orientation, this model predicts a $\pi/4$ rotation in the plane of the film below the superconducting transition. At a rotation of $\pi/4$ with respect to the crystal axes, the triplet generation is minimized, which maximizes the superconducting condensation energy required for the **M** rotation.

These predictions were recently demonstrated in magnetic tunnel junctions containing epitaxial V/MgO/Fe/MgO/Fe/Co (González-Ruano *et al.*, 2021), grown using molecular beam epitaxy. The Rashba SOC arises from the MgO/Fe interface, which is also responsible for a well-defined perpendicular magnetic anisotropy in addition to the required cubic symmetry of Fe(001). The top Fe/Co bilayer detects superconductivity-driven orientational changes of the Fe(001) layer through the tunneling magnetoresistance (TMR) effect. Below $T_c$ of the V layer, the Fe layer showed a pronounced reduction in the field required to orient the OOP **M** or, for larger junctions, a spontaneous reorientation in the OOP direction at zero field. An electric field effect was also reported in the superconducting state, where the OOP switching fields depends on the strength and direction of the applied field (González-Ruano *et al.*, 2021). This field-dependent behavior arises from an electric-field-induced modification of the Rashba SOC. A similar effect, albeit an IP rotation of the Fe(001) layer magnetic moment, was also observed in this system (González-Ruano *et al.*, 2020), as predicted by the previously described theoretical model. While the free energy considerations are somewhat similar, this is fundamentally different from the superconducting exchange coupling observed in GdN/Nb/GdN trilayers (Zhu *et al.*, 2017) and originally predicted by de Gennes (1966).

### D. Interfacial magnetoanisotropy

TMR (Tsymbal and Žutić, 2019) is an important effect in spintronics where the tunneling probability, and thus the resistance, of $F$/insulator/$F$ trilayers depend on the orientation of the two ferromagnets. In a $N/F$ bilayer with an interfacial SOC, the resistance can depend on the **M** orientation from TAMR (Gould *et al.*, 2004; Moser *et al.*, 2007); recall Sec. II.A. TAMR devices have an advantage over TMR equivalents, as they require only a single $F$, thereby reducing the number of interfaces and potential alignment problems due to magnetostatic coupling between the two $F$ layers.

When the normal metal is replaced by a superconductor, Andreev reflection provides an additional source of magnetoanisotropy through a process known as magnetoanisotropic Andreev reflection (MAAR) (Högl *et al.*, 2015). The transport properties of such a bilayer were explored by Vezin *et al.* (2020) using the BTK formalism outlined in Sec. II.D.4, within which the interfacial SOC may be included as a boundary potential. With the $F/S$ interface located at $z=0$, the Hamiltonian is $H = \hbar^2\boldsymbol{k}^2/2m - \mu + \boldsymbol{h}\cdot\boldsymbol{\sigma}\theta(z) + V_B(z)$, where $\boldsymbol{h}$ is the $F$ exchange field and $\theta(z)$ is the step function. The boundary potential is assumed to contain a spin-independent contribution $V_0$, as well as Rashba SOC $V_B(z) = [V_0 d + \alpha(k_x\sigma_y - k_y\sigma_x)]\delta(z)$, with $d$ the barrier thickness. It is convenient to introduce the dimensionless quantities: spin polarization $P = |\boldsymbol{h}|/2\mu_F$, barrier $Z = V_0 d\sqrt{m}/\hbar^2\sqrt{k_F q_F}$, and Rashba SOC $\lambda = 2\alpha\sqrt{m}/\hbar^2$ strengths, where $\mu_F$ is the chemical potential in the $F$ region, $m$ is the effective mass, and $k_F$ ($q_F$) is the magnitude of the spin-averaged wave vector in the $F$ ($S$) region. Even a small $P$ and $\lambda$ yield a notable increase in the zero-bias conductance due to spin-flip Andreev reflection (Vezin *et al.*, 2020). For $P = 40\%$ the MAAR is already 10 times greater than the normal-state TAMR. In the half-metallic limit, the MAAR depends universally on spin-orbit fields only (Högl *et al.*, 2015).

The existence of a large OOP MAAR has been demonstrated in all-epitaxial Fe/MgO/V junctions (Martínez *et al.*, 2020). By defining an angle $\theta$, measured between **M** and the interface normal, both an OOP TAMR and MAAR can be expressed from the magnetoanisotropy of the conductance $G$,

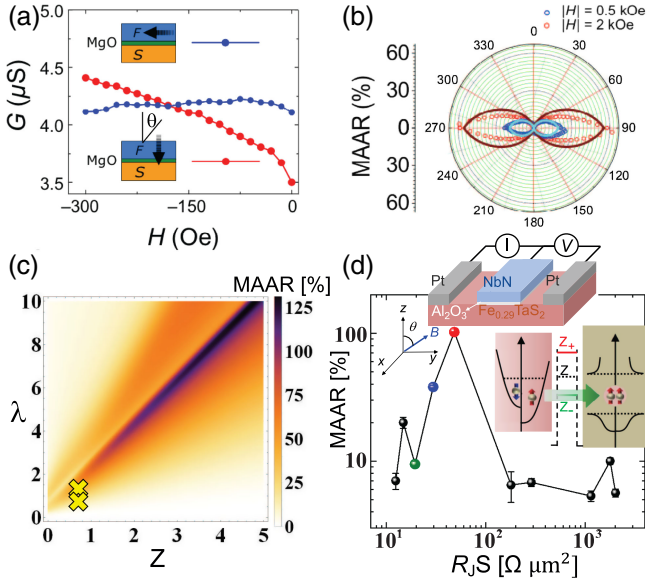


FIG. 6. (a) Evolution of $G(V=0)$ in the Fe/MgO/V junctions, with IP and OOP $H$. The two remanent, perpendicularly oriented $\mathbf{M}$ (thick black arrows) with different $G(0)$ reveal a MAAR $\sim 17\%$ at $H=0$. (b) OOP MAAR at $H=0.5$, 2 kOe (blue and red dots) and indicated by arrows compared with a phenomenological model (outer red and inner blue lines). The results are for $T=0.3$ K. Adapted from Martínez *et al.*, 2020. (c) OOP MAAR amplitude at $V=0$ as a function of the interfacial barrier $Z$ and the Rashba SOC $\lambda$ for spin polarization $P=0.7$. The crosses represent the parameters for the Fe/MgO/V junctions (Martínez *et al.*, 2020). From Vezin *et al.*, 2020. (d) Upper inset: OOP MAAR amplitude of the $Fe_{0.29}TaS_2/Al_2O_3/NbN$ junctions on the interface resistance area product $R_JS$ near $V=0$, where $R_J=V/I$. Lower inset: SOC-modified barrier. From Cai *et al.*, 2021.

$$\mathrm{TAMR(MAAR)}=[G(0^\circ)-G(\theta)]/G(\theta). \tag{18}$$

In the same Fe/MgO/V junction, the conductance anisotropy and TAMR can be measured by rotating $\mathbf{M}$, either by raising the temperature above $T_c$ or by applying the bias, to exceed $\Delta$ for V, as shown in Fig. 6(a). While with a modest SOC in the Fe/MgO/V junction there is only a negligible TAMR of $\sim 0.01\%$ at applied field $|H|=1$ kOe, at the same temperature of $T=0.3$ K, a measured zero-bias conductance anisotropy in Figs. 6(b)–6(d) reveals that the MAAR is enhanced by several orders of magnitude. By carefully designing the magnetic anisotropies, one can obtain two remanent states with perpendicular $\mathbf{M}$ in Fe/MgO/V junctions (Martínez *et al.*, 2020). The observed large increase of MAAR $\sim 17\%$ at $H=0$ thus excludes that, and the enhanced MAAR is due to an applied magnetic field.

A large MAAR is connected to the proximity-induced equal-spin-triplet superconductivity (Vezin *et al.*, 2020). The Green's function $G$ from the spin-flip Andreev reflection dominates the same triangular region, which is shown in Fig. 6(c) to have an enhanced MAAR (Vezin *et al.*, 2020). The nonmonotonic behavior of the spin-flip Andreev reflection arises from the effective barrier strength $Z^{\pm}_{\mathrm{eff}}=Z\pm\lambda k_{\parallel}/2\sqrt{k_Fq_F}$, where $Z^{+}_{\mathrm{eff}}$ ($Z^{-}_{\mathrm{eff}}$) is for inner (outer) Rashba bands (Vezin *et al.*, 2020); see Fig. 1. When $Z\geq 0$ and $\lambda\geq 0$, $Z^{+}_{\mathrm{eff}}\geq Z$ cannot be suppressed. However, at $k_{\parallel}=(2Z/\lambda)\sqrt{k_Fq_F}$, $Z^{-}_{\mathrm{eff}}$ becomes transparent and gives a dramatically increased $G$. The maximum of the total $G$ is achieved when the amount of the open channels $\propto k_{\parallel}$ is maximized. Therefore, the maximum spin-flip Andreev reflection is near $q_F=(2Z/\lambda)\sqrt{k_Fq_F}$, i.e., $\lambda=2Z$ for $k_F=q_F$.

Unlike common expectations that a strong SOC is desirable for equal-spin-triplet superconductivity, a desirable SOC strength nonmonotonically depends on the interfacial barrier. This trend is confirmed in Fig. 6(d) for quasi-2D van der Waals (vdW) $F/S$ junctions where, together with a large MAAR, such a measurement supports the equal-spin-triplet superconductivity (Cai *et al.*, 2021). Conversely, while a weak interfacial barrier that enables a robust proximity-induced superconductivity seems suitable to enhance the spin-triplet superconductivity, its largest contribution is obtained for the interfacial barrier that nonmonotonically depends on the SOC strength. A large $G$ anisotropy is also found in all-vdW $F/S$ tunnel junctions (Lv *et al.*, 2018; Kang *et al.*, 2021). Not only does the MAAR support large spin-valve signals with a single $F$, its analysis could be used to identify equal-spin-triplet superconductivity and probe elusive MZMs. For the MAAR, it would be important to realize a tunable SOC in a single sample.

Combined interfacial Rashba and Dresselhaus SOC was investigated by Högl *et al.* (2015), Costa, Matos-Abiague, and Fabian (2019), and Costa and Fabian (2020). Since the interfacial barrier depends on spin and $\boldsymbol{k}$, it was found that so-called skewed Andreev processes, where the reflection amplitude is asymmetric in $\boldsymbol{k}$ space, resulted in a large anomalous Hall effect. Another manifestation of spin anisotropy due to SOC occurs at the interface of a ballistic $S$/HM bilayer when the symmetry breaking axis $\boldsymbol{n}$ of the spin-orbit field is rotated (Johnsen, Svalland, and Linder, 2020). Such an effect may be achieved by combining bulk and interfacial SOC. Depending on the direction of $\boldsymbol{n}$, a modulation of $T_c$ was found due to anisotropic conversion of the conventional $s$-wave even-frequency superconducting correlations into other pair correlations of different symmetries.

### E. Josephson junctions

JJs with weak links featuring SOC have been studied for decades in the form of supercurrents through 2DEGs (Takayanagi and Kawakami, 1985; Mayer *et al.*, 2020). Recent developments for JJs involving SOC typically include magnetic elements for (i) inducing MZM and related topological phenomena, (ii) creating long-range triplet supercurrents carrying both charge and spin, or (iii) creating phase batteries where the ground-state phase difference in the JJ is arbitrary (not only 0 or $\pi$).

*Long-range triplet supercurrents*. Whereas magnetically inhomogeneous structures are known to support long-range spin-polarized supercurrents in diffusive systems, despite the pair-breaking effect of an exchange field SOC can accomplish this in homogeneous ferromagnets. Consider an inhomogeneous $\mathbf{M}$ along the $x$ direction, such as a domain wall, written as $\boldsymbol{h}=h\sin(Qx)\hat{\boldsymbol{y}}+h\cos(Qx)\hat{\boldsymbol{z}}$, where $Q$ is the wave vector describing the $\mathbf{M}$ rotation (Bergeret and Tokatly, 2014).

By performing a unitary transformation $U$ on the Green's function describing such a system, corresponding to a local SU(2) rotation $U(x) = e^{-(i/2)Qx\sigma_x}$, one finds that the resulting equation of motion for the transformed Green's function describes a system with homogeneous $\mathbf{M}$ $\boldsymbol{h} = h\hat{\boldsymbol{z}}$, but now with an effective SOC that enters the gradient operator $\tilde{\boldsymbol{\nabla}}$ like an SU(2) gauge field $\tilde{\boldsymbol{\nabla}} = \boldsymbol{\nabla} + (iQ/2)[\sigma^x, \cdot]\hat{\boldsymbol{x}}$ (Bergeret and Tokatly, 2014). The result of this transformation is that the singlet-triplet conversion in a $S$/inhomogeneous $F$ structure is equivalent to the singlet-triplet conversion in a $S$/homogeneous $F$ structure with SOC. Considering a ferromagnetic nanowire with an easy-axis anisotropy proximitized to superconducting leads and neglecting all forms of intrinsic SOC, one can also produce long-range triplet correlations by bending the nanowire. If the resulting curvature is not sufficiently large that the exchange interaction of $\mathbf{M}$ overcomes the anisotropy, $\mathbf{M}$ follows the bend of the wire, thereby producing a rotation of $\mathbf{M}$. As a result, an artificial, effective SOC appears. This can therefore give rise to long-range triplet supercurrents and induce 0 to $\pi$ transitions in JJs (Salamone *et al.*, 2021). Other ways to manipulate supercurrents via SOC were discussed by Shekhter *et al.* (2016, 2017) and Entin-Wohlman *et al.* (2018).

The first experiments to detect long-range triplets were carried out in JJs with disordered magnetic interface (Keizer *et al.*, 2006) or spin-mixer layers (Khaire *et al.*, 2010; Robinson, Witt, and Blamire, 2010; Eschrig, 2011). These spin-mixer layers generated the triplets that were subsequently passed through a thick $F$ (such as Co) to filter out the singlets. Therefore, the proposal to create triplets in JJs with SOC weak links is attractive, as it removes the requirement of complex spin-mixer layers.

To date direct experimental evidence in this direction in thin-film hybrids has been inconclusive. Initial attempts with Nb/Pt/$F$/Pt/Nb, where $F$ is a synthetic antiferromagnet composed of Co/Ru/Co, showed a significant enhancement in the characteristic voltage of the JJs compared to devices without the Pt layer (Satchell and Birge, 2018). However, the decay length of the supercurrent as a function of the Co layer thickness was not as expected for long-range triplets. The major limitation is the predominant IP magnetic anisotropy of the $F$ layer instead of the canted magnetic anisotropy required to observe the long-range triplets (Jacobsen, Ouassou, and Linder, 2015). Overcoming this limitation by replacing the Pt/$F$/Pt weak link with a $[\mathrm{Co/Ni}]_n$/Co multilayer with a canted magnetic anisotropy also failed to show evidence of triplet supercurrents. It is not clear whether this discrepancy between theory and experiments is due merely to a poor singlet-to-triplet conversion efficiency in these systems or something more fundamental.

Lateral JJs with the current flowing in the plane of the layers are more flexible in terms of satisfying the conditions for SOC-mediated triplet generation. The original experiment observing supercurrent flow through half-metallic $CrO_2$ in a lateral JJ can similarly be explained as arising from the SOC in the contact region instead of surface magnetic inhomogeneity in $CrO_2$, as previously assumed (Bergeret and Tokatly, 2014). This SOC can be attributed to structural inversion asymmetry (Ast *et al.*, 2007; Miron *et al.*, 2010). In the lateral geometry in a disk-shaped JJ containing a Nb/Co bilayer, triplet supercurrents have been detected that are confined to the rim of the disk (Fermin, van Dinter *et al.*, 2022). This confinement arises from an effective SOC due to the vortex in Co.

An additional advantage of the lateral geometry is the possibility of studying the dependence of the triplet supercurrent as a function of the $\mathbf{M}$ direction of $F$ as proposed theoretically first by Eskilt *et al.* (2019) and later by Bujnowski, Biele, and Bergeret (2019). Here a lateral JJ with SOC is in contact with an underlying $F$ with IP anisotropy. The supercurrent was shown to be highly sensitive to the IP $\mathbf{M}$ rotation with the triplet supercurrent reducing by several orders of magnitude with a $\pi/2$ rotation. This is evidence of the presence of triplet supercurrents, and the device also acts as a magnetic transistor for supercurrents without the constraint for complex magnetic anisotropies.

While the normal-state properties of heterostructures typically consider $k$-linear SOC described by models such as Eq. (5), there is a growing class of materials where the $k$-cubic SOC is not merely a small perturbation but rather a dominant contribution (Winkler *et al.*, 2002; Krich and Halperin, 2007; Nakamura, Koga, and Kimura, 2012; Liu *et al.*, 2018; Cottier *et al.*, 2020). The role of such SOC in JJs is largely unexplored (Alidoust, Shen, and Žutić, 2021). The corresponding Hamiltonian can be written as $H_{\mathrm{SO}} = (i\alpha_c/2)(k_-^3\sigma_+ - k_+^3\sigma_-) - (\beta_c/2)(k_-^2 k_+\sigma_+ + k_+^2 k_-\sigma_-)$, using cubic strengths $\alpha_c$ and $\beta_c$, for Rashba and Dresselhaus terms, where $k_\pm = k_x \pm ik_y$ and $\sigma_\pm = \sigma_x \pm i\sigma_y$. Without symmetry constraints to prevent $k$-linear SOC, the relative $k$-cubic SOC contribution depends on the carrier density (Žutić, Fabian, and Das Sarma, 2004; Krich and Halperin, 2007). Therefore, assuming a simple $k$-linear SOC may not in general be adequate. HMs in superconducting heterostructures do not have small Fermi pockets, and the interpretation for the long-range triplet decay may need to be revisited. Furthermore, from Fig. 2 we see that the emergent interfacial SOC is not $k$ linear and can strongly modify transport properties.

A hallmark of JJs with cubic SOC goes beyond current-phase relations (including the anomalous Josephson effect, discussed later in the context of phase batteries) and also influences the spin structure and symmetry properties of superconducting proximity effects. Unlike the $p$ wave for linear SOC, the $f$-wave symmetry of superconducting correlations is the fingerprint for cubic SOC, which supports MZMs (Alidoust, Shen, and Žutić, 2021). Cubic Rashba SOC also provides an effective low-energy description for the heavy holes in Ge-based planar JJs (Luethi *et al.*, 2023; Tosato *et al.*, 2023).

*Phase batteries*. The supercurrent flowing through JJs depends sensitively on the phase difference $\phi$ between the superconductors. A finite phase difference usually drives a supercurrent through the system, and the ground state of the system is usually $\phi = 0$ or $\pi$. But this is not always the case (Golubov, Kupriyanov, and Il'ichev, 2004). The phase difference $\phi$ of the superconducting order parameters by $2\pi n$, where $n$ is an integer, should correspond to exactly the same physical state. Moreover, a dc supercurrent flows if a gradient exists in the phase of the superconducting order parameter in the

junction. If $I(0) = 0$, it follows that $I(2\pi n) = 0$. Finally, performing a time-reversal operation on the system must reverse any supercurrent present. Since time reversal includes complex conjugation, the phase changes sign and $\phi \to -\phi$. Therefore, one usually has $I(\phi) = -I(-\phi)$.

From the aforementioned properties, it follows that $I = 0$ whenever $\phi = \pi n$. Therefore, the ground-state phase difference of a JJ, as the state with no supercurrent, is usually either 0 or $\pi$. This can change if time-reversal symmetry (TRS) and inversion symmetry is broken. In JJs with superconductors breaking TRS, such as $d + \mathrm{i}d$ superconductors, the relation $I(\phi) = -I(-\phi)$ is not necessarily fulfilled (Liu, Xu, and Wang, 2017). Instead, the phase difference $\phi$ that minimizes the Josephson energy of the system can be neither 0 nor $\pi$, but instead a different value denoted by $\phi_0$. There is no supercurrent for the ground-state phase difference $\phi_0$, so $I(\phi_0) = 0$.

JJs where the ground-state phase difference is neither 0 nor $\pi$, but rather some arbitrary value $\phi_0$ known as a $\phi_0$ junction (Buzdin, 2008). This behavior was also found in earlier studies by Geshkenbein and Larkin (1986) and Millis, Rainer, and Sauls (1988), who considered JJs with unconventional superconductors, SOC, and magnetically active interfaces. Assuming that the value of $\phi_0$ is tunable, a suitable name for such systems is in fact phase batteries. By tuning $\phi_0$ via external parameters, one provides a phase bias to a macroscopic wave function in a quantum circuit. This is conceptually similar to how a classical battery provides a voltage bias. The question then is whether controllable $\phi_0$ junctions can be tailored by combining materials with the right properties into a JJ.

One way to achieve a phase battery using conventional superconductors is combining antisymmetric SOC with a spin-splitting Zeeman field in the weak link. This breaks TRS and inversion symmetry, which can result in a finite supercurrent even at zero phase difference (Buzdin, 2008; Zazunov *et al.*, 2009). Here "breaking inversion symmetry" means that some particular operation on the spatial degrees of freedom in the system, such as a mirror, parity, or rotation operation (or a combination thereof), does not leave the Hamiltonian of the weak link invariant. The precise description of which spatial symmetry that needs to be broken for the $\phi_0$ junction to appear is system specific, depending on the direction of the spin-splitting field (Liu and Chan, 2010; Rasmussen *et al.*, 2016).

A microscopic explanation of the $\phi_0$ effect in JJs with quantum dots (QDs) was given by Zazunov *et al.* (2009) and Szombati *et al.* (2016). The Hamiltonian of a two-level QD with SOC and spin splitting is (Szombati *et al.*, 2016) $H_{\mathrm{QD}} = (E_{\mathrm{orb}}\tau_z - \mu\tau_0)\sigma_0 + B\tau_0\sigma_z + \alpha\tau_y\sigma z$, where $\mu$ is the chemical potential, $E_{\mathrm{orb}}$ is the orbital energy, $\alpha$ parametrizes the SOC strength, $B$ is the Zeeman splitting, and $\tau_{0,x,y,z}$ and $\sigma_{0,x,y,z}$ are the identity and Pauli matrices acting on orbital and spin space, respectively. Without SOC, $\alpha = 0$ and the two orbitals do not mix. Transfer of electrons in the Cooper pair through the QD then takes place on one level at the time. Consider one electron tunneling via level 1 and the second via level 2: the corresponding matrix element for such a process is $t_L^{(1)} t_R^{(1)} t_L^{(2)} t_R^{(2)}$, where $t_L^{(i)}$ are the hybridization amplitudes between level $i$ in the QD and the left lead and can be taken as real for $\phi = 0$; a similar approach is taken for $t_R(i)$. Therefore, the matrix element describing tunneling from right to left is exactly the same as it is for describing tunneling from left to right when $\phi = 0$; hence, no current flows.

When $\alpha \neq 0$, the $H_{\mathrm{QD}}$ eigenstates are a mix of the two orbital states. As shown by Szombati *et al.* (2016), this results in new single-level hybridization amplitudes $T_L^{(1,2)}$ for levels 1 and 2 with the left lead (determining the probability for electron transfer between the level and the lead). For spin-↑ electrons, $T_L^{(1)} = t_L^{(1)} \cos\varepsilon + \mathrm{i}\sin\varepsilon t_L^{(2)}$ and $T_L^{(2)} = t_L^{(2)} \cos\varepsilon - \mathrm{i}\sin\varepsilon t_L^{(1)}$. The expressions for $T_R^{(i)}$ are obtained by $L \to R$. For spin-down electrons, the aforementioned plus and minus signs are exchanged.

A key observation is that the amplitudes $T_{L(R)}^{i}$ are now complex. This means that as electrons make their way across the QD, they gain a finite phase. The phase of the resulting matrix element is the opposite for electrons tunneling in one direction (say, left to right) compared to the opposite direction (right to left). Since the imaginary part of the rightward and leftward total tunneling coefficients are then different, leftward and rightward tunneling do not cancel each other exactly for a given spin species $\sigma$. If the tunneling probabilities are now also different in magnitude for spin ↑ and ↓ (for $B \neq 0$), the Cooper pairs acquire a net phase upon tunneling despite $\phi = 0$.

Predictions for $\phi_0$ have also been made in JJs with metallic interlayers, such as multilayered ferromagnets (Braude and Nazarov, 2007; Grein *et al.*, 2009; Liu and Chan, 2010; Kulagina and Linder, 2014) and through metallic weak links that contain both SOC and ferromagnetic order (Buzdin, 2008). This effect can be understood in terms of Andreev bound states, which comprise counterpropagating electrons and holes that transfer Cooper pairs between superconductors via Andreev reflection. These bound states come in pairs $\pm E_i$ where $i$ is an index characterizing internal degrees of freedom such as the spin of the electron and hole that compose the bound state. Consider first a simple $S/F/S$ JJ. In the limit of weak Zeeman splitting $h$ and assuming a high-transparency junction for simplicity, one finds energies (Annunziata *et al.*, 2011) $E_i = E_\sigma = E_0 \cos(\phi/2 + \sigma ch)$, $\sigma = \pm 1$, where $c$ is a geometry-dependent constant and $E_0 = \Delta$. The current carried by these Andreev bound states is proportional to $dE_\sigma/d\phi$. While each bound state is phase shifted by $\sigma ch$, the total current at $\phi = 0$ vanishes since the magnitude of each current is identical.

The situation changes in a $S/F_1/F_2/F_3/S$ junction. When the magnetization $\mathbf{M}_i$ of the ferromagnets is such that the spin chirality defined as $\mathbf{M}_1 \cdot (\mathbf{M}_2 \times \mathbf{M}_3)$ is nonzero, an anomalous $\phi_0$ JJ emerges. When all $\mathbf{M}$ are perpendicular to each other, the spin chirality is maximized. The reason for why the spin chirality needs to be finite is precisely that both time-reversal symmetry and inversion symmetry are now broken in a manner that permits the $\phi_0$ effect (recall that $\mathbf{M}_j$ is a pseudovector). The Andreev bound states are (Liu and Chan, 2010) $E_i = E_\eta = E_{\eta,0} \cos(\phi + \eta c' h)$, $\eta = \pm 1$, where $c'$ is a new constant, under the simplifying assumptions that the Zeeman splitting in each $F$ layer is equal and that the spin-chirality product is maximized. The index $\eta$ is related to the spin of the Andreev bound state. The crucial difference from the $S/F/S$ case is that the amplitude $E_{\eta,0}$ of the bound state is

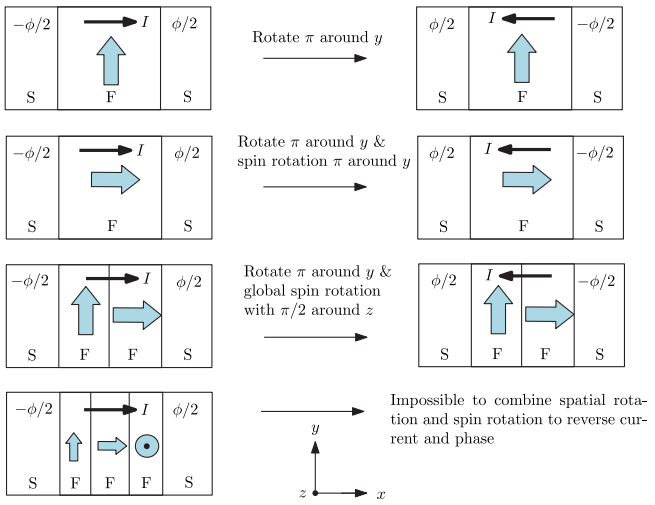


FIG. 7. Illustration showing how a combination of spatial rotation of the entire junction and a global spin rotation allows one to prove that $I(\phi) = -I(-\phi)$ for magnetic JJs with zero spin chirality. The blue (light gray) arrows show **M** in each layer.

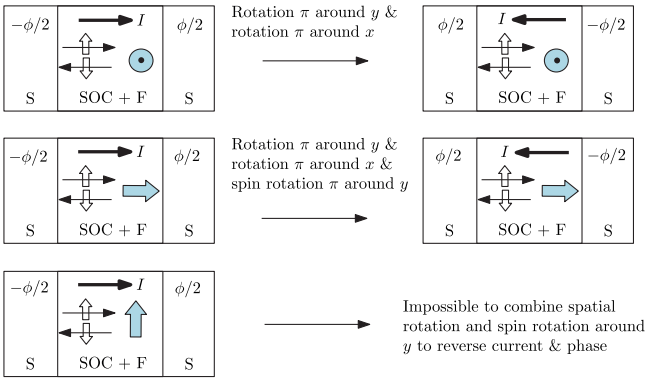


FIG. 8. Illustration showing how a combination of spatial rotation of the entire junction and a particular global spin rotation allows one to prove $I(\phi) = -I(-\phi)$ for magnetic JJs with SOC. A Rashba-type SOC $k_x\sigma_z$ is considered. The illustration of SOC indicates that ↑ have lower energy when moving in one direction, whereas ↓ have lower energy when moving in the opposite direction.

now unequal for the two bound states $\eta = \pm 1$. Therefore, the total current at $\phi = 0$ does not cancel out and a net anomalous supercurrent exists even at zero phase difference.

A pictorial argument shows when a $\phi_0$ effect can appear, which is intuitively easier to understand than using matrix symmetry operations applied to the Hamiltonian of the system. Consider first a magnetic JJ with an arbitrary number of magnetic layers. Without SOC, there is no coupling between the spin degree of freedom and orbital motions of the electrons. Therefore, a global spin rotation should leave the supercurrent invariant: if all **M** are rotated in the same way, the current stays the same. The goal now is to use this global spin rotation invariance as well as a spatial rotation of the entire JJ to prove that $I(\phi) = -I(-\phi)$. As explained in Fig. 7, this is possible to accomplish for arbitrary **M** directions with both one and two ferromagnets, but not with three (lower row) if the spin chirality is finite. The pictorial proof shown in the figures can thus be used to prove if the $\phi_0$ effect is absent. We note that the same type of pictorial proof should be possible to use for nonreciprocal dissipative transport by replacing the superconducting phase differences $\pm\phi/2$ with voltages $\pm V/2$.

We can use the pictorial proof also for a $S/F/S$ junction with SOC to infer which **M** directions do not permit a $\phi_0$ state. We consider a Rashba-type SOC $\propto \alpha\sigma_z k_x$ in a 1D geometry for simplicity since this suffices to show the principle. This is shown in Fig. 8. The upper row shows that if **M** points in the $z$ direction, physically rotating the entire junction two times brings it back to its original state except for a reversed current and phase. Therefore, one concludes that $I(\phi) = -I(-\phi)$: i.e., no $\phi_0$ state. When the **M** points along the $x$ direction, a global spin rotation around the $y$ axis is still permitted without changing the supercurrent. The reason is that performing this spin rotation changes neither the SOC term nor the absolute or relative magnitude of the momentum-dependent total exchange field of the carriers. Combined with a physical rotation of the entire system, one again proves that $I(\phi) = -I(-\phi)$. This is not possible to do when **M** points in the $y$ direction, which is consistent with the known result that such a system hosts a $\phi_0$ state. A further manipulation of such a $\phi_0$ state is possible with the contribution of Rashba and Dresselhaus SOC (Alidoust, 2020) and experimentally demonstrated gate-controlled SOC (Mayer *et al.*, 2020; Dartiailh *et al.*, 2021).

Besides the phase shift obtained due to the broken time-reversal and inversion symmetry in the junction, the magnitude of the critical current also becomes direction dependent, which we further discuss in Sec. IV.F. Finally, the presence of SOC in magnetic JJs has also been shown to induce electrically controlled **M** dynamics (Nashaat *et al.*, 2019) and specific magnetization trajectories along *I-V* characteristics of $\phi_0$ JJs (Shukrinov, 2022), as well as anomalous Gilbert damping and Duffing features (Shukrinov *et al.*, 2021; Abdelmoneim *et al.*, 2022).

### F. Supercurrent diodes

There has been a resurgence in the interest of the superconducting diode effect that shares a curious history with the spin Hall effect, which was predicted decades before (D'yakonov and Perel', 1971a, 1971b) the current terminology was established (Hirsch, 1999). Swartz and Hart (1967) found a rectifying behavior in a superconducting Pb-based bimetallic strip in an applied magnetic field. The magnitude of $I_c^+$ in the forward direction mismatched to $I_c^-$ in the reverse direction, behavior noted independently in the abstract of Edelstein (1996). This means that there is a magnitude range $I_c^- < I < I_c^+$ where the current $I$ is dissipationless in one direction, but resistive in the other. The term *Josephson diode* was used by Hu, Wu, and Dai (2007) with the proposed implementation of the $p$- and $n$-doped regions resembling conventional semiconductor diodes without SOC, but with a broken inversion symmetry and a rectifying behavior (Shockley, 1949). Before the recent observation by Ando *et al.* (2020), early experimental (Touitou *et al.*, 2004; Vodolazov *et al.*, 2005) and theoretical (Grein *et al.*, 2009; Silaev *et al.*, 2014) studies of the superconducting diode effect with

ferromagnets that do not invoke SOC were summarized by Satchell *et al.* (2023).

Many recent experimental realizations of the superconducting diode effect have closely followed theory (Reynoso *et al.*, 2008), appearing in JJs with spin splitting and SOC. However, while some measurements show the diode effect (Mayer *et al.*, 2020; Dartiailh *et al.*, 2021), prior to the work of Ando *et al.* (2020), such an effect was overlooked. Figures 5(c) and 5(d) show such a supercurrent diode effect, where the normalized critical current asymmetry reaches ≈10–20% (Dartiailh *et al.*, 2021).

Theory (Davydova, Prembabu, and Fu, 2022; He, Tanaka, and Nagaosa, 2022; Ilić and Bergeret, 2022; Scammell, Li, and Scheurer, 2022; Yuan and Fu, 2022; Hou *et al.*, 2023) and experiments (Ando *et al.*, 2020; Baumgartner *et al.*, 2022; Pal *et al.*, 2022) have investigated nonreciprocal critical currents in superconducting wires or films. The supercurrent diode effect in a JJ is related to the appearance of an anomalous phase, but it is possible to have a $\phi_0$ JJ without any accompanying diode effect. A current-phase relation of $I = I_0 \sin(\phi + \phi_0)$ gives an anomalous phase difference but no diode effect since the positive and negative critical currents match. Since $\delta \sin(\phi + \phi_0)$ can be written as $\alpha \sin\phi + \beta \cos\phi$ for the real coefficients $\alpha, \beta, \delta$, $\phi_0$, for the diode effect one additionally requires higher-order harmonics in the current-phase relation beyond $\sin\phi$ and $\cos\phi$ in order to achieve different magnitudes of the positive and negative critical currents (Baumgartner *et al.*, 2022). A skewed current-phase relation is therefore a necessary condition.

Several studies have focused on superconducting systems where time reversal and inversion symmetry breaking are modeled via ferromagnetism or a magnetic field and antisymmetric SOC interactions, such as Rashba SOC. Nonreciprocal supercurrents have also been observed in materials with valley-Zeeman SOC where, unlike the Rashba SOC, the rectification of supercurrent depends on the OOP magnetic field (Bauriedl *et al.*, 2022). Figure 9 shows rectification efficiency of 60% measured in transition metal dichalcogenide $NbSe_2$ sandwiched between *h*-BN layers, which is significantly larger

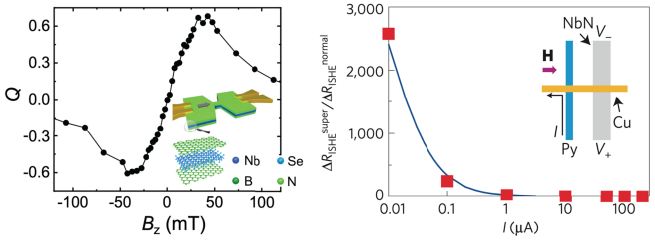


FIG. 9. Left panel: supercurrent rectification efficiency $Q \equiv 2(I_c^+ - |I_c^-|)/(I_c^+ + |I_c^-|)$ as a function of the OOP applied magnetic field measured at 1.3 K. $Q$ is maximal around 35 mT. Inset: device structure with a 250 nm long and wide central constriction. The $z$ direction is perpendicular to the crystal plane. A 10 nm *h*-BN encapsulates two-, three-, or five-layer $NbSe_2$. From Bauriedl *et al.*, 2022. Right panel: inverse spin Hall signal at 3 K quantified by $\Delta R_{ISHE}^{super}$ vs injected spin current $I$. The signal is normalized by the measured value at 20 K in the normal state $\Delta R_{ISHE}^{normal}$. The blue (light gray) line is the fit to the model. From Wakamura *et al.*, 2015.

than those observed in Rashba SOC systems. The rectification saturates at low temperature with a maximum observed around $T = T_c/2$, unlike the observations by Ando *et al.* (2020), where the diode effect was observed near $T_c$. The unusual temperature dependence together with the rectification appearing with an OOP applied magnetic field indicates a fundamentally different origin of the diode effect than that observed for Rashba superconductors.

There are aspects of the supercurrent diode effect that remain poorly understood. For instance, the experimental observation of the diode effect by Ando *et al.* (2020) occurred only near $T_c$, vanishing far below $T_c$. This suggests that a key role is played by fluctuations in $\Delta$.

### G. Spin pumping

Traditional studies of spin transport involve quasiparticle injection at voltages above the superconducting gap. They show evidence for spin and charge decoupling (Hübler *et al.*, 2012; Quay *et al.*, 2013) and enhancement of the spin-relaxation times (Yang *et al.*, 2010; Wakamura *et al.*, 2014). Previous experiments demonstrated that Andreev reflection excludes transport of dynamically driven spin currents through the superconducting energy gap, so the spin-current-induced broadening of the FMR linewidth is suppressed by the opening of the superconducting gap (Bell *et al.*, 2008).

Jeon *et al.* (2018) compared FMR results on Nb/Py/Nb trilayers with Pt/Nb/Py/Nb/Pt structures in which the outer Pt layers are effective spin sinks with strong SOC. They investigated the $T$ dependence of the FMR linewidth ($\mu_0 \Delta H \propto \alpha$) and the resonance field $\mu_0 H_{res}$ across $T_c$. Where Pt (or other large SOC spin sinks) are present, a substantially increased FMR damping for a *S*-layer thickness of the order of the coherence length is interpreted as evidence for superconducting pure spin (triplet) supercurrent pumping. The key mechanism driving the spin current through superconducting Nb involves an interaction of the SOC in Pt with a proximity exchange field from Py, which passes through Nb. Theoretically this requires Landau-Fermi liquid interactions and a non-negligible spin splitting in Pt, which creates a triplet channel in the superconducting density of states of Nb around zero energy (Montiel and Eschrig, 2018). Jeon *et al.* (2020) substituted Pt for a perpendicularly magnetized Pt/Co/Pt spin sink, thereby allowing tunability of the pure spin supercurrent by controlling the **M** angle of Co with respect to the SOC.

An alternative explanation of the FMR results was suggested by Müller *et al.* (2021), who studied spin injection into superconducting NbN from an adjacent Py layer. Here the enhanced $\mu_0 \Delta H$ is attributed to an increased inhomogeneous broadening rather than increased damping. Note that even though Müller *et al.* (2021) used NbN that was thicker than the coherence length, they saw an enhanced $\mu_0 \Delta H$, while Jeon *et al.* (2018) observed this enhancement only in thinner Nb layers. In thicker Nb layers, they observed a decrease of the linewidth below the $T_c$, indicating that comparisons of results between different systems may not be straightforward and that more work is required to understand the discrepancies.

### H. Spin Hall phenomena with superconductors

The spin Hall effect (Sinova *et al.*, 2015) and its inverse are key in spintronics, providing a method to electrically detect spin currents. The spin Hall effect also takes place theoretically in superconducting materials, where a longitudinal flow of charge or spin converts to a transverse flow of spin or charge. Experimentally demonstrating a superconducting spin Hall effect would provide a means to electrically detect the polarization of spin supercurrents and potentially control spin in the superconducting state.

To understand this prospect, we start with the magnetoelectric phenomena in superconductors that were previously studied by Edelstein (1995). Considering $S$ lacking spatial reflection symmetry, Edelstein predicted that the supercurrent must be accompanied by an induced spin polarization among the itinerant electrons. Spin Hall effects in superconductors were later considered by Mal'shukov and Chu (2008), who predicted an induced edge spin polarization in a JJ with a spin-orbit coupled layer separating the superconductors. Kontani, Goryo, and Hirashima (2009) instead considered the dissipative spin Hall effect in $S$ with Rashba SOC, predicting a large negative spin Hall conductivity in the superconducting state. Several works considering the spin Hall effect in different JJ geometries followed, including an ac Josephson bias (Mal'shukov, Sadjina, and Brataas, 2010; Mal'shukov and Chu, 2011).

An important experimental breakthrough of Wakamura *et al.* (2015), motivated by theoretical predictions (Takahashi and Maekawa, 2002, 2008; Maekawa, 2006), reported a large quasiparticle-mediated inverse spin Hall effect in the superconductor NbN that exceeded the effect in the normal state by 3 orders of magnitude. The signal diminished when the distance between the voltage probes in the setup exceeded the charge imbalance length, indicating that the inverse spin Hall signal was indeed carried by quasiparticles. This quasiparticle-mediated spin Hall effect in the superconducting state was measured with the spin absorption technique using a lateral structure composed of Py and a superconducting NbN wire joined by a nonmagnetic Cu bridge, as illustrated in the inset of Fig. 9. The spin current injected via Py diffuses toward the NbN wire and is partly absorbed by it owing to the high SOC in NbN, where it is converted to a charge current (quasiparticle current in the superconducting state) via the inverse spin Hall effect.

Theoretical studies utilizing the quasiclassical theory of superconductivity followed shortly (Espedal *et al.*, 2017; Huang, Tokatly, and Bergeret, 2018). With this methodology, one derives kinetic equations for the distribution functions for energy, charge, and spin-excited modes in the system, which permits computation of the currents. The coefficients in these kinetic equations are determined by the spectral properties of the material and therefore can be much different in the normal and superconducting states. Espedal *et al.* (2017) computed the various contributions to the spin Hall effect in a conventional superconductor, including side-jump, skew scattering, and anomalous velocity operators. They found that the inverse spin Hall current (i.e., a charge current) $j_i^{\mathrm{sH}}$ flowing in the $i$ direction could be computed from the injected spin current $j_{jk}^{s}$ flowing in the $j$ direction and polarized along the $k$ direction according to

$$j_i^{\mathrm{sH}} = \theta^{\mathrm{sH}} \varepsilon_{ijk} j_{jk}^{s}, \tag{19}$$

where $\varepsilon_{ijk}$ is the Levi-Civita tensor, while $\theta^{\mathrm{sH}}$ is the spin Hall angle. In the superconducting state, in the diffusive limit the spin Hall angle is $\theta^{\mathrm{sH}} = \chi^{\mathrm{sH}} N_S D/D_E$. Here $\chi^{\mathrm{sH}}$ is the normal-state spin Hall angle, whereas $D$ and $D_E$ are renormalized, energy-dependent diffusion coefficients in the superconducting state with a ratio $D/D_E$ that depends only weakly on energy. The key factor in the expression for $\theta^{\mathrm{sH}}$ is the superconducting density of states $N_S$, which strongly depends on energy near the gap edge $E \simeq \Delta$. This result predicts a strong enhancement in the spin Hall angle for quasiparticle energies near the gap $\Delta$, a result that is consistent with the experimental findings of Wakamura *et al.* (2015). However, the total accumulation due to the spin Hall effect, obtained by integrating over all energies, does not show nearly the same magnitude of enhancement as in the experiment. Thus, a complete explanation of the experimental results remains an open question. Additional studies reported efficient spin-charge conversion in spin-split (Jeon, Jeon *et al.*, 2020) and Ising superconductors (Jeon *et al.*, 2021), and a recent theoretical work reported the same enhancement by orders of magnitude in the spin-split case as seen experimentally (Kamra and Linder, 2023). Moreover, a theory incorporating the roles of both intrinsic and extrinsic SOC in the kinetic equations determining the spin-charge conversion was reported (Virtanen, Bergeret, and Tokatly, 2021, 2022).

Another interesting aspect regarding spin Hall phenomena involves pure supercurrent transport: conversion of Cooper pair charge currents to Cooper pair spin currents, and vice versa. Yang, Yang, and Wang (2012) and Linder, Amundsen, and Risinggård (2017) considered this phenomenon in JJs with interfacial SOC and a Zeeman field. They found that applying a phase gradient between the superconductors produced a transversal spin current at the junction interfaces. The physical origin of this effect stems from the $p$-wave superconducting correlations induced by the SOC. As explained in Sec. II.D.1, these correlations can give rise to equilibrium spin currents, provided that they are not phase shifted by $\pi/2$ with respect to the singlet correlations. In a $S/F$ bilayer, the Zeeman field in $F$ will indeed cause such $(\pi/2)$-shifted $p$-wave triplets to appear, having seemingly no observable consequences. However, in a JJ with a phase gradient, $p$-wave triplets induced at the interface to one of the superconductors can be nonzero at the other $S$ interface, modifying the singlet-triplet phase shift and thereby yielding spin currents.

In typical spin Hall phenomenology, an injected current in a given direction is deflected transversely to the injected current while being polarized in a direction transverse to both the injection and deflection axis. The previously considered spin Hall supercurrent behaves similarly, with the polarization of the triplet Cooper pairs carrying the current taking the role of the spin polarization of the resistive current in the conventional case. The superspin Hall effect was later studied in a finite size structure (Risinggård and Linder, 2019), demonstrating that the induced transverse spin supercurrent flow would produce an edge spin $\mathbf{M}$ in a manner similar to the conventional resistive spin Hall effect. The prediction of an

anomalous supercurrent Hall effect in $F$ with a nontrivial spin texture (Yokoyama, 2015) suggests that similar effects could take place in homogeneously magnetized systems with SOC since conversion processes between singlet and triplet Cooper pairs can be shown to be similar in systems with inhomogeneous **M** and systems with homogeneous **M** and SOC (Bergeret and Tokatly, 2014). Indeed, Costa and Fabian (2020) predicted an anomalous Josephson Hall effect and transverse spin supercurrents in JJs with a macrospin $F$ and interfacial SOC.

Whereas the aforementioned studies considered intrinsic Rashba SOC, Bergeret and Tokatly (2016) predicted that dissipationless magnetoelectric phenomena like spin Hall effects with supercurrents should also occur with extrinsic (impurity) SOC. In the diffusive transport, they predicted a nondissipative spin-galvanic effect corresponding to the generation of a supercurrent by a spin-splitting field, in addition to its inverse: a magnetic moment induced by a supercurrent. Edge **M** induced by supercurrents due to interfacial SOC was studied by Silaev, Bobkova, and Bobkov (2020) and Linder and Amundsen (2022). Long-range triplets and controllable $0-\pi$ switching has also been predicted in such systems (Mazanik and Bobkova, 2022). Another path to achieving spin-Hall-like phenomena is to exploit the orbital degrees of freedom (Chirolli *et al.*, 2022; Mercaldo *et al.*, 2022).

## V. OPEN QUESTIONS AND FUTURE DIRECTIONS

As a growing class of novel materials is considered, the understanding of SOC in superconducting hybrid structures and how it can be utilized continues to evolve. SOC, beyond common Rashba and Dresselhaus models, modifies both Cooper pairs and quasiparticle excitations. However, in junctions with common elemental superconductors and conventional semiconductors, even simple SOC models can accurately capture the observed generation of spin-triplet Cooper pairs, the transition to topological superconductivity (Dartiailh *et al.*, 2021), an anomalous phase in Josephson junctions (Mayer *et al.*, 2020), and nonreciprocal phenomena (Nadeem, Fuhrer, and Wang, 2023).

Compared to the generation of spin-triplet superconductivity with multiple ferromagnets or magnetic textures, the presence of SOC can simplify the structure and offer a desirable gate-controlled tunability. With a proximity-induced triplet superconductivity, this gate-tunable SOC is predicted to control superconducting $T_c$ (Ouassou *et al.*, 2016), and its feasibility is experimentally supported by the singlet-to-triplet transition in measurements from Figs. 5(c) and 5(d). An alternative approach is to use tunable magnetic textures and the resulting fringing fields, which have been experimentally shown to yield synthetic SOC in proximity-induced superconductivity (Desjardins *et al.*, 2019). An open experimental challenge is to electrically control tunable magnetic configurations employed in spintronics (Tsymbal and Žutić, 2019), which, in the context of superconducting hybrid structures, could generate spin supercurrents and define topological structures, not by epitaxy but by tunable magnetic textures (Fatin *et al.*, 2016; Zhou *et al.*, 2019; Güngördü and Kovalev, 2022).

The prospect of equal-spin-triplet superconductivity poses many questions for dynamical and nonequilibrium phenomena. For example, how could the resulting spin supercurrents modify magnetization dynamics? In the absence of SOC, supercurrent-induced magnetization dynamics was proposed two decades ago (Waintal and Brouwer, 2002) and studied from first principles (Wang, Tang, and Xia, 2010). The role of SOC, including the spin-orbit and spin-transfer torques generated by spin-triplet supercurrents (Zhao and Sauls, 2008), was also considered (Brydon, Asano, and Timm, 2011; Hals, 2016; Takashima, Fujimoto, and Yokoyama, 2017; Nashaat *et al.*, 2019). Experimentally supercurrent densities are generally too low to compete with the magnetic anisotropy of ferromagnets, although they may influence a nanomagnet (Cai and Chudnovsky, 2010). This suggests that spin supercurrents could modify various magnetic nanotextures (Buzdin, 2008; Linder and Yokoyama, 2011), including domain walls and skyrmions (Kulagina and Linder, 2014; Rabinovich *et al.*, 2019; Tsymbal and Žutić, 2019), potentially to change their topology or implement superconducting counterparts of magnetic racetrack (Hayashi *et al.*, 2008).

Magnetization dynamics in superconducting hybrid structures is an example of nonequilibrium phenomena where, in addition to solving the kinetic equations, suitable boundary conditions describing the interfaces between the different layers are also required. Recently the time-dependent interplay between SOC and superconducting order in a single layer was successfully modeled (Bobkova, Bobkov, and Silaev, 2021). A gate-controlled time-dependent SOC can strongly modify the current-phase relations and drive the JJ dynamics even without any bias current (Monroe, Alidoust, and Žutić, 2022). This work, which has been supported by experiments in planar JJs (Dartiailh *et al.*, 2021), has implications for superconducting spintronics, Majorana states, emerging qubits (Krantz *et al.*, 2019), and enhanced neuromorphic computing (Crotty, Schult, and Segall, 2010). Changes to the current-phase relations for improved $\pi$ qubits using ferromagnetic or $d$-wave JJs (Ioffe *et al.*, 1999; Yamashita *et al.*, 2005) can be generalized via time-dependent gate-tunable SOC and can also realize other paths toward fault-tolerant operations (Brooks, Kitaev, and Preskill, 2013; Larsen *et al.*, 2020; Pita-Vidal *et al.*, 2020; De Simoni *et al.*, 2021; Mercaldo, Ortix, and Cuoco, 2023).

Developing new materials and identifying optimal materials is an active area of investigation that will determine the progress in several of the previously outlined challenges. A prominent example is the growing family of vdW materials where strong SOC can coexist with superconductivity and ferromagnetism (Saito *et al.*, 2016; de la Barrera *et al.*, 2018; Žutić *et al.*, 2019; Sierra *et al.*, 2021), thereby offering a fertile playground to realize nonreciprocal transport, anomalous Josephson effect, topological superconductivity, and triplet supercurrents (Kezilebieke *et al.*, 2020; Cai *et al.*, 2021; Bauriedl *et al.*, 2022; Holleis *et al.*, 2023; Hu *et al.*, 2023; Xie *et al.*, 2023). Controlling superconductivity in vdW materials can be enhanced with chiral molecules (Wan *et al.*, 2023). Their chirality-induced spin selectivity (Naaman, Paltiel, and Waldeck, 2020) connects the chiral structure and the electron spin, which mimics the effects of SOC and magnetism and therefore could support spin-triplet and topological states with

conventional superconductors (Alpern *et al.*, 2021; Ozeri *et al.*, 2023).

Existing materials will continue to play a crucial role for future developments, and a considerable amount of work still needs to be done to understand the full impact of interfaces, particularly interfacial electronic and spin states. Understanding this impact is especially important in oxide systems, where generation of triplet Cooper pairs have long been attributed to noncollinear spins or SOC at the $S/F$ interface without direct experimental observation (Sefrioui *et al.*, 2003; Peña *et al.*, 2004; Keizer *et al.*, 2006; Dybko *et al.*, 2009; Kalcheim *et al.*, 2011; Visani *et al.*, 2012; Yates *et al.*, 2013; Bergeret and Tokatly, 2014; Sanchez-Manzano *et al.*, 2022). While a detailed review of the progress in oxide materials is beyond the scope of this Colloquium, we refer the interested reader to the papers cited by Cuoco and Di Bernardo (2022), which could be relevant for future work on triplet pairing from SOC in oxide systems.

Finally, an interesting direction is combining the emerging field of orbitronics with superconductivity (Fukaya *et al.*, 2018, 2022; Mercaldo *et al.*, 2020, 2022). Since the orbital $M$ can be much greater than spin $M$, this can lead to enhanced magnetoelectric phenomena such as the large supercurrent-induced Edelstein effect (Chirolli *et al.*, 2022).

## LIST OF SYMBOLS AND ABBREVIATIONS

| | |
|---|---|
| 1D | one-dimensional |
| 2D | two-dimensional |
| 2DEG | two-dimensional electron gas |
| ac | alternating current |
| BCS | Bardeen-Cooper-Schrieffer |
| BTK | Blonder-Tinkham-Klapwijk |
| BIA | bulk inversion asymmetry |
| DOS | density of states |
| $F$ | ferromagnet |
| FMR | ferromagnetic resonance |
| FFLO | Fulde-Ferrell-Larkin-Ovchinnikov |
| HM | heavy metal |
| ISHE | inverse spin Hall effect |
| IP | in-plane |
| $I$-$V$ | current-voltage |
| JJ | Josephson junction |
| LE-$\mu$SR | low-energy muon spin rotation |
| MAAR | magnetoanisotropic Andreev reflection |
| MR | magnetoresistance |
| MZM | Majorana zero mode |
| $N$ | normal metal |
| $N/F$ | normal metal/ferromagnet |
| OOP | out-of-plane |
| Py | NiFe, permalloy |
| QD | quantum dot |
| $S$ | superconductor |
| SEM | scanning electron microscope |
| $S/F$ | superconductor/ferromagnet |
| $S/F/S$ | superconductor/ferromagnet/superconductor |
| $S$/HM | superconductor/heavy metal |
| $S$/HM/$F$ | superconductor/heavy metal/ferromagnet |
| SIA | structure inversion asymmetry |
| SPOT | symmetries in the indices of spin, parity, orbit, and time |
| SQUID | superconducting quantum interference device |
| SOC | spin-orbit coupling |
| SOC/$S$ | spin-orbit coupling/superconductor |
| TAMR | tunneling anisotropic magnetoresistance |
| TMR | tunneling magnetoresistance |
| TRS | time-reversal symmetry |
| vdW | van der Waals |

## ACKNOWLEDGMENTS

The authors thank M. Alidoust, F. Aliev, A. Bobkov, I. Bobokova, D. Caso, R. de Sousa, J. Fabian, E. H. Fyhn, F. Giazotto, C. Gonzalez-Ruano, J. E. Han, W. Han, S. Jacobsen, L. G. Johnsen, A. Matos-Abiague, L. A. B. Olde Olthof, J. A. Ouassou, V. Risinggård, J. Shabani, C. Shen, and T. Zhou for the useful discussions. J. L. was supported by the Research Council of Norway through Grant No. 323766, and through its Norwegian Centres of Excellence funding scheme "QuSpin" (Grant No. 262633). J. L. also acknowledges support from Sigma2—the National Infrastructure for High Performance Computing and Data Storage in Norway, Project No. NN9577K. J. W. A. R. acknowledges funding from the EPSRC Programme Grant "Superspin" (Grant No. EP/N017242/1) and EPSRC International Network Grant "Oxide Superspin" (Grant No. EP/P026311/1). I. Ž. was supported by U.S. DOE, Office of Science BES, Award No. DE-SC0004890, the U.S. ONR through Grants No. N000141712793 and MURI No. N000142212764, U.S. NSF ECCS Grants No. 2130845 and No. 1810266, and U.S. AFOSR Grant No. FA9550-22-1-0349. N. B. acknowledges funding from the EPSRC (Grant No. EP/S016430/1) and the support of Loughborough University. J. W. A. R. and N. B. also acknowledge support from EPSRC Henry Royce Institute Recurrent Grant No. EP/R00661X/1. Nordita is funded in part by NordForsk.

## REFERENCES

Aasen, D., *et al.*, 2016, "Milestones toward Majorana-Based Quantum Computing," Phys. Rev. X **6**, 031016.

Abdelmoneim, S. A., Y. M. Shukrinov, K. V. Kulikov, H. ElSamman, and M. Nashaat, 2022, "Locking of magnetization and Josephson oscillations at ferromagnetic resonance in a $\varphi_0$ junction under external radiation," Phys. Rev. B **106**, 014505.

Abrikosov, A. A., L. P. Gor'kov, and Dzyaloshinski, 1975, *Methods of Quantum Field Theory in Statistical Physics* (Dover Publications, New York).

Aguado, R., 2017, "Majorana quasiparticles in condensed matter," Riv. Nuovo Cimento **40**, 523–593.

Alicea, J., 2010, "Majorana fermions in a tunable semiconductor device," Phys. Rev. B **81**, 125318.

Alicea, J., Y. Oreg, G. Refael, F. Von Oppen, and M. P. Fisher, 2011, "Non-Abelian statistics and topological quantum information processing in 1D wire networks," Nat. Phys. **7**, 412–417.

Alidoust, M., 2020, "Critical supercurrent and $\varphi_0$ state for probing a persistent spin helix," Phys. Rev. B **101**, 155123.

Alidoust, M., and K. Halterman, 2015a, "Long-range spin-triplet correlations and edge spin currents in diffusive spin-orbit coupled SNS hybrids with a single spin-active interface," J. Phys. Condens. Matter **27**, 235301.

Alidoust, M., and K. Halterman, 2015b, "Spontaneous edge accumulation of spin currents in finite-size two-dimensional diffusive spin–orbit coupled *SFS* heterostructures," New J. Phys. **17**, 033001.

Alidoust, M., C. Shen, and I. Žutić, 2021, "Cubic spin-orbit coupling and anomalous Josephson effect in planar junctions," Phys. Rev. B **103**, L060503.

Alpern, H., *et al.*, 2021, "Unconventional Meissner screening induced by chiral molecules in a conventional superconductor," Phys. Rev. Mater. **5**, 114801.

Amundsen, M., and J. Linder, 2017, "Supercurrent vortex pinball via a triplet Cooper pair inverse Edelstein effect," Phys. Rev. B **96**, 064508.

Amundsen, M., and J. Linder, 2019, "Quasiclassical theory for interfaces with spin-orbit coupling," Phys. Rev. B **100**, 064502.

Ando, F., Y. Miyasaka, T. Li, J. Ishizuka, T. Arakawa, Y. Shiota, T. Moriyama, Y. Yanase, and T. Ono, 2020, "Observation of superconducting diode effect," Nature (London) **584**, 373–376.

Annunziata, G., H. Enoksen, J. Linder, M. Cuoco, C. Noce, and A. Sudbø, 2011, "Josephson effect in $S/F/S$ junctions: Spin bandwidth asymmetry versus Stoner exchange," Phys. Rev. B **83**, 144520.

Aoki, D., F. Hardy, A. Miyake, V. Taufour, T. D. Matsuda, and J. Flouquet, 2011, "Properties of ferromagnetic superconductors," C.R. Phys. **12**, 573–583.

Armitage, N. P., E. J. Mele, and A. Vishwanath, 2018, "Weyl and Dirac semimetals in three-dimensional solids," Rev. Mod. Phys. **90**, 015001.

Ast, C. R., J. Henk, A. Ernst, L. Moreschini, M. C. Falub, D. Pacilé, P. Bruno, K. Kern, and M. Grioni, 2007, "Giant Spin Splitting through Surface Alloying," Phys. Rev. Lett. **98**, 186807.

Baladié, I., A. Buzdin, N. Ryzhanova, and A. Vedyayev, 2001, "Interplay of superconductivity and magnetism in superconductor/ferromagnet structures," Phys. Rev. B **63**, 054518.

Banerjee, A., *et al.*, 2023, "Signatures of a topological phase transition in a planar Josephson junction," Phys. Rev. B **107**, 245304.

Banerjee, N., J. A. Ouassou, Y. Zhu, N. A. Stelmashenko, J. Linder, and M. G. Blamire, 2018, "Controlling the superconducting transition by spin-orbit coupling," Phys. Rev. B **97**, 184521.

Banerjee, N., J. W. A. Robinson, and M. G. Blamire, 2014, "Reversible control of spin-polarized supercurrents in ferromagnetic Josephson junctions," Nat. Commun. **5**, 4771.

Baumgartner, C., *et al.*, 2022, "Supercurrent rectification and magnetochiral effects in symmetric Josephson junctions," Nat. Nanotechnol. **17**, 39–44.

Bauriedl, L., *et al.*, 2022, "Supercurrent diode effect and magnetochiral anisotropy in few-layer $NbSe_2$," Nat. Commun. **13**, 4266.

Beenakker, C. W. J., 2020, "Search for non-Abelian Majorana braiding statistics in superconductors," SciPost Phys. Lect. Notes **15**, 2.

Bell, C., S. Milikisyants, M. Huber, and J. Aarts, 2008, "Spin Dynamics in a Superconductor-Ferromagnet Proximity System," Phys. Rev. Lett. **100**, 047002.

Belzig, W., F. K. Wilhelm, C. Bruder, G. Schön, and A. D. Zaikin, 1999, "Quasiclassical Green's function approach to mesoscopic superconductivity," Superlattices Microstruct. **25**, 1251–1288.

Benalcazar, W. A., B. A. Bernevig, and T. L. Hughes, 2017, "Quantized electric multipole insulators," Science **357**, 61–66.

Berezinskii, V. L., 1974, "New model of the anisotropic phase of superfluid $He^3$," JETP Lett. **20**, 287–289.

Bergeret, F. S., M. Silaev, P. Virtanen, and T. T. Heikkilä, 2018, "Colloquium: Nonequilibrium effects in superconductors with a spin-splitting field," Rev. Mod. Phys. **90**, 041001.

Bergeret, F. S., and I. V. Tokatly, 2013, "Singlet-Triplet Conversion and the Long-Range Proximity Effect in Superconductor-Ferromagnet Structures with Generic Spin Dependent Fields," Phys. Rev. Lett. **110**, 117003.

Bergeret, F. S., and I. V. Tokatly, 2014, "Spin-orbit coupling as a source of long-range triplet proximity effect in superconductor-ferromagnet hybrid structures," Phys. Rev. B **89**, 134517.

Bergeret, F. S., and I. V. Tokatly, 2016, "Manifestation of extrinsic spin Hall effect in superconducting structures: Nondissipative magnetoelectric effects," Phys. Rev. B **94**, 180502.

Bergeret, F. S., A. F. Volkov, and K. B. Efetov, 2001, "Long-Range Proximity Effects in Superconductor-Ferromagnet Structures," Phys. Rev. Lett. **86**, 4096–4099.

Bergeret, F. S., A. F. Volkov, and K. B. Efetov, 2005, "Odd triplet superconductivity and related phenomena in superconductor-ferromagnet structures," Rev. Mod. Phys. **77**, 1321–1373.

Birge, N. O., and M. Houzet, 2019, "Spin-singlet and spin-triplet Josephson junctions for cryogenic memory," IEEE Magn. Lett. **10**, 4509605.

Blamire, M. G., A. Aziz, and J. W. A. Robinson, 2011, "Nanopillar junctions," Phil. Trans. R. Soc. A **369**, 3198–3213.

Blamire, M. G., C. B. Smiet, N. Banerjee, and J. W. A. Robinson, 2013, "Field modulation of the critical current in magnetic Josephson junctions," Supercond. Sci. Technol. **26**, 055017.

Blonder, G. E., M. Tinkham, and T. M. Klapwijk, 1982, "Transition from metallic to tunneling regimes in superconducting microconstrictions: Excess current, charge imbalance, and supercurrent conversion," Phys. Rev. B **25**, 4515–4532.

Bobkova, I. V., and A. M. Bobkov, 2015, "Long-range spin imbalance in mesoscopic superconductors under Zeeman splitting," JETP Lett. **101**, 118–124.

Bobkova, I. V., and A. M. Bobkov, 2017, "Quasiclassical theory of magnetoelectric effects in superconducting heterostructures in the presence of spin-orbit coupling," Phys. Rev. B **95**, 184518.

Bobkova, I. V., A. M. Bobkov, and M. A. Silaev, 2021, "Dynamic Spin-Triplet Order Induced by Alternating Electric Fields in Superconductor-Ferromagnet-Superconductor Josephson Junctions," Phys. Rev. Lett. **127**, 147701.

Boden, K. M., W. P. Pratt, and N. O. Birge, 2011, "Proximity-induced density-of-states oscillations in a superconductor/strong-ferromagnet system," Phys. Rev. B **84**, 020510(R).

Boutin, S., J. C. Lemyre, and I. Garate, 2018, "Majorana bound state engineering via efficient real-space parameter optimization," Phys. Rev. B **98**, 214512.

Braude, V., and Y. V. Nazarov, 2007, "Fully Developed Triplet Proximity Effect," Phys. Rev. Lett. **98**, 077003.

Bregazzi, A. T., J. A. Ouassou, A. G. T. Coveney, N. A. Stelmashenko, A. Child, A. T. N'Diaye, J. W. A. Robinson, F. K. Dejene, J. Linder, and N. Banerjee, 2024, "Enhanced controllable triplet proximity effect in superconducting spin-orbit coupled spin valves with modified superconductor/ferromagnet interfaces," Appl. Phys. Lett. **124**, 162602.

Brooks, P., A. Kitaev, and J. Preskill, 2013, "Protected gates for superconducting qubits," Phys. Rev. A **87**, 052306.

Brouwer, P. W., M. Duckheim, A. Romito, and F. von Oppen, 2011, "Topological superconducting phases in disordered quantum wires with strong spin-orbit coupling," Phys. Rev. B **84**, 144526.

Brydon, P. M. R., Y. Asano, and C. Timm, 2011, "Spin Josephson effect with a single superconductor," Phys. Rev. B **83**, 180504(R).

Bujnowski, B., R. Biele, and F. S. Bergeret, 2019, "Switchable Josephson current in junctions with spin-orbit coupling," Phys. Rev. B **100**, 224518.

Buzdin, A., 2008, "Direct Coupling Between Magnetism and Superconducting Current in the Josephson $\varphi_0$ Junction," Phys. Rev. Lett. **101**, 107005.

Buzdin, A. I., 2005, "Proximity effects in superconductor-ferromagnet heterostructures," Rev. Mod. Phys. **77**, 935–976.

Bychkov, E. I., and Y. A. Rashba, 1984, "Properties of a 2D electron gas with lifted spectral degeneracy," JETP Lett. **39**, 78–81, https://ui.adsabs.harvard.edu/abs/1984JETPL..39...78B.

Cai, L., and E. M. Chudnovsky, 2010, "Interaction of a nanomagnet with a weak superconducting link," Phys. Rev. B **82**, 104429.

Cai, R., I. Žutić, and W. Han, 2023, "Superconductor/ferromagnet heterostructures: A platform for superconducting spintronics and quantum computation," Adv. Quantum Technol. **6**, 2200080.

Cai, R., *et al.*, 2021, "Evidence for anisotropic spin-triplet Andreev reflection at the 2D van der Waals ferromagnet/superconductor interface," Nat. Commun. **12**, 6725.

Cayao, J., and A. M. Black-Schaffer, 2017, "Odd-frequency superconducting pairing and subgap density of states at the edge of a two-dimensional topological insulator without magnetism," Phys. Rev. B **96**, 155426.

Cayao, J., and A. M. Black-Schaffer, 2018, "Odd-frequency superconducting pairing in junctions with Rashba spin-orbit coupling," Phys. Rev. B **98**, 075425.

Cayao, J., P. Dutta, P. Burset, and A. M. Black-Schaffer, 2022, "Phase-tunable electron transport assisted by odd-frequency Cooper pairs in topological Josephson junctions," Phys. Rev. B **106**, L100502.

Chandrasekhar, V., 2004, *Proximity Coupled Systems: Quasiclassical Theory of Superconductivity*, Vol. 2 (Springer-Verlag, Berlin).

Chang, C. H., and C. Ortix, 2017, "Theoretical prediction of a giant anisotropic magnetoresistance in carbon nanoscrolls," Nano Lett. **17**, 3076–3080.

Chantis, A. N., K. D. Belashchenko, E. Y. Tsymbal, and M. van Schilfgaarde, 2007, "Tunneling Anisotropic Magnetoresistance Driven by Resonant Surface States: First-Principles Calculations on an Fe(001) Surface," Phys. Rev. Lett. **98**, 046601.

Chen, Z. Y., A. Biswas, I. Žutić, T. Wu, S. B. Ogale, R. L. Greene, and T. Venkatesan, 2001, "Spin-polarized transport across a $La_{0.7}Sr_{0.3}MnO_3$ / $YBa_2Cu_3O_{7-x}$ interface: Role of Andreev bound states," Phys. Rev. B **63**, 212508.

Chirolli, L., M. T. Mercaldo, C. Guarcello, F. Giazotto, and M. Cuoco, 2022, "Colossal Orbital Edelstein Effect in Noncentrosymmetric Superconductors," Phys. Rev. Lett. **128**, 217703.

Chou, P. H., C. H. Chen, S. W. Liu, C. H. Chung, and C. Y. Mou, 2021, "Geometry-induced topological superconductivity," Phys. Rev. B **103**, 014508.

Costa, A., and J. Fabian, 2020, "Anomalous Josephson Hall effect charge and transverse spin currents in superconductor/ferromagnetic-insulator/ superconductor junctions," Phys. Rev. B **101**, 104508.

Costa, A., A. Matos-Abiague, and J. Fabian, 2019, "Skew Andreev reflection in ferromagnet/superconductor junctions," Phys. Rev. B **100**, 060507.

Cottier, R. J., B. D. Koehne, J. T. Miracle, D. A. Currie, N. Theodoropoulou, L. Pantelidis, A. Hernandez-Robles, and A. Ponce, 2020, "Strong spin-orbit interactions in a correlated two-dimensional electron system formed in $SrTiO_3(001)$ films grown epitaxially on $p$-Si(001)," Phys. Rev. B **102**, 125423.

Crotty, P., D. Schult, and K. Segall, 2010, "Josephson junction simulation of neurons," Phys. Rev. E **82**, 011914.

Culcer, D., A. C. Keser, Y. Li, and G. Tkachov, 2020, "Transport in two-dimensional topological materials: Recent developments in experiment and theory," 2D Mater. **7**, 022007.

Cuoco, M., and A. Di Bernardo, 2022, "Materials challenges for $SrRuO_3$: From conventional to quantum electronics," APL Mater. **10**, 090902.

Dartiailh, M. C., W. Mayer, J. Yuan, K. S. Wickramasinghe, A. Matos-Abiague, I. Žutić, and J. Shabani, 2021, "Phase Signature of Topological Transition in Josephson Junctions," Phys. Rev. Lett. **126**, 036802 [arXiv:1906.01179].

Das, A., Y. Ronen, Y. Most, Y. Oreg, M. Heiblum, and H. Shtrikman, 2012, "Zero-bias peaks and splitting in an Al–InAs nanowire topological superconductor as a signature of Majorana fermions," Nat. Phys. **8**, 887–895.

Das, K. S., D. Makarov, P. Gentile, M. Cuoco, B. J. Van Wees, C. Ortix, and I. J. Vera-Marun, 2019, "Independent geometrical control of spin and charge resistances in curved spintronics," Nano Lett. **19**, 6839–6844.

Das Sarma, S., M. Freedman, and C. Nayak, 2015, "Majorana zero modes and topological quantum computation," npj Quantum Inf. **1**, 15001.

Das Sarma, S., and H. Pan, 2021, "Disorder-induced zero-bias peaks in Majorana nanowires," Phys. Rev. B **103**, 195158.

Davydova, M., S. Prembabu, and L. Fu, 2022, "Universal Josephson diode effect," Sci. Adv. **8**, eabo0309.

Dayton, I. M., *et al.*, 2018, "Experimental demonstration of a Josephson magnetic memory cell with a programmable $\pi$-junction," IEEE Magn. Lett. **9**, 3301905.

de Gennes, P. G., 1966, "Coupling between ferromagnets through a superconducting layer," Phys. Lett. **23**, 10–11.

de Gennes, P. G., 1999, *Superconductivity of Metals and Alloys*, 2nd ed., Advanced Books Classics (Perseus Books, New York).

de la Barrera, S. C., *et al.*, 2018, "Tuning Ising superconductivity with layer and spin–orbit coupling in two-dimensional transition-metal dichalcogenides," Nat. Commun. **9**, 1427.

Deng, M. T., C. L. Yu, G. Y. Huang, M. Larsson, P. Caroff, and H. Q. Xu, 2012, "Anomalous zero-bias conductance peak in a Nb–InSb nanowire–Nb hybrid device," Nano Lett. **12**, 6414–6419.

Dery, H., H. Wu, B. Ciftcioglu, M. Huang, Y. Song, R. K. Kawakami, J. Shi, I. Krivorotov, I. Žutić, and L. J. Sham, 2012, "Nanospintronics based on magnetologic gates," IEEE Trans. Electron Devices **59**, 259–262.

De Simoni, G., S. Battisti, N. Ligato, M. T. Mercaldo, M. Cuoco, and F. Giazotto, 2021, "Gate control of the current-flux relation of a Josephson quantum interferometer based on proximitized metallic nanojuntions," ACS Appl. Electron. Mater. **3**, 3927–3935.

Desjardins, M. M., *et al.*, 2019, "Synthetic spin-orbit interaction for Majorana devices," Nat. Mater. **18**, 1060–1064.

de Sousa, R., and S. Das Sarma, 2003, "Gate control of spin dynamics in III-V semiconductor quantum dots," Phys. Rev. B **68**, 155330.

Deutscher, G., 2005, "Andreev–Saint-James reflections: A probe of cuprate superconductors," Rev. Mod. Phys. **77**, 109–135.

Di Bernardo, A., *et al.*, 2015, "Intrinsic Paramagnetic Meissner Effect due to $s$-Wave Odd-Frequency Superconductivity," Phys. Rev. X **5**, 041021.

Dirac, P., 1928, "The quantum theory of the electron," Proc. R. Soc. A **117**, 610–624.

Dresselhaus, G., 1955, "Spin-orbit coupling effects in zinc blende structures," Phys. Rev. **100**, 580–586.

Droghetti, A., I. Rungger, A. Rubio, and I. V. Tokatly, 2022, "Spin-orbit induced equilibrium spin currents in materials," Phys. Rev. B **105**, 024409.

D'yakonov, M. I., and V. I. Perel', 1971a, "Current-induced spin orientation of electrons in semiconductors," Phys. Lett. **35A**, 459–460.

D'yakonov, M. I., and V. I. Perel', 1971b, "Possibility of orienting electron spins with current," Pis'ma Zh. Eksp. Teor. Fiz. **13**, 657–670 [JETP Lett. **13**, 467–469 (1971)].

Dybko, K., K. Werner-Malento, P. Aleshkevych, M. Wojcik, M. Sawicki, and P. Przyslupski, 2009, "Possible spin-triplet superconducting phase in the $La_{0.7}Sr_{0.3}MnO_3/YBa_2Cu_3O_7/La_{0.7}Sr_{0.3}MnO_3$ trilayer," Phys. Rev. B **80**, 144504.

Dzyaloshinsky, I., 1958, "A thermodynamic theory of 'weak' ferromagnetism of antiferromagnetics," J. Phys. Chem. Solids **4**, 241–255.

Edelstein, V. M., 1995, "Magnetoelectric Effect in Polar Superconductors," Phys. Rev. Lett. **75**, 2004–2007.

Edelstein, V. M., 1996, "The Ginzburg-Landau equation for superconductors of polar symmetry," J. Phys. Condens. Matter **8**, 339–349.

Edelstein, V. M., 2003, "Triplet superconductivity and magnetoelectric effect near the *s*-wave-superconductor–normal-metal interface caused by local breaking of mirror symmetry," Phys. Rev. B **67**, 020505.

Eilenberger, G., 1968, "Transformation of Gorkov's equation for type II superconductors into transport-like equations," Z. Phys. **214**, 195–213.

Elliot, S. R., and M. Franz, 2015, "Colloquium: Majorana fermions in nuclear, particle, and solid-state physics," Rev. Mod. Phys. **87**, 137–163.

Entin-Wohlman, O., R. I. Shekhter, M. Jonson, and A. Aharony, 2018, "Rashba proximity states in superconducting tunnel junctions," Low Temp. Phys. **44**, 543–551.

Eschrig, M., 2011, "Spin-polarized supercurrents for spintronics," Phys. Today **64**, No. 1, 43–49.

Eschrig, M., 2015, "Spin-polarized supercurrents for spintronics: A review of current progress," Rep. Prog. Phys. **78**, 104501.

Eschrig, M., 2018, "Theory of Andreev bound states in *S-F-S* junctions and *S-F* proximity devices," Phil. Trans. R. Soc. A **376**, 20150149.

Eschrig, M., C. Iniotakis, and Y. Tanaka, 2012, *Properties of Interfaces and Surfaces in Non-centrosymmetric Superconductors* (Springer-Verlag, Berlin), pp. 313–357.

Eschrig, M., J. Kopu, J. C. Cuevas, and G. Schön, 2003, "Theory of Half-Metal/Superconductor Heterostructures," Phys. Rev. Lett. **90**, 137003.

Eskilt, J. R., M. Amundsen, N. Banerjee, and J. Linder, 2019, "Long-ranged triplet supercurrent in a single in-plane ferromagnet with spinorbit coupled contacts to superconductors," Phys. Rev. B **100**, 224519.

Espedal, C., P. Lange, S. Sadjina, A. G. Mal'shukov, and A. Brataas, 2017, "Spin Hall effect and spin swapping in diffusive superconductors," Phys. Rev. B **95**, 054509.

Espedal, C., T. Yokoyama, and J. Linder, 2016, "Anisotropic Paramagnetic Meissner Effect by Spin-Orbit Coupling," Phys. Rev. Lett. **116**, 127002.

Fabian, J., A. Matos-Abiague, C. Ertler, P. Stano, and I. Žutić, 2007, "Semiconductor spintronics," Acta Phys. Slovaca **57**, 565–907.

Faraday, M., 1846, "I. Experimental researches in electricity.—Nineteenth series," Phil. Trans. R. Soc. London **136**, 1–20.

Fatin, G. L., A. Matos-Abiague, B. Scharf, and I. Žutić, 2016, "Wireless Majorana Bound States: From Magnetic Tunability to Braiding," Phys. Rev. Lett. **117**, 077002.

Feng, D. C., M. Z. Zheng, Y. Qun, Z. P. Niu, and D. Y. Xing, 2008, "Origin of the spin-triplet Andreev reflection at ferromagnet/*s*-wave superconductor interface," J. Appl. Phys. **103**, 023921.

Feofanov, A. K., *et al.*, 2010, "Implementation of superconductor/ferromagnet/superconductor $\pi$-shifters in superconducting digital and quantum circuits," Nat. Phys. **6**, 593–597.

Fermin, R., N. M. A. Scheinowitz, J. Aarts, and K. Lahabi, 2022, "Mesoscopic superconducting memory based on bistable magnetic textures," Phys. Rev. Res. **4**, 033136.

Fermin, R., D. van Dinter, M. Hubert, B. Woltjes, M. Silaev, J. Aarts, and K. Lahabi, 2022, "Superconducting triplet rim currents in a spin-textured ferromagnetic disk," Nano Lett. **22**, 2209–2216.

Ferriani, P., K. Von Bergmann, E. Y. Vedmedenko, S. Heinze, M. Bode, M. Heide, G. Bihlmayer, S. Blügel, and R. Wiesendanger, 2008, "Atomic-Scale Spin Spiral with a Unique Rotational Sense: Mn Monolayer on W(001)," Phys. Rev. Lett. **101**, 027201.

Fittipaldi, R., *et al.*, 2021, "Unveiling unconventional magnetism at the surface of $Sr_2RuO_4$," Nat. Commun. **12**, 5792.

Flokstra, M. G., S. J. Ray, S. J. Lister, J. Aarts, H. Luetkens, T. Prokscha, A. Suter, E. Morenzoni, and S. L. Lee, 2014, "Measurement of the spatial extent of inverse proximity in a Py/Nb/Py superconducting trilayer using low-energy muon-spin rotation," Phys. Rev. B **89**, 054510.

Flokstra, M. G., R. Stewart, N. Satchell, G. Burnell, H. Luetkens, T. Prokscha, A. Suter, E. Morenzoni, S. Langridge, and S. L. Lee, 2018, "Observation of Anomalous Meissner Screening in Cu/Nb and Cu/Nb/Co Thin Films," Phys. Rev. Lett. **120**, 247001.

Flokstra, M. G., *et al.*, 2016, "Remotely induced magnetism in a normal metal using a superconducting spin-valve," Nat. Phys. **12**, 57–61.

Fominov, Y. V., A. A. Golubov, T. Y. Karminskaya, M. Y. Kupriyanov, R. G. Deminov, and L. R. Tagirov, 2010, "Superconducting triplet spin valve," JETP Lett. **91**, 308–313.

Fornieri, A., *et al.*, 2019, "Evidence of topological superconductivity in planar Josephson junctions," Nature (London) **569**, 89–92.

Francica, G., M. Cuoco, and P. Gentile, 2020, "Topological superconducting phases and Josephson effect in curved superconductors with time reversal invariance," Phys. Rev. B **101**, 094504.

Francica, G., P. Gentile, and M. Cuoco, 2019, "Effects of geometry on spin-orbit Kramers states in semiconducting nanorings," Europhys. Lett. **127**, 30001.

Fu, L., and C. L. Kane, 2008, "Superconducting Proximity Effect and Majorana Fermions at the Surface of a Topological Insulator," Phys. Rev. Lett. **100**, 096407.

Fukaya, Y., S. Tamura, K. Yada, Y. Tanaka, P. Gentile, and M. Cuoco, 2018, "Interorbital topological superconductivity in spin-orbit coupled superconductors with inversion symmetry breaking," Phys. Rev. B **97**, 174522.

Fukaya, Y., Y. Tanaka, P. Gentile, K. Yada, and M. Cuoco, 2022, "Anomalous Josephson coupling and high-harmonics in non-centrosymmetric superconductors with *S*-wave spin-triplet pairing," npj Quantum Mater. **7**, 99.

Fulde, P., and R. A. Ferrell, 1964, "Superconductivity in a strong spin-exchange field," Phys. Rev. **135**, A550–A563.

Gentile, P., M. Cuoco, and C. Ortix, 2015, "Edge States and Topological Insulating Phases Generated by Curving a Nanowire with Rashba Spinorbit Coupling," Phys. Rev. Lett. **115**, 256801.

Gentile, P., M. Cuoco, A. Romano, C. Noce, D. Manske, and P. M. R. Brydon, 2013, "Spin-Orbital Coupling in a Triplet Superconductor-Ferromagnet Junction," Phys. Rev. Lett. **111**, 097003.

Geshkenbein, V. B., and A. I. Larkin, 1986, "The Josephson effect in superconductors with heavy fermions," Pis'ma Zh. Eksp. Teor. Fiz. **43**, 306–309 [JETP Lett. **43**, 395–399 (1986)].

Ginzburg, V. L., and L. D. Landau, 1950, "On the theory of superconductivity," Zh. Eksp. Teor. Fiz. **20**, 1064–1082.

Giroud, M., H. Courtois, K. Hasselbach, D. Mailly, and B. Pannetier, 1998, "Superconducting proximity effect in a mesoscopic ferromagnetic wire," Phys. Rev. B **58**, R11872.

Gmitra, M., A. Matos-Abiague, C. Draxl, and J. Fabian, 2013, "Magnetic Control of Spin-Orbit Fields: A First-Principles Study of Fe/GaAs Junctions," Phys. Rev. Lett. **111**, 036603.

Golovchanskiy, I., N. Abramov, V. Stolyarov, V. Chichkov, M. Silaev, I. Shchetinin, A. Golubov, V. Ryazanov, A. Ustinov, and M. Kupriyanov, 2020, "Magnetization Dynamics in Proximity-Coupled Superconductor-Ferromagnet-Superconductor Multilayers," Phys. Rev. Appl. **14**, 024086.

Golubov, A. A., M. Y. Kupriyanov, and E. Il'ichev, 2004, "The current-phase relation in Josephson junctions," Rev. Mod. Phys. **76**, 411–469.

González-Ruano, C., D. Caso, L. G. Johnsen, C. Tiusan, M. Hehn, N. Banerjee, J. Linder, and F. G. Aliev, 2021, "Superconductivity assisted change of the perpendicular magnetic anisotropy in V/MgO/Fe junctions," Sci. Rep. **11**, 19041.

González-Ruano, C., L. G. Johnsen, D. Caso, C. Tiusan, M. Hehn, N. Banerjee, J. Linder, and F. G. Aliev, 2020, "Superconductivityinduced change in magnetic anisotropy in epitaxial ferromagnetsuperconductor hybrids with spin-orbit interaction," Phys. Rev. B **102**, 020405.

Gorini, C., P. Schwab, R. Raimondi, and A. L. Shelankov, 2010, "Non-Abelian gauge fields in the gradient expansion: Generalized Boltzmann and Eilenberger equations," Phys. Rev. B **82**, 195316.

Gor'kov, L. P., 1959, "Microscopic derivation of the Ginzburg-Landau equations in the theory of superconductivity," Sov. Phys. JETP **36**, 1364–1367.

Gor'kov, L. P., and E. I. Rashba, 2001, "Superconducting 2D System with Lifted Spin Degeneracy: Mixed Singlet-Triplet State," Phys. Rev. Lett. **87**, 037004.

Gould, C., C. Rüster, T. Jungwirth, E. Girgis, G. M. Schott, R. Giraud, K. Brunner, G. Schmidt, and L. W. Molenkamp, 2004, "Tunneling Anisotropic Magnetoresistance: A Spin-Valve-Like Tunnel Magnetoresistance Using a Single Magnetic Layer," Phys. Rev. Lett. **93**, 117203.

Grein, R., M. Eschrig, G. Metalidis, and G. Schön, 2009, "Spin-Dependent Cooper Pair Phase and Pure Spin Supercurrents in Strongly Polarized Ferromagnets," Phys. Rev. Lett. **102**, 227005.

Griffin, A., and J. Demers, 1971, "Tunneling in the normal-metal-insulator-superconductor geometry using the Bogoliubov equations of motion," Phys. Rev. B **4**, 2202–2208.

Gu, J. Y., C.-Y. You, J. S. Jiang, J. Pearson, Y. B. Bazaliy, and S. D. Bader, 2002, "Magnetization-Orientation Dependence of the Superconducting Transition Temperature in the Ferromagnet-Superconductor-Ferromagnet System: CuNi/Nb/CuNi," Phys. Rev. Lett. **89**, 267001.

Güngördü, U., and A. A. Kovalev, 2022, "Majorana bound states with chiral magnetic textures," J. Appl. Phys. **132**, 041101.

Güngördü, U., S. Sandhoefner, and A. A. Kovalev, 2018, "Stabilization and control of Majorana bound states with elongated skyrmion," Phys. Rev. B **97**, 115136.

Hals, K. M. D., 2016, "Supercurrent-induced spin-orbit torques," Phys. Rev. B **93**, 115431.

Halterman, K., and O. T. Valls, 2009, "Emergence of triplet correlations in superconductor/half-metallic nanojunctions with spin-active interfaces," Phys. Rev. B **80**, 104502.

Halterman, K., O. T. Valls, and C.-T. Wu, 2015, "Charge and spin currents in ferromagnetic Josephson junctions," Phys. Rev. B **92**, 174516.

Hayashi, M., L. Thomas, R. Moriya, C. Rettner, and S. S. P. Parkin, 2008, "Current-controlled magnetic domain-wall nanowire shift register," Science **320**, 209–211.

He, J. J., Y. Tanaka, and N. Nagaosa, 2022, "A phenomenological theory of superconductor diodes," New J. Phys. **24**, 053014.

Heinze, S., K. Von Bergmann, M. Menzel, J. Brede, A. Kubetzka, R. Wiesendanger, G. Bihlmayer, and S. Blügel, 2011, "Spontaneous atomic-scale magnetic skyrmion lattice in two dimensions," Nat. Phys. **7**, 713–718.

Hell, M., K. Flensberg, and M. Leijnse, 2017, "Coupling and braiding Majorana bound states in networks defined in two-dimensional electron gases with proximity-induced superconductivity," Phys. Rev. B **96**, 035444.

Hell, M., M. Leijnse, and K. Flensberg, 2017, "Two-Dimensional Platform for Networks of Majorana Bound States," Phys. Rev. Lett. **118**, 107701.

Hillier, A. D., *et al.*, 2022, "Muon spin spectroscopy," Nat. Rev. Methods Primers **2**, 5.

Hirohata, A., K. Yamada, Y. Nakatani, L. Prejbeanu, B. Diény, P. Pirro, and B. Hillebrands, 2020, "Review on spintronics: Principles and device applications," J. Magn. Magn. Mater. **509**, 166711.

Hirsch, J. E., 1999, "Spin Hall Effect," Phys. Rev. Lett. **83**, 1834.

Högl, P., A. Matos-Abiague, I. Žutić, and J. Fabian, 2015, "Magnetoanisotropic Andreev Reflection in Ferromagnet-Superconductor Junctions," Phys. Rev. Lett. **115**, 116601.

Holleis, L., C. L. Patterson, Y. Zhang, H. M. Yoo, H. Zhou, T. Taniguchi, K. Watanabe, S. Nadj-Perge, and A. F. Young, 2023, "Ising superconductivity and nematicity in Bernal bilayer graphene with strong spin orbit coupling," arXiv:2303.00742.

Holmes, D. S., A. L. Ripple, and M. A. Manheimer, 2013, "Energy-efficient superconducting computing - power budgets and requirements," IEEE Trans. Appl. Supercond. **23**, 1701610.

Hou, Y., *et al.*, 2023, "Ubiquitous Superconducting Diode Effect in Superconductor Thin Films," Phys. Rev. Lett. **131**, 027001.

Hu, G., C. Wang, S. Wang, Y. Zhang, Y. Feng, Z. Wang, Q. Niu, Z. Zhang, and B. Xiang, 2023, "Long-range skin Josephson supercurrent across a van der Waals ferromagnet," Nat. Commun. **14**, 1779.

Hu, J., C. Wu, and X. Dai, 2007, "Proposed Design of a Josephson Diode," Phys. Rev. Lett. **99**, 067004.

Huang, C., I. V. Tokatly, and F. S. Bergeret, 2018, "Extrinsic spin-charge coupling in diffusive superconducting systems," Phys. Rev. B **98**, 144515.

Huang, Y.-P., and P. Kotetes, 2023, "Mechanisms for magnetic skyrmion catalysis and topological superconductivity," Phys. Rev. Res. **5**, 013125.

Hübler, F., M. J. Wolf, D. Beckmann, and H. v. Löhneysen, 2012, "Long-Range Spin-Polarized Quasiparticle Transport in Mesoscopic Al Superconductors with a Zeeman Splitting," Phys. Rev. Lett. **109**, 207001.

Ikegaya, S., W. B. Rui, D. Manske, and A. P. Schnyder, 2021, "Tunable Majorana corner modes in noncentrosymmetric superconductors: Tunneling spectroscopy and edge imperfections," Phys. Rev. Res. **3**, 023007.

Ilić, S., and F. S. Bergeret, 2022, "Theory of the Supercurrent Diode Effect in Rashba Superconductors with Arbitrary Disorder," Phys. Rev. Lett. **128**, 177001.

Ioffe, L. B., V. B. Geshkenbein, M. V. Feigel'man, A. L. Fauchére, and G. Blatter, 1999, "Environmentally decoupled *sds*-wave

Josephson junctions for quantum computing," Nature (London) **398**, 679–681.
Ivanov, D. A., 2001, "Non-Abelian Statistics of Half-Quantum Vortices in *p*-Wave Superconductors," Phys. Rev. Lett. **86**, 268–271.
Jackson, J. D., 1998, *Classical Electrodynamics*, 3rd ed. (Wiley, Hoboken, NJ).
Jacobsen, S. H., I. Kulagina, and J. Linder, 2016, "Controlling superconducting spin flow with spin-flip immunity using a single homogeneous ferromagnet," Sci. Rep. **6**, 23926.
Jacobsen, S. H., J. A. Ouassou, and J. Linder, 2015, "Critical temperature and tunneling spectroscopy of superconductor-ferromagnet hybrids with intrinsic Rashba-Dresselhaus spin-orbit coupling," Phys. Rev. B **92**, 024510.
Jeon, K.-R., K. Cho, A. Chakraborty, J.-C. Jeon, J. Yoon, H. Han, J.-K. Kim, and S. S. P. Parkin, 2021, "Role of two-dimensional ising superconductivity in the nonequilibrium quasiparticle spin-to-charge conversion efficiency," ACS Nano **15**, 16819–16827.
Jeon, K.-R., C. Ciccarelli, A. J. Ferguson, H. Kurebayashi, L. F. Cohen, X. Montiel, M. Eschrig, J. W. Robinson, and M. G. Blamire, 2018, "Enhanced spin pumping into superconductors provides evidence for superconducting pure spin currents," Nat. Mater. **17**, 499–503.
Jeon, K.-R., C. Ciccarelli, H. Kurebayashi, L. F. Cohen, X. Montiel, M. Eschrig, S. Komori, J. W. A. Robinson, and M. G. Blamire, 2019, "Exchange-field enhancement of superconducting spin pumping," Phys. Rev. B **99**, 024507.
Jeon, K.-R., J.-C. Jeon, X. Zhou, A. Migliorini, J. Yoon, and S. S. P. Parkin, 2020, "Giant transition-state quasiparticle spin-Hall effect in an exchange-spin-split superconductor detected by nonlocal magnon spin transport," ACS Nano **14**, 15874–15883.
Jeon, K.-R., *et al.*, 2019, "Effect of Meissner Screening and Trapped Magnetic Flux on Magnetization Dynamics in Thick $Nb/Ni_{80}Fe_{20}/Nb$ Trilayers," Phys. Rev. Appl. **11**, 014061.
Jeon, K.-R., *et al.*, 2020, "Tunable Pure Spin Supercurrents and the Demonstration of Their Gateability in a Spin-Wave Device," Phys. Rev. X **10**, 031020.
Johnsen, L. G., N. Banerjee, and J. Linder, 2019, "Magnetization reorientation due to the superconducting transition in heavy-metal heterostructures," Phys. Rev. B **99**, 134516.
Johnsen, L. G., K. Svalland, and J. Linder, 2020, "Controlling the Superconducting Transition by Rotation of an Inversion Symmetry-Breaking Axis," Phys. Rev. Lett. **125**, 107002.
Jones, N., 2018, "The information factories," Nature (London) **561**, 163–166.
Joynt, R., and L. Taillefer, "The superconducting phases of $UPt_3$," 2002, Rev. Mod. Phys. **74**, 235–294.
Kadigrobov, A., R. I. Shekhter, and M. Jonson, 2001, "Quantum spin fluctuations as a source of long-range proximity effects in diffusive ferromagnet-super conductor structures," Europhys. Lett. **54**, 394.
Kalcheim, Y., I. Felner, O. Millo, T. Kirzhner, G. Koren, A. Di Bernardo, M. Egilmez, M. G. Blamire, and J. W. A. Robinson, 2014, "Magnetic field dependence of the proximity-induced triplet superconductivity at ferromagnet/superconductor interfaces," Phys. Rev. B **89**, 180506.
Kalcheim, Y., T. Kirzhner, G. Koren, and O. Millo, 2011, "Long-range proximity effect in $La_{2/3}Ca_{1/3}MnO_3/(100)YBa_2Cu_3O_{7-\delta}$ ferromagnet/superconductor bilayers: Evidence for induced triplet superconductivity in the ferromagnet," Phys. Rev. B **83**, 064510.
Kalcheim, Y., O. Millo, A. Di Bernardo, A. Pal, and J. W. A. Robinson, 2015, "Inverse proximity effect at superconductor-ferromagnet interfaces: Evidence for induced triplet pairing in the superconductor," Phys. Rev. B **92**, 060501(R).
Kalcheim, Y., O. Millo, M. Egilmez, J. W. A. Robinson, and M. G. Blamire, 2012, "Evidence for anisotropic triplet superconductor order parameter in half-metallic ferromagnetic $La_{0.7}Ca_{0.3}Mn_3O$ proximity coupled to superconducting $Pr_{1.85}Ce_{0.15}CuO_4$,," Phys. Rev. B **85**, 104504.
Kallin, C., 2012, "Chiral *p*-wave order in $Sr_2RuO_4$," Rep. Prog. Phys. **75**, 042501.
Kamra, L. J., and J. Linder, 2023, "Inverse spin-Hall effect and spin-swapping in spin-split superconductors," arXiv:2305.18525.
Kang, K., S. Jiang, H. Berger, K. Watanabe, T. Taniguchi, L. Forró, J. Shan, and K. F. Mak, 2021, "Giant anisotropic magnetoresistance in Ising superconductor-magnetic insulator tunnel junctions," arXiv:2101.01327.
Kaur, R. P., D. F. Agterberg, and M. Sigrist, "Helical Vortex Phase in the Noncentrosymmetric $CePt_3Si$," 2005, Phys. Rev. Lett. **94**, 137002.
Keizer, R. S., S. T. B. Goennenwein, T. M. Klapwijk, G. Miao, and A. Gupta, 2006, "A spin triplet supercurrent through the half-metallic ferromagnet $CrO_2$," Nature (London) **439**, 825–827.
Kerr, J., 1877, "XLIII. On rotation of the plane of polarization by reflection from the pole of a magnet," Philos. Mag. **3**, 321–343.
Kezilebieke, S., M. N. Huda, V. Vaňo, M. Aapro, S. C. Ganguli, O. J. Silveira, S. Glodzik, A. S. Foster, T. Ojanen, and P. Liljeroth, 2020, "Topological superconductivity in a van der Waals heterostructure," Nature (London) **588**, 424–428.
Khaire, T. S., M. A. Khasawneh, W. P. Pratt, and N. O. Birge, 2010, "Observation of Spin-Triplet Superconductivity in Co-Based Josephson Junctions," Phys. Rev. Lett. **104**, 137002.
Kim, H., A. Palacio-Morales, T. Posske, L. Rózsa, K. Palotás, L. Szunyogh, M. Thorwart, and R. Wiesendanger, 2018, "Toward tailoring Majorana bound states in artificially constructed magnetic atom chains on elemental superconductors," Sci. Adv. **4**, eaar5251.
Kim, S. K., S. Tewari, and Y. Tserkovnyak, 2015, "Control and braiding of Majorana fermions bound to magnetic domain walls," Phys. Rev. B **92**, 020412(R).
Kitaev, A. Y., 2001, "Unpaired Majorana fermions in quantum wires," Phys. Usp. **44**, 131–136.
Kitaev, A. Y., 2003, "Fault-tolerant quantum computation by anyons," Ann. Phys. (Amsterdam) **303**, 2–30.
Kjaergaard, M., K. Wölms, and K. Flensberg, 2012, "Majorana fermions in superconducting nanowires without spin-orbit coupling," Phys. Rev. B **85**, 020503(R).
Kjaergaard, M., *et al.*, 2016, "Quantized conductance doubling and hard gap in a two-dimensional semiconductor-superconductor heterostructure," Nat. Commun. **7**, 12841.
Klinovaja, J., P. Stano, and D. Loss, 2012, "Transition from Fractional to Majorana Fermions in Rashba Nanowires," Phys. Rev. Lett. **109**, 236801.
Konschelle, F., I. V. Tokatly, and F. S. Bergeret, 2015, "Theory of the spingalvanic effect and the anomalous phase shift $\varphi_0$ in superconductors and Josephson junctions with intrinsic spin-orbit coupling," Phys. Rev. B **92**, 125443.
Konschelle, F., I. V. Tokatly, and F. S. Bergeret, 2016, "Ballistic Josephson junctions in the presence of generic spin dependent fields," Phys. Rev. B **94**, 014515.
Kontani, H., J. Goryo, and D. S. Hirashima, 2009, "Intrinsic Spin Hall Effect in the *s*-Wave Superconducting State: Analysis of the Rashba Model," Phys. Rev. Lett. **102**, 086602.
Kontos, T., M. Aprili, J. Lesueur, F. Genêt, B. Stephanidis, and R. Boursier, 2002, "Josephson Junction through a Thin Ferromagnetic Layer: Negative Coupling," Phys. Rev. Lett. **89**, 137007.

Krantz, P., M. Kjaergaard, F. Yan, T. P. Orlando, S. Gustavsson, and W. D. Oliver, 2019, "A quantum engineer's guide to superconducting qubits," Appl. Phys. Rev. **6**, 021318.

Krich, J. J., and B. I. Halperin, 2007, "Cubic Dresselhaus Spin-Orbit Coupling in 2D Electron Quantum Dots," Phys. Rev. Lett. **98**, 226802.

Kriener, M., K. Segawa, Z. Ren, S. Sasaki, and Y. Ando, 2011, "Bulk Superconducting Phase with a Full Energy Gap in the Doped Topological Insulator $Cu_xBi_2Se_3$," Phys. Rev. Lett. **106**, 127004.

Kulagina, I., and J. Linder, 2014, "Spin supercurrent, magnetization dynamics, and $\varphi$-state in spin-textured Josephson junctions," Phys. Rev. B **90**, 054504.

Lahtinen, V. T., and J. K. Pachos, 2017, "A short introduction to topological quantum computation," SciPost Phys. **3**, 021.

Larkin, Y. N., and A. I. Ovchinnikov, 1964, "Inhomogeneous state of superconductors," Zh. Eksp. Teor. Fiz. **47**, 1136–1146 [Sov. Phys. JETP **20**, 762–769 (1965)].

Larsen, T. W., M. E. Gershenson, L. Casparis, A. Kringhoj, N. J. Pearson, R. P. G. McNeil, F. Kuemmeth, P. Krogstrup, K. D. Petersson, and C. M. Marcus, 2020, "Parity-Protected Superconductor-Semiconductor Qubit," Phys. Rev. Lett. **125**, 056801.

Lawrence, M. D., and N. Giordano, 1999, "Proximity effects in superconductor-ferromagnet junctions," J. Phys. Condens. Matter **11**, 1089–1094.

Lee, S., and Y.-K. Kwon, 2020, "Unveiling giant hidden Rashba effects in two-dimensional $Si_2Bi_2$," npj 2D Mater. Appl. **4**, 45.

Leggett, A. J., 1975, "A theoretical description of the new phases of liquid $^3$He," Rev. Mod. Phys. **47**, 331–414.

Leksin, P. V., N. N. Garif'yanov, I. A. Garifullin, Y. V. Fominov, J. Schumann, Y. Krupskaya, V. Kataev, O. G. Schmidt, and B. Büchner, 2012, "Evidence for Triplet Superconductivity in a Superconductor-Ferromagnet Spin Valve," Phys. Rev. Lett. **109**, 057005.

Li, L.-L., Y.-L. Zhao, X.-X. Zhang, and Y. Sun, 2018, "Possible evidence for spin-transfer torque induced by spin-triplet supercurrents," Chin. Phys. Lett. **35**, 077401.

Lindemann, M., G. Xu, T. Pusch, R. Michalzik, M. R. Hofmann, I. Žutić, and N. C. Gerhardt, 2019, "Ultrafast spin-lasers," Nature (London) **568**, 212–215.

Linder, J., and M. Amundsen, 2022, "Quasiclassical boundary conditions for spin-orbit coupled interfaces with spin-charge conversion," Phys. Rev. B **105**, 064506.

Linder, J., M. Amundsen, and V. Risinggård, 2017, "Intrinsic superspin Hall current," Phys. Rev. B **96**, 094512.

Linder, J., and A. V. Balatsky, 2019, "Odd-frequency superconductivity," Rev. Mod. Phys. **91**, 045005.

Linder, J., and J. W. A. Robinson, 2015, "Superconducting spintronics," Nat. Phys. **11**, 307–315.

Linder, J., and T. Yokoyama, 2011, "Supercurrent-induced magnetization dynamics in a Josephson junction with two misaligned ferromagnetic layers," Phys. Rev. B **83**, 012501.

Linder, J., T. Yokoyama, and A. Sudbø, 2009, "Theory of superconducting and magnetic proximity effect in $S/F$ structures with inhomogeneous magnetization textures and spin-active interfaces," Phys. Rev. B **79**, 054523.

Liu, H., E. Marcellina, A. R. Hamilton, and D. Culcer, 2018, "Strong Spin-Orbit Contribution to the Hall Coefficient of Two-Dimensional Hole Systems," Phys. Rev. Lett. **121**, 087701.

Liu, J.-F., and K. S. Chan, 2010, "Anomalous Josephson current through a ferromagnetic trilayer junction," Phys. Rev. B **82**, 184533.

Liu, J.-F., Y. Xu, and J. Wang, 2017, "Identifying the chiral $d$-wave superconductivity by Josephson $\varphi_0$-states," Sci. Rep. **7**, 43899.

Luethi, M., K. Laubscher, S. Bosco, D. Loss, and J. Klinovaja, 2023, "Planar Josephson junctions in germanium: Effect of cubic spin-orbit interaction," Phys. Rev. B **107**, 035435.

Lutchyn, R. M., J. D. Sau, and S. Das Sarma, 2010, "Majorana Fermions and a Topological Phase Transition in Semiconductor-Superconductor Heterostructures," Phys. Rev. Lett. **105**, 077001.

Lv, P., Y.-F. Zhou, N.-X. Yang, and Q.-F. Sun, 2018, "Magneto-anisotropic spin-triplet Andreev reflection in ferromagnet-Ising superconductor junctions," Phys. Rev. B **97**, 144501.

Mackenzie, A. P., and Y. Maeno, 2003, "The superconductivity of $Sr_2RuO_4$ and the physics of spin-triplet pairing," Rev. Mod. Phys. **75**, 657–712.

Maekawa, S., 2006, Ed., *Concepts in Spin Electronics* (Oxford University Press, Oxford).

Maekawa, S., S. Valenzuela, E. Saitoh, and T. Kimura, 2012, Eds., *Spin Current* (Oxford University Press, New York).

Maeno, Y., H. Hashimoto, K. Yoshida, S. Nishizaki, T. Fujita, J. G. Bednorz, and F. Lichtenberg, 1994, "Superconductivity in a layered perovskite without copper," Nature (London) **372**, 532–534.

Mal'shukov, A. G., and C. S. Chu, 2008, "Spin Hall effect in a Josephson contact," Phys. Rev. B **78**, 104503.

Mal'shukov, A. G., and C. S. Chu, 2011, "Spin-Hall current and spin polarization in an electrically biased SNS Josephson junction," Phys. Rev. B **84**, 054520.

Mal'shukov, A. G., S. Sadjina, and A. Brataas, 2010, "Inverse spin Hall effect in superconductor/normal-metal/superconductor Josephson junctions," Phys. Rev. B **81**, 060502.

Manna, S., P. Wei, Y. Xie, and J. S. Moodera, 2020, "Signature of a pair of Majorana zero modes in superconducting gold surface states," Proc. Natl. Acad. Sci. U.S.A. **117**, 8775–8782.

Marder, M. P., 2010, *Condensed Matter Physics*, 2nd ed. (Wiley, Hoboken, NJ).

Marra, P., and M. Cuoco, 2017, "Controlling Majorana states in topologically inhomogeneous superconductors," Phys. Rev. B **95**, 140504(R).

Martínez, I., *et al.*, 2020, "Interfacial Spin-Orbit Coupling: A Platform for Superconducting Spintronics," Phys. Rev. Appl. **13**, 014030.

Matos-Abiague, A., J. Shabani, A. D. Kent, G. L. Fatin, B. Scharf, and I. Žutić, 2017, "Tunable magnetic textures: From Majorana bound states to braiding," Solid State Commun. **262**, 1–6.

Mayer, W., M. C. Dartiailh, J. Yuan, K. S. Wickramasinghe, E. Rossi, and J. Shabani, 2020, "Gate controlled anomalous phase shift in Al/InAs Josephson junctions," Nat. Commun. **11**, 212.

Mazanik, A. A., and I. V. Bobkova, 2022, "Supercurrent-induced long-range triplet correlations and controllable Josephson effect in superconductor/ferromagnet hybrids with extrinsic spin-orbit coupling," Phys. Rev. B **105**, 144502.

Meier, F., and B. P. Zakharchenya, 1984, *Optical Orientation* (North-Holland, New York).

Mel'Nikov, A. S., A. V. Samokhvalov, S. M. Kuznetsova, and A. I. Buzdin, 2012, "Interference Phenomena and Long-Range Proximity Effect in Clean Superconductor-Ferromagnet Systems," Phys. Rev. Lett. **109**, 237006.

Mercaldo, M. T., C. Ortix, and M. Cuoco, 2023, "High orbital-moment cooper pairs by crystalline symmetry breaking," Adv. Quantum Technol. **6**, 2300081.

Mercaldo, M. T., C. Ortix, F. Giazotto, and M. Cuoco, 2022, "Orbital vortices in $s$-wave spin-singlet superconductors in zero magnetic field," Phys. Rev. B **105**, L140507.

Mercaldo, M. T., P. Solinas, F. Giazotto, and M. Cuoco, 2020, "Electrically Tunable Superconductivity Through Surface Orbital Polarization," Phys. Rev. Appl. **14**, 034041.

Meservey, R., and P. M. Tedrow, 1994, "Spin-polarized electron tunneling," Phys. Rep. **238**, 173–243.

Millis, A., D. Rainer, and J. A. Sauls, 1988, "Quasiclassical theory of superconductivity near magnetically active interfaces," Phys. Rev. B **38**, 4504–4515.

Miron, I. M., G. Gaudin, S. Auffret, B. Rodmacq, A. Schuhl, S. Pizzini, J. Vogel, and P. Gambardella, 2010, "Current-driven spin torque induced by the Rashba effect in a ferromagnetic metal layer," Nat. Mater. **9**, 230–234.

Mironov, S., and A. Buzdin, 2017, "Spontaneous Currents in Superconducting Systems with Strong Spin-Orbit Coupling," Phys. Rev. Lett. **118**, 077001.

Mironov, S. V., and A. Buzdin, 2014, "Standard, inverse, and triplet spinvalve effects in $F_1/S/F_2$ systems," Phys. Rev. B **89**, 144505.

Mohanta, N., T. Zhou, J. Xu, J. E. Han, A. D. Kent, J. Shabani, I. Žutić, and A. Matos-Abiague, 2019, "Electrical Control of Majorana Bound States Using Magnetic Stripes," Phys. Rev. Appl. **12**, 034048.

Monroe, D., M. Alidoust, and I. Žutić, 2022, "Tunable Planar Josephson Junctions Driven by Time-Dependent Spin-Orbit Coupling," Phys. Rev. Appl. **18**, L031001.

Montiel, X., and M. Eschrig, 2018, "Generation of pure superconducting spin current in magnetic heterostructures via nonlocally induced magnetism due to Landau Fermi liquid effect," Phys. Rev. B **98**, 104513.

Moraru, I. C., W. P. Pratt, and N. O. Birge, 2006, "Observation of standard spin-switch effects in ferromagnet/superconductor/ferromagnet trilayers with a strong ferromagnet," Phys. Rev. B **74**, 220507.

Moriya, T., 1960, "Anisotropic superexchange interaction and weak ferromagnetism," Phys. Rev. **120**, 91–98.

Moser, J., A. Matos-Abiague, D. Schuh, W. Wegscheider, J. Fabian, and D. Weiss, 2007, "Tunneling Anisotropic Magnetoresistance and Spin-Orbit Coupling in Fe/GaAs/Au Tunnel Junctions," Phys. Rev. Lett. **99**, 056601.

Mourik, V., K. Zuo, S. M. Frolov, S. R. Plissard, E. P. Bakkers, and L. P. Kouwenhoven, 2012, "Signatures of Majorana fermions in hybrid superconductor-semiconductor nanowire devices," Science **336**, 1003–1007.

Müller, M., L. Liensberger, L. Flacke, H. Huebl, A. Kamra, W. Belzig, R. Gross, M. Weiler, and M. Althammer, "Temperature-Dependent Spin Transport and Current-Induced Torques in Superconductor-Ferromagnet Heterostructures," 2021, Phys. Rev. Lett. **126**, 087201.

Naaman, R., Y. Paltiel, and D. H. Waldeck, 2020, "Chiral induced spin selectivity gives a new twist on spin-control in chemistry," Acc. Chem. Res. **53**, 2659–2667.

Nadeem, M., M. S. Fuhrer, and X. Wang, 2023, "The superconducting diode effect," Nat. Rev. Phys. **5**, 558–577.

Nadj-Perge, S., I. K. Drozdov, J. Li, H. Chen, S. Jeon, J. Seo, A. H. MacDonald, B. A. Bernevig, and A. Yazdani, 2014, "Observation of Majorana fermions in ferromagnetic atomic chains on a superconductor," Science **346**, 602–607.

Nagasawa, F., D. Frustaglia, H. Saarikoski, K. Richter, and J. Nitta, 2013, "Control of the spin geometric phase in semiconductor quantum rings," Nat. Commun. **4**, 2526.

Nakamura, H., T. Koga, and T. Kimura, 2012, "Experimental Evidence of Cubic Rashba Effect in an Inversion-Symmetric Oxide," Phys. Rev. Lett. **108**, 206601.

Nashaat, M., I. V. Bobkova, A. M. Bobkov, Y. M. Shukrinov, I. R. Rahmonov, and K. Sengupta, 2019, "Electrical control of magnetization in superconductor/ferromagnet/superconductor junctions on a three-dimensional topological insulator," Phys. Rev. B **100**, 054506.

Nayak, C., S. H. Simon, A. Stern, M. Freedman, and S. Das Sarma, 2008, "Non-Abelian anyons and topological quantum computation," Rev. Mod. Phys. **80**, 1083–1159.

Nelson, K. D., Z. Q. Mao, Y. Maeno, and Y. Liu, 2004, "Odd-parity superconductivity in $Sr_2RuO_4$," Science **306**, 1151–1154.

Nishikawa, Y., A. Tackeuchi, S. Nakamura, S. Muto, and N. Yokoyama, 1995, "All-optical picosecond switching of a quantum well etalon using spin-polarization relaxation," Appl. Phys. Lett. **66**, 839–841.

Ohnishi, K., S. Komori, G. Yang, K.-R. Jeon, L. Olde Olthof, X. Montiel, M. G. Blamire, and J. W. A. Robinson, 2020, "Spin-transport in superconductors," Appl. Phys. Lett. **116**, 130501.

Olthof, Olde, L. A. B., X. Montiel, J. W. A. Robinson, and A. I. Buzdin, 2019, "Superconducting vortices generated via spin-orbit coupling at superconductor/ferromagnet interface," Phys. Rev. B **100**, 220505.

Oreg, Y., G. Refael, and F. von Oppen, 2010, "Helical Liquids and Majorana Bound States in Quantum Wires," Phys. Rev. Lett. **105**, 177002.

Ouassou, J. A., A. Di Bernardo, J. W. A. Robinson, and J. Linder, 2016, "Electric control of superconducting transition through a spin-orbit coupled interface," Sci. Rep. **6**, 29312.

Ozeri, M., *et al.*, 2023, "Scanning SQUID imaging of reduced superconductivity due to the effect of chiral molecule islands adsorbed on Nb," Adv. Mater. Interfaces **10**, 2201899.

Pahomi, T. E., M. Sigrist, and A. A. Soluyanov, 2020, "Braiding Majorana corner modes in a second-order topological superconductor," Phys. Rev. Res. **2**, 032068.

Pal, B., *et al.*, 2022, "Josephson diode effect from Cooper pair momentum in a topological semimetal," Nat. Phys. **18**, 1228–1233.

Park, B. G., J. Wunderlich, D. A. Williams, S. J. Joo, K. Y. Jung, K. H. Shin, K. Olejník, A. B. Shick, and T. Jungwirth, 2008, "Tunneling Anisotropic Magnetoresistance in Multilayer-$(Co/Pt)/AlO_x/Pt$ Structures," Phys. Rev. Lett. **100**, 087204.

Park, J.-H., C. H. Kim, J.-W. Rhim, and J. H. Han, 2012, "Orbital Rashba effect and its detection by circular dichroism angle-resolved photoemission spectroscopy," Phys. Rev. B **85**, 195401.

Park, S. R., C. H. Kim, J. Yu, J. H. Han, and C. Kim, 2011, "Orbital-Angular-Momentum Based Origin of Rashba-Type Surface Band Splitting," Phys. Rev. Lett. **107**, 156803.

Paudel, P. P., T. Cole, B. D. Woods, and T. D. Stanescu, 2021, "Enhanced topological superconductivity in spatially modulated planar Josephson junctions," Phys. Rev. B **104**, 155428.

Pekerten, B., J. D. Pakizer, B. Hawn, and A. Matos-Abiague, 2022, "Anisotropic topological superconductivity in Josephson junctions," Phys. Rev. B **105**, 054504.

Peña, V., Z. Sefrioui, D. Arias, C. Leon, J. Santamaria, M. Varela, S. J. Pennycook, and J. L. Martinez, 2004, "Coupling of superconductors through a half-metallic ferromagnet: Evidence for a long-range proximity effect," Phys. Rev. B **69**, 224502.

Petrashov, V. T., V. N. Antonov, S. V. Maksimov, and S. R. Shaikhadarov, 1994, "Conductivity of mesoscopic structures with ferromagnetic and superconducting regions," Pis'ma Zh. Eksp. Teor. Fiz. **59**, 523–526 [JETP Lett. **59**, 551–555 (1994), http://jetpletters.ru/ps/1309/article_19787.pdf].

Petrashov, V. T., I. A. Sosnin, I. Cox, A. Parsons, and C. Troadec, 1999, "Giant Mutual Proximity Effects in Ferromagnetic/Superconducting Nanostructures," Phys. Rev. Lett. **83**, 3281–3284.

Petsch, A. N., M. Zhu, M. Enderle, Z. Q. Mao, Y. Maeno, I. I. Mazin, and S. M. Hayden, 2020, "Reduction of the Spin Susceptibility in

the Superconducting State of $Sr_2RuO_4$ Observed by Polarized Neutron Scattering," Phys. Rev. Lett. **125**, 217004.
Pientka, F., A. Keselman, E. Berg, A. Yacoby, A. Stern, and B. I. Halperin, 2017, "Topological Superconductivity in a Planar Josephson Junction," Phys. Rev. X **7**, 021032.
Pita-Vidal, M., A. Bargerbos, C.-K. Yang, D. J. van Woerkom, W. Pfaff, N. Haider, P. Krogstrup, L. P. Kouwenhoven, G. de Lange, and A. Kou, 2020, "Gate-Tunable Field-Compatible Fluxonium-Phys. Rev. Appl. **14**, 064038.
Quay, C. H. L., D. Chevallier, C. Bena, and M. Aprili, 2013, "Spin imbalance and spin-charge separation in a mesoscopic superconductor," Nat. Phys. **9**, 84–88.
Rabinovich, D. S., I. V. Bobkova, A. M. Bobkov, and M. A. Silaev, 2019, "Resistive State of Superconductor-Ferromagnet-Superconductor Josephson Junctions in the Presence of Moving Domain Walls," Phys. Rev. Lett. **123**, 207001.
Raimondi, R., P. Schwab, C. Gorini, and G. Vignale, 2012, "Spin-orbit interaction in a two-dimensional electron gas: A SU(2) formulation," Ann. Phys. (Berlin) **524**, 153–162.
Rammer, J., and H. Smith, 1986, "Quantum field-theoretical methods in transport theory of metals," Rev. Mod. Phys. **58**, 323–359.
Rashba, E. I., 2003, "Spin currents in thermodynamic equilibrium: The challenge of discerning transport currents," Phys. Rev. B **68**, 241315.
Rasmussen, A., J. Danon, H. Suominen, F. Nichele, M. Kjaergaard, and K. Flensberg, 2016, "Effects of spin-orbit coupling and spatial symmetries on the Josephson current in SNS junctions," Phys. Rev. B **93**, 155406.
Read, N., and D. Green, 2000, "Paired states of fermions in two dimensions with breaking of parity and time-reversal symmetries and the fractional quantum Hall effect," Phys. Rev. B **61**, 10267–10297.
Reeg, C. R., and D. L. Maslov, 2015, "Proximity-induced triplet superconductivity in Rashba materials," Phys. Rev. B **92**, 134512.
Ren, H., *et al.*, 2019, "Topological superconductivity in a phase-controlled Josephson junction," Nature (London) **569**, 93–98.
Reynoso, A. A., G. Usaj, C. A. Balseiro, D. Feinberg, and M. Avignon, 2008, "Anomalous Josephson Current in Junctions with Spin Polarizing Quantum Point Contacts," Phys. Rev. Lett. **101**, 107001.
Risinggård, V., and J. Linder, 2019, "Direct and inverse superspin Hall effect in two-dimensional systems: Electrical detection of spin supercurrents," Phys. Rev. B **99**, 174505.
Robinson, J. W. A., F. Chiodi, M. Egilmez, G. B. Halasz, and M. G. Blamire, 2012, "Supercurrent enhancement in Bloch domain walls," Sci. Rep. **2**, 699.
Robinson, J. W. A., A. V. Samokhvalov, and A. I. Buzdin, 2019, "Chirality-controlled spontaneous currents in spin-orbit coupled superconducting rings," Phys. Rev. B **99**, 180501.
Robinson, J. W. A., J. D. S. Witt, and M. G. Blamire, 2010, "Controlled injection of spin-triplet supercurrents into a strong ferromagnet," Science **329**, 59–61.
Rogers, M., *et al.*, 2021, "Spin-singlet to triplet Cooper pair converter interface," Commun. Phys. **4**, 69.
Rokhinson, L. P., X. Liu, and J. K. Furdyna, 2012, "The fractional a.c. Josephson effect in a semiconductor–superconductor nanowire as a signature of Majorana particles," Nat. Phys. **8**, 795–799.
Rosenbach, D., *et al.*, 2021, "Reappearance of first Shapiro step in narrow topological Josephson junctions," Sci. Adv. **7**, eabf1854.
Rößler, U. K., A. N. Bogdanov, and C. Pfleiderer, 2006, "Spontaneous skyrmion ground states in magnetic metals," Nature (London) **442**, 797–801.
Rusanov, A. Y., S. Habraken, and J. Aarts, 2006, "Inverse spin switch effects in ferromagnet-superconductor-ferromagnet trilayers with strong ferromagnets," Phys. Rev. B **73**, 060505.
Saito, Y., *et al.*, 2016, "Superconductivity protected by spin–valley locking in ion-gated $MoS_2$," Nat. Phys. **12**, 144–149.
Salamone, T., H. G. Hugdal, M. Amundsen, and S. H. Jacobsen, 2022, "Curvature control of the superconducting proximity effect in diffusive ferromagnetic nanowires," Phys. Rev. B **105**, 134511.
Salamone, T., M. B. M. Svendsen, M. Amundsen, and S. Jacobsen, 2021, "Curvature-induced long-range supercurrents in diffusive superconductor-ferromagnet-superconductor Josephson junctions with a dynamic 0–$\pi$ transition," Phys. Rev. B **104**, L060505.
Samokhin, K. V., 2004, "Magnetic properties of superconductors with strong spin-orbit coupling,," Phys. Rev. B **70**, 104521.
Samokhin, K. V., 2009, "Spin-orbit coupling and semiclassical electron dynamics in noncentrosymmetric metals," Ann. Phys. (Amsterdam) **324**, 2385–2407.
Sanchez-Manzano, D., *et al.*, 2022, "Extremely long-range, high-temperature Josephson coupling across a half-metallic ferromagnet," Nat. Mater. **21**, 188–194.
SanGiorgio, P., S. Reymond, M. R. Beasley, J. H. Kwon, and K. Char, 2008, "Anomalous Double Peak Structure in Superconductor/Ferromagnet Tunneling Density of States," Phys. Rev. Lett. **100**, 237002.
Sasaki, S., M. Kriener, K. Segawa, K. Yada, Y. Tanaka, M. Sato, and Y. Ando, 2011, "Topological Superconductivity in $Cu_xBi_2Se_3$," Phys. Rev. Lett. **107**, 217001.
Satchell, N., and N. O. Birge, 2018, "Supercurrent in ferromagnetic Josephson junctions with heavy metal interlayers," Phys. Rev. B **97**, 214509.
Satchell, N., R. Loloee, and N. O. Birge, 2019, "Supercurrent in ferromagnetic Josephson junctions with heavy-metal interlayers. II. Canted magnetization," Phys. Rev. B **99**, 174519.
Satchell, N., P. M. Shepley, M. C. Rosamond, and G. Burnell, 2023, "Supercurrent diode effect in thin film Nb tracks," J. Appl. Phys. **133**, 203901.
Sau, J. D., R. M. Lutchyn, S. Tewari, and S. Das Sarma, 2010, "Generic New Platform for Topological Quantum Computation Using Semiconductor Heterostructures," Phys. Rev. Lett. **104**, 040502.
Scammell, H. D., J. I. A. Li, and M. S. Scheurer, 2022, "Theory of zero-field superconducting diode effect in twisted trilayer graphene," 2D Mater. **9**, 025027.
Schindler, F., A. M. Cook, M. G. Vergniory, Z. Wang, S. S. Parkin, B. A. Bernevig, and T. Neupert, 2018, "Higher-order topological insulators," Sci. Adv. **4**, aat0346.
Schindler, F., *et al.*, 2018, "Higher-order topology in bismuth," Nat. Phys. **14**, 918–924.
Sefrioui, Z., D. Arias, V. Peña, J. E. Villegas, M. Varela, P. Prieto, C. León, J. L. Martinez, and J. Santamaria, 2003, "Ferromagnetic/superconducting proximity effect in $La_{0.7}Ca_{0.3}MnO_3/YBa_2Cu_3O_{7-\delta}$ superlattices," Phys. Rev. B **67**, 214511.
Sengupta, K., I. Žutić, H.-J. Kwon, V. M. Yakovenko, and S. Das Sarma, 2001, "Midgap edge states and pairing symmetry of quasi-onedimensional organic superconductors," Phys. Rev. B **63**, 144531.
Serene, J. W., and D. Rainer, 1983, "The quasiclassical approach to superfluid $^3$He," Phys. Rep. **101**, 221–311.
Setiawan, F., C.-T. Wu, and K. Levin, 2019, "Full proximity treatment of topological superconductors in Josephson-junction architectures," Phys. Rev. B **99**, 174511.

Shabani, J., *et al.*, 2016, "Two-dimensional epitaxial superconductor-semiconductor heterostructures: A platform for topological superconducting networks," Phys. Rev. B **93**, 155402.
Shekhter, R. I., O. Entin-Wohlman, M. Jonson, and A. Aharony, 2016, Rashba Splitting of Cooper Pairs," Phys. Rev. Lett. **116**, 217001.
Shekhter, R. I., O. Entin-Wohlman, M. Jonson, and A. Aharony, 2017, "Spin precession in spin-orbit coupled weak links: Coulomb repulsion and Pauli quenching," Phys. Rev. B **96**, 241412.
Shelankov, A. L., 1985, "On the derivation of quasiclassical equations for superconductors," J. Low Temp. Phys. **60**, 29–44.
Shen, S.-Q., 2012, *Topological Insulators: Dirac Equation in Condensed Matters* (Springer, Berlin).
Shishidou, T., H. G. Suh, P. M. R. Brydon, M. Weinert, and D. F. Agterberg, 2021, "Topological band and superconductivity in $UTe_2$," Phys. Rev. B **103**, 104504.
Shockley, W., 1949, "The theory of *p-n* junctions in semiconductors and *p-n* junction transistors," Bell Syst. Tech. J. **28**, 435–489.
Shockley, W., 1952, "Electrons and holes in semiconductors," Phys. Today **5**, No. 12, 18–19.
Shukrinov, Y. M., 2022, "Anomalous Josephson effect," Phys. Usp. **65**, 317–354, https://ufn.ru/en/articles/2022/4/a/.
Shukrinov, Y. M., I. R. Rahmonov, A. Janalizadeh, and M. R. Kolahchi, 2021, "Anomalous Gilbert damping and duffing features of the superconductor-ferromagnet-superconductor $\varphi_0$ Josephson junction," Phys. Rev. B **104**, 224511.
Sierra, J. F., J. Fabian, R. K. Kawakami, S. Roche, and S. O. Valenzuela, 2021, "van der Waals heterostructures for spintronics and opto-spintronics," Nat. Nanotechnol. **16**, 856–868.
Silaev, M., 2022, "Anderson-Higgs Mass of Magnons in Superconductor-Ferromagnet-Superconductor Systems," Phys. Rev. Appl. **18**, L061004.
Silaev, M., P. Virtanen, F. S. Bergeret, and T. T. Heikkilä, 2015, "Long-Range Spin Accumulation from Heat Injection in Mesoscopic Superconductors with Zeeman Splitting," Phys. Rev. Lett. **114**, 167002.
Silaev, M. A., A. Y. Aladyshkin, M. V. Silaeva, and A. S. Aladyshkina, 2014, "The diode effect induced by domain-wall superconductivity," J. Phys. Condens. Matter **26**, 095702.
Silaev, M. A., I. V. Bobkova, and A. M. Bobkov, 2020, "Odd triplet superconductivity induced by a moving condensate," Phys. Rev. B **102**, 100507.
Silaev, M. A., I. V. Tokatly, and F. S. Bergeret, 2017, "Anomalous current in diffusive ferromagnetic Josephson junctions," Phys. Rev. B **95**, 184508.
Simensen, H. T., and J. Linder, 2018, "Tunable superconducting critical temperature in ballistic hybrid structures with strong spin-orbit coupling,," Phys. Rev. B **97**, 054518.
Singh, A., S. Voltan, K. Lahabi, and J. Aarts, 2015, "Colossal Proximity Effect in a Superconducting Triplet Spin Valve Based on the Half-Metallic Ferromagnet $CrO_2$," Phys. Rev. X **5**, 021019.
Sinova, J., S. O. Valenzuela, J. Wunderlich, C. H. Back, and T. Jungwirth, 2015, "Spin Hall effects," Rev. Mod. Phys. **87**, 1213–1259.
Smidman, M., M. B. Salamon, H. Q. Yuan, and D. F. Agterberg, 2017, "Superconductivity and spin-orbit coupling in non-centrosymmetric materials: A review," Rep. Prog. Phys. **80**, 036501.
Sonin, E. B., 2007, "Equilibrium spin currents in the Rashba medium," Phys. Rev. B **76**, 033306.
Sonin, E. B., 2010, "Spin currents and spin superfluidity," Adv. Phys. **59**, 181–255.
Sosnin, I., H. Cho, V. T. Petrashov, and A. F. Volkov, 2006, "Superconducting Phase Coherent Electron Transport in Proximity Conical Ferromagnets," Phys. Rev. Lett. **96**, 157002.
Steffensen, D., M. H. Christensen, B. M. Andersen, and P. Kotetes, 2022, "Topological superconductivity induced by magnetic texture crystals," Phys. Rev. Res. **4**, 013225.
Stern, A., and E. Berg, 2019, "Fractional Josephson Vortices and Braiding of Majorana Zero Modes in Planar Superconductor-Semiconductor Heterostructures," Phys. Rev. Lett. **122**, 107701.
Swartz, P. S., and H. R. Hart, Jr., 1967, "Asymmetries of the critical surface current in type-II superconductors," Phys. Rev. **156**, 412–420.
Szombati, D. B., S. Nadj-Perge, D. Car, S. R. Plissard, E. P. A. M. Bakkers, and L. P. Kouwenhoven, 2016, "Josephson $\phi_0$-junction in nanowire quantum dots," Nat. Phys. **12**, 568–572.
Tafuri, F., 2019, Ed., *Fundamentals and Frontiers of the Josephson Effect* (Springer Nature, Cham, Switzerland).
Tagirov, L. R., 1999, "Low-Field Superconducting Spin Switch Based on a Superconductor/Ferromagnet Multilayer," Phys. Rev. Lett. **83**, 2058–2061.
Takahashi, S., and S. Maekawa, 2002, "Hall Effect Induced by a Spin-Polarized Current in Superconductors," Phys. Rev. Lett. **88**, 116601.
Takahashi, S., and S. Maekawa, 2008, "Spin current in metals and superconductors," J. Phys. Soc. Jpn. **77**, 031009.
Takashima, R., S. Fujimoto, and T. Yokoyama, "Adiabatic and nonadiabatic spin torques induced by a spin-triplet supercurrent," 2017, Phys. Rev. B **96**, 121203(R).
Takayanagi, H., and T. Kawakami, 1985, "Superconducting Proximity Effect in the Native Inversion Layer on InAs," Phys. Rev. Lett. **54**, 2449–2452.
Tanaka, Y., Y. Mizuno, T. Yokoyama, K. Yada, and M. Sato, 2010, "Anomalous Andreev Bound State in Noncentrosymmetric Superconductors," Phys. Rev. Lett. **105**, 097002.
Tanaka, Y., T. Yokoyama, A. V. Balatsky, and N. Nagaosa, 2009, "Theory of topological spin current in noncentrosymmetric superconductors," Phys. Rev. B **79**, 060505.
Tedrow, P. M., and R. Meservey, 1971, "Direct Observation of Spin-State Mixing in Superconductors," Phys. Rev. Lett. **27**, 919–921.
Thomson, W., 1857, "XIX. On the electro-dynamic qualities of metals—Effects of magnetization on the electric conductivity of nickel and of iron," Proc. R. Soc. London **8**, 546–550.
Tkachov, G., 2017, "Magnetoelectric Andreev Effect due to Proximity-Induced Nonunitary Triplet Superconductivity in Helical Metals," Phys. Rev. Lett. **118**, 016802.
Tokatly, I. V., 2008, "Equilibrium Spin Currents: Non-Abelian Gauge Invariance and Color Diamagnetism in Condensed Matter," Phys. Rev. Lett. **101**, 106601.
Tokatly, I. V., 2017, "Usadel equation in the presence of intrinsic spin-orbit coupling: A unified theory of magnetoelectric effects in normal and superconducting systems," Phys. Rev. B **96**, 060502.
Tosato, A. A., *et al.*, 2023, "Hard superconducting gap in germanium," Commun. Mater. **4**, 23.
Touitou, N., P. Bernstein, J. F. Hamet, C. Simon, L. Méchin, J. P. Contour, and E. Jacquet, 2004, "Nonsymmetric current-voltage characteristics in ferromagnet/superconductor thin film structures," Appl. Phys. Lett. **85**, 1742–1744.
Tsymbal, E. Y., and I. Žutić, 2019, Eds., *Spintronics Handbook*, 2nd ed. (CRC Press, Boca Raton).
Usman, I. T. M., *et al.*, 2011, "Evidence for spin mixing in holmium thin film and crystal samples," Phys. Rev. B **83**, 144518.
Valls, O. T., 2022, *Superconductor/Ferromagnet Nanostructures* (World Scientific, Hackensack, NJ).
Vas'ko, V. A., V. A. Larkin, P. A. Kraus, K. R. Nikolaev, D. E. Grupp, C. A. Nordman, and A. M. Goldman, 1997, "Critical Current Suppression in a Superconductor by Injection of Spin-Polarized Carriers from a Ferromagnet," Phys. Rev. Lett. **78**, 1134–1137.

Vezin, T., C. Shen, J. E. Han, and I. Žutić, 2020, "Enhanced spin-triplet pairing in magnetic junctions with *s*-wave superconductors," Phys. Rev. B **101**, 014515.

Virtanen, P., F. S. Bergeret, and I. V. Tokatly, 2021, "Magnetoelectric effects in superconductors due to spin-orbit scattering: Nonlinear *s*-model description," Phys. Rev. B **104**, 064515.

Virtanen, P., F. S. Bergeret, and I. V. Tokatly, 2022, "Nonlinear $\sigma$ model for disordered systems with intrinsic spin-orbit coupling," Phys. Rev. B **105**, 224517.

Visani, C., Z. Sefrioui, J. Tornos, C. Leon, J. Briatico, M. Bibes, A. Barthélémy, J. Santamaría, and J. E. Villegas, 2012, "Equal-spin Andreev reflection and long-range coherent transport in high-temperature superconductor/half-metallic ferromagnet junctions," Nat. Phys. **8**, 539–543.

Vodolazov, D. Y., B. A. Gribkov, S. A. Gusev, A. Y. Klimov, Y. N. Nozdrin, V. V. Rogov, and S. N. Vdovichev, 2005, "Considerable enhancement of the critical current in a superconducting film by a magnetized magnetic strip," Phys. Rev. B **72**, 064509.

Vorontsov, A. B., I. Vekhter, and M. Eschrig, 2008, "Surface Bound States and Spin Currents in Noncentrosymmetric Superconductors," Phys. Rev. Lett. **101**, 127003.

Waintal, X., and P. W. Brouwer, 2002, "Magnetic exchange interaction induced by a Josephson current," Phys. Rev. B **65**, 054407.

Wakamura, T., H. Akaike, Y. Omori, Y. Niimi, S. Takahashi, A. Fujimaki, S. Maekawa, and Y. Otani, 2015, "Quasiparticle-mediated spin Hall effect in a superconductor," Nat. Mater. **14**, 675–678.

Wakamura, T., N. Hasegawa, K. Ohnishi, Y. Niimi, and Y. Otani, 2014, "Spin Injection into a Superconductor with Strong Spin-Orbit Coupling," Phys. Rev. Lett. **112**, 036602.

Wan, Z., A. Kazakov, M. J. Manfra, L. N. Pfeiffer, K. W. West, and L. P. Rokhinson, 2015, "Induced superconductivity in high-mobility two-dimensional electron gas in gallium arsenide heterostructures," Nat. Commun. **6**, 7426.

Wan, Z., *et al.*, "Signatures of chiral superconductivity in chiral molecule intercalated tantalum disulfide," 2023, arXiv:2302.05078.

Wang, S., L. Tang, and K. Xia, 2010, "Spin transfer torque in the presence of Andreev reflections," Phys. Rev. B **81**, 094404.

Wang, X. L., A. Di Bernardo, N. Banerjee, A. Wells, F. S. Bergeret, M. G. Blamire, and J. W. A. Robinson, 2014, "Giant triplet proximity effect in superconducting pseudo spin valves with engineered anisotropy," Phys. Rev. B **89**, 140508(R).

Wei, J. Y. T., N.-C. Yeh, C. C. Fui, and R. P. Vasquez, 1999, "Tunneling spectroscopy study of spin-polarized quasiparticle injection effects in cuprate/manganite heterostructures," J. Appl. Phys. **85**, 5350–5352.

Wei, P., S. Manna, M. Eich, P. Lee, and J. Moodera, 2019, "Superconductivity in the Surface State of Noble Metal Gold and Its Fermi Level Tuning by EuS Dielectric," Phys. Rev. Lett. **122**, 247002.

Wendin, G., 2017, "Quantum information processing with superconducting circuits: A review," Rep. Prog. Phys. **80**, 106001.

Winkler, R., 2003, *Spin-Orbit Coupling Effects in Two-Dimensional Electron and Hole Systems* (Springer, New York).

Winkler, R., H. Noh, E. Tutuc, and M. Shayegan, 2002, "Anomalous Rashba spin splitting in two-dimensional hole systems," Phys. Rev. B **65**, 245417.

Wu, C.-T., B. M. Anderson, W. H. Hsiao, and K. Levin, 2017, "Majorana zero modes in spintronics devices," Phys. Rev. B **95**, 014519.

Wu, C.-T., F. Setiawan, B. M. Anderson, W. H. Hsiao, and K. Levin, 2018, "Quantum phase transitions in proximitized Josephson junction," Phys. Rev. B **98**, 064504.

Xie, Y.-M., É. Lantagne-Hurtubise, A. F. Young, S. Nadj-Perge, and J. Alicea, 2023, "Gate-Defined Topological Josephson Junctions in Bernal Bilayer Graphene," Phys. Rev. Lett. **131**, 146601.

Yada, K., M. Sato, Y. Tanaka, and T. Yokoyama, 2011, "Surface density of states and topological edge states in noncentrosymmetric superconductors," Phys. Rev. B **83**, 064505.

Yamashita, T., K. Tanikawa, S. Takahashi, and S. Maekawa, 2005, "Superconducting $\pi$ Qubit with a Ferromagnetic Josephson Junction," Phys. Rev. Lett. **95**, 097001.

Yang, G., C. Ciccarelli, and J. W. A. Robinson, 2021, "Boosting spintronics with superconductivity," APL Mater. **9**, 050703.

Yang, G., P. Stano, J. Klinovaja, and D. Loss, 2016, "Majorana bound states in magnetic skyrmions," Phys. Rev. B **93**, 224505.

Yang, H., S.-H. Yang, S. Takahashi, S. Maekawa, and S. S. P. Parkin, 2010, "Extremely long quasiparticle spin lifetimes in superconducting aluminium using MgO tunnel spin injectors," Nat. Mater. **9**, 586–593.

Yang, Z.-H., Y.-H. Yang, and J. Wang, 2012, "Interfacial spin Hall current in a Josephson junction with Rashba spin-orbit coupling," Chin. Phys. B **21**, 057402.

Yao, Y., R. Cai, T. Yu, Y. Ma, W. Xing, Y. Ji, X.-C. Xie, S.-H. Yang, and W. Han, 2021, "Giant oscillatory Gilbert damping in superconductor/ferromagnet/superconductor junctions," Sci. Adv. **7**, eabh3686.

Yates, K. A., M. S. Anwar, J. Aarts, O. Conde, M. Eschrig, T. Löfwander, and L. F. Cohen, 2013, "Andreev spectroscopy of $CrO_2$ thin films on $TiO_2$ and $Al_2O_3$," Europhys. Lett. **103**, 67005.

Yazdani, A., 2019, "Conjuring Majorana with synthetic magnetism," Nat. Mater. **18**, 1036–1037.

Ying, Z. J., M. Cuoco, C. Ortix, and P. Gentile, 2017, "Tuning pairing amplitude and spin-triplet texture by curving superconducting nanostructures," Phys. Rev. B **96**, 100506.

Ying, Z. J., P. Gentile, C. Ortix, and M. Cuoco, 2016, "Designing electron spin textures and spin interferometers by shape deformations," Phys. Rev. B **94**, 081406.

Yokoyama, T., 2015, "Anomalous Josephson Hall effect in magnet/triplet superconductor junctions," Phys. Rev. B **92**, 174513.

Yokoyama, T., M. Eto, and Y. V. Nazarov, 2014, "Anomalous Josephson effect induced by spin-orbit interaction and Zeeman effect in semiconductor nanowires," Phys. Rev. B **89**, 195407.

Yokoyama, T., Y. Tanaka, and J. Inoue, 2006, "Charge transport in two-dimensional electron gas/insulator/superconductor junctions with Rashba spin-orbit coupling," Phys. Rev. B **74**, 035318.

Yu, P., J. Chen, M. Gomanko, G. Badawy, E. P. A. M. Bakkers, K. Zuo, V. Mourik, and S. M. Frolov, 2021, "Non-Majorana states yield nearly quantized conductance in proximatized nanowires," Nat. Phys. **17**, 482–488.

Yuan, N. F. Q., and L. Fu, 2022, "Supercurrent diode effect and finite-momentum superconductors," Proc. Natl. Acad. Sci. U.S.A. **119**, e2119548119.

Zazunov, A., R. Egger, T. Jonckheere, and T. Martin, 2009, "Anomalous Josephson Current through a Spin-Orbit Coupled Quantum Dot," Phys. Rev. Lett. **103**, 147004.

Zhao, E., and J. A. Sauls, 2008, "Theory of nonequilibrium spin transport and spin-transfer torque in superconducting-ferromagnetic nanostructures," Phys. Rev. B **78**, 174511.

Zhou, T., M. C. Dartiailh, W. Mayer, J. E. Han, A. Matos-Abiague, J. Shabani, and I. Žutić, 2020, "Phase Control of Majorana Bound States in a Topological X Junction," Phys. Rev. Lett. **124**, 137001.

Zhou, T., M. C. Dartiailh, K. Sardashti, J. E. Han, A. Matos-Abiague, J. Shabani, and I. Žutić, 2022, "Fusion of Majorana bound states with mini-gate control in two-dimensional systems," Nat. Commun. **13**, 1738.

Zhou, T., N. Mohanta, J. E. Han, A. Matos-Abiague, and I. Žutić, 2019, "Tunable magnetic textures in spin valves: From spintronics to Majorana bound states," Phys. Rev. B **99**, 134505.

Zhu, J.-X., 2016, *Bogoliubov–de Gennes Method and Its Applications*, Lecture Notes in Physics, 1st ed. (Springer International Publishing, Cham, Switzerland).

Zhu, X., 2018, "Tunable Majorana corner states in a two-dimensional second-order topological superconductor induced by magnetic fields," Phys. Rev. B **97**, 205134.

Zhu, Y., A. Pal, M. G. Blamire, and Z. H. Barber, 2017, "Superconducting exchange coupling between ferromagnets," Nat. Mater. **16**, 195–199.

Žutić, I., and S. Das Sarma, 1999, "Spin-polarized transport and Andreev reflection in semiconductor/superconductor hybrid structures," Phys. Rev. B **60**, R16322–R16325.

Žutić, I., J. Fabian, and S. Das Sarma, 2004, "Spintronics: Fundamentals and applications," Rev. Mod. Phys. **76**, 323–410.

Žutić, I., A. Matos-Abiague, B. Scharf, H. Dery, and K. Belashchenko, 2019, "Proximitized materials," Mater. Today **22**, 85–107.

Žutić, I., and I. Mazin, 2005, "Phase-Sensitive Tests of the Pairing State Symmetry in $Sr_2RuO_4$," Phys. Rev. Lett. **95**, 217004.